Evaluation of Crumb Rubber in Hot Mix Asphalt

Final Report
July 2004

Thomas Bennert
Senior Research Engineer and
Supervisor of the RAPL

Ali Maher
Professor and Director

Joseph Smith
Research Engineer

Center for Advanced Infrastructure and Transportation (CAIT)
Rutgers Asphalt/Pavement Laboratory (RAPL)
Rutgers University
Department of Civil and Environmental Engineering
623 Bowser Road
Piscataway, NJ 08854

In Cooperation with

BAYSHORE RECYCLING CORP.
P.O. Box 290
75 Crows Mill Road
Keasbey, NJ 08862

Disclaimer Statement

"The contents of this report reflect the views of the author(s) who is (are) responsible for the facts and the accuracy of the data presented herein. The contents do not necessarily reflect the official views or policies of the New Jersey Department of Transportation or the Federal Highway Administration. This report does not constitute a standard, specification, or regulation."

The contents of this report reflect the views of the authors, who are responsible for the facts and the accuracy of the information presented herein. This document is disseminated under the sponsorship of the Department of Transportation, University Transportation Centers Program, in the interest of information exchange. The U.S. Government assumes no liability for the contents or use thereof.

TECHNICAL REPORT STANDARD TITLE PAGE

1. Report No.	2. Government Accession No.	3. Recipient's Catalog No.

4. Title and Subtitle	5. Report Date
Evaluation of Crumb Rubber in Hot Mix Asphalt	July, 2004
	6. Performing Organization Code CAIT/Rutgers
7. Author(s) Mr. Thomas Bennert, Dr. Ali Maher, and Mr. Joseph Smith	8. Performing Organization Report No.
9. Performing Organization Name and Address	10. Work Unit No.
	11. Contract or Grant No.
	13. Type of Report and Period Covered Final Report 9/2003 – 7/2004
12. Sponsoring Agency Name and Address U.S.D.O.T, Research and Special Programs Administration 400 7th Street, SW Washington, D.C. 20590-0001	14. Sponsoring Agency Code
15. Supplementary Notes	

16. Abstract

An asphalt-rubber hot mix asphalt (AR-HMA) design was created using a Superpave 12.5mm gradation and a #30 (-) mesh crumb rubber at 20% total weight of the asphalt binder. At this point in time, asphalt rubber has only been used with HMA that contains a more open graded nature, such as open graded friction course (OGFC). However, OGFC is limited on it use due to its potential problems (i.e. clogging and winter maintenance). However, a 12.5mm Superpave mix may be used on almost any roadway in New Jersey and is most commonly found as the surface course. It is used for both new construction and rehabilitation projects. Therefore, this mix type has the largest potential for usage, meaning that more tires can eventually be recycled. However, two factors need to be considered prior to acceptance; performance and cost.

Four HMA mixes were constructed and tested in this study. Three baseline mixes using a PG64-22, PG70-22, and a PG76-22 asphalt binder, as well as the AR-HMA mix which used crumb rubber blended with the same PG64-22 asphalt binder. The influence of crumb rubber particle size on the compaction properties during the mixture design procedure was also evaluated. This would provide a method of comparing the final mixture performance of different performance graded binders to the AR-HMA mix. This type of methodology of testing the mixtures is extremely important due to the necessity of ensuring the crumb rubber complying to the aggregate gradation volume limitations, and how the crumb rubber interacts with this volume limitation under performance testing. Therefore, a number of different performance tests were conducted on the four different HMA mixes: 1) Asphalt Pavement Analyzer, 2) Repeated Load Permanent Deformation testing using the Simple Performance test specifications, 3) Dynamic Modulus, 4) Repeated Shear at Constant Height, 5) Frequency Sweep at Constant Height,and 6) Simple Shear at Constant Height.

The results from the mixture design portion concluded that to provide consistent compactibility when using crumb rubber in a 12.5mm Superpave design, the maximum particle size should not be greater than a #30 mesh. The performance tests concluded that the AR-HMA mix performed as well as or better than the PG76-22 for every test conducted. For example, the dynamic modulus test results showed that the AR-HMA had similar stiffnesses to the PG76-22 at the high test temperatures, however, the AR-HMA had a much less stiffness at the low test temperature. This indicates that the AR-HMA mix design in this study will provide excellent rut resistance, while also providing excellent low temperature cracking resistance. Essentially, by adding the crumb rubber to the PG64-22, the working temperature range of the asphalt binder increased on both the high and low sides. Also, by performing similarily to the PG76-22, Bayshore Recycling now can establish a cost comparison using the difference in cost between a HMA with a PG64-22 and a PG76-22.

17. Key Words	18. Distribution Statement
Asphalt Rubber, Dynamic Modulus, Superpave Shear Tester, Asphalt Pavement Analyzer, Simple Performance Test	

19. Security Classif (of this report)	20. Security Classif. (of this page)	21. No of Pages	22. Price
Unclassified	Unclassified	72	

Form DOT F 1700.7 (8-69)

TABLE OF CONTENTS

Page #

LIST OF FIGURES

LIST OF TABLES

INTRODUCTION

An asphalt rubber, hot mix asphalt (AR-HMA) was designed for BAYSHORE RECYCLING CORPORATION. and is described in a previously submitted report entitled, "Evaluation of Crumb Rubber in Hot Mix Asphalt – Summary of Tasks I and II". The previous report encompassed the following:

- The establishment of an aggregate gradation that would be classified as a 12.5mm HMA in the Superpave Mixture System;
- The development of a baseline mix design using conventional and polymer-modified asphalt binders;
- A compatibility check of the crumb rubber and asphalt binder using viscosity guidelines;
- The use of different sized crumb rubber to incorporate into an asphalt rubber, hot mix asphalt; and
- The final recommendation of an optimal sized crumb rubber size that could be blended into a 12.5mm Superpave HMA. The crumb rubber particle size that was recommended for further testing was a #30(-) mesh.

The purpose of this report is to describe the results of the performance testing that was conducted on the final AR-HMA, as well as the baseline mixes. The baseline mixes had the identical gradation as the AR-HMA, with asphalt binder grades of PG64-22, PG70-22, and PG76-22. The testing provides a means of comparing the performance of the AR-HMA mixture to the typically used asphalt mixes. Based on the performance comparisons, BAYSHORE RECYCLING can establish a cost/performance ratio of the AR-HMA corresponds to the cost/performance ratio of the conventional baseline mixes.

REVIEW OF VOLUMETRIC PROPERTIES

The most common asphalt mix type used by the New Jersey Department of Transportation (NJDOT) is the 12.5mm Superpave mix. This mix type may be used on almost any roadway in New Jersey and is most commonly found as the surface course. It is used for both new construction and rehabilitation projects. Therefore, to provide the greatest potential for using the most crumb rubber possible, the 12.5mm surface course mix was selected.

The final aggregate gradation selected for the mix design is shown in Figure 1. It is a 12.5mm Superpave mix, however, the nature of the gradation is coarse/open. Also shown in the figure are the two asphalt rubber mixes currently in service in New Jersey. Both of the in-service mixes are Open Graded Friction Course (OGFC) and have a much different gradation characteristic than the 12.5mm gradation selected for analysis. Due to the excessive amount of air voids in the OGFC mixes, the crumb rubber can exist within the aggregate skeleton without hampering the performance/compaction of the material. However, dense graded hot mix asphalt mixes, such as the 12.5 mm Superpave mix, is designed for a much lower air void content, therefore not easily allowing for the introduction of crumb rubber.

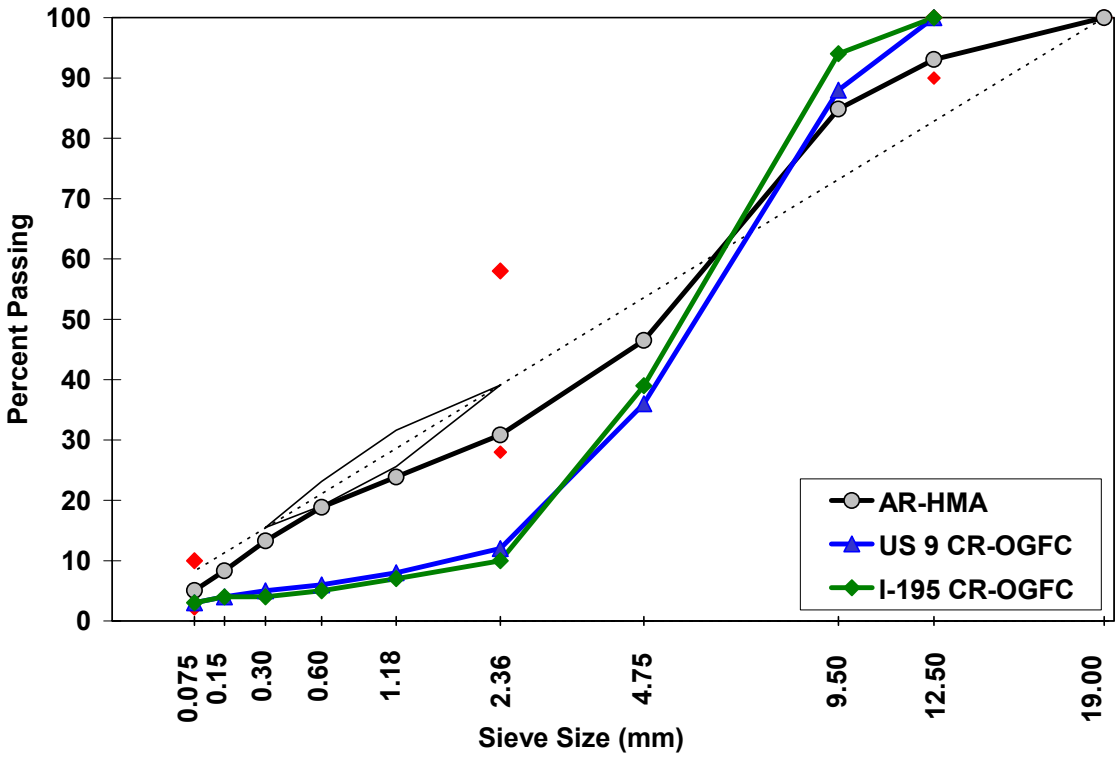

Figure 1 – Aggregate Gradation Used for the 12.5mm Superpave Design (AR-HMA) with Two In-Service OGFC Mixes Modified with Crumb Rubber (CR)

The HMA used in the testing program was a 12.5 mm Superpave mix using a PG64-22, PG70-22, and PG76-22 asphalt binders from the Citgo Refineries in Paulsboro, NJ. The AR-HMA was constructed using the PG64-22 with 20% crumb rubber by weight of the asphalt binder. The crumb rubber was blended with the PG64-22 for one hour prior to mixing with the aggregates. The final design of the mix was based on an Equivalent Single Axle Loads (ESAL's) range of 3.0 to 30 million. This represents a majority of moderate to heavy trafficked roads in New Jersey. Table 1 provides the final volumetric properties for all mixtures tested.

Table 1 – Final Volumetric Properties of Baseline Samples

Volumetric Property	PG76-22	PG70-22	PG64-22	AR-HMA
Asphalt Content (%)	5.1	5.1	5.1	6.1
VMA (> 14%)	15.7	15.7	15.7	17.9
VFA (65 to 75%)	74.3	74.3	74.3	77.4
Dust/Binder (0.6 to 1.2%)	1.1	1.1	1.1	0.9
TSR (> 80%)	96	91.6	87.3	93.4

VMA – Voids in Mineral Aggregate; VFA – Voids Filled with Asphalt
TSR – Tensile Strength Ratio

PERFORMANCE TESTING

Past experience has shown that the addition of crumb rubber to hot mix asphalt (HMA) can actually enhance the overall working properties of the HMA. The general benefits are shown with an increase in the resilience of the asphalt binder and the ability to withstand oxidation aging more easily. This can be further broken down into temperature ranges for which the HMA must work at:

High Temperatures

At high temperatures, the asphalt binder tends to flow easier due to the natural decrease of viscosity associated with higher temperatures. This condition creates a "softer" HMA, which is prone to rutting. The addition of crumb rubber to the HMA provides an increased viscosity contribution, thus stiffening the HMA at higher temperatures (Takallou et al., 1997; Chipps et al., 2001).

Intermediate Temperatures

At intermediate temperatures, the HMA must be able to withstand cyclic loading so as minimize tensile strains. The tensile strains occur at the bottom of the asphalt layer due to excessive bending and migrate upward (called reflective cracking). This ultimately compromises the structural integrity of the HMA layer. By adding crumb rubber to the HMA, an increase in resilience within the layer occurs, providing more elasticity during bending. Work conducted by Gopal et al. (2001) concluded that the addition of crumb rubber aids in the energy absorption properties of the HMA, therefore reducing the potential for failure due to cyclic loading. However, the authors also recommended that an optimum rubber content should be determined for each particular crumb rubber size and asphalt binder type.

Low Temperatures

At low temperature, the HMA must not be too stiff. It is well known that if a HMA has a high modulus at low temperatures, it will be very prone to cracking. Therefore, to help withstand cracking at low temperatures, the HMA must have a lower stiffness and a higher creep. Creep is defined as the deflection of the HMA under a constant load. Results from a number of researchers have shown that the addition of crumb rubber both decreases the stiffness and increases the creep properties of the HMA (Bahia and Davies, 1994; Takallou et al., 1997; Kim et al., 2001; Gopal et al., 2002).

In-Service Life (Every-Day Temperatures)

The addition of crumb rubber to HMA has also been found to resist age hardening. During the natural aging (hot-cooling cycles), the asphalt binder undergoes age hardening. The age hardening essentially describes the increase of stiffness with the increase of in-service life of the HMA. The first significant hardening occurs at the mixing plant during the mixing process where the HMA is heated to temperatures

ranging from 275 to 325^{o}F. After the mixing, the age hardening continues, although at a much slower rate. However, the addition of crumb rubber to HMA has been found to help reduce the effects of age hardening. Work conducted by Raad et al. (2001) revolved around evaluating the age hardening of AR-HMA. Laboratory testing was conducted on both un-modified HMA and AR-HMA. The testing was conducted immediately after field compaction and then after 10 years of service. Laboratory fatigue test results indicated that the recently placed and the 10 ten-year old AR-HMA were similar, indicating that the AR-HMA had undergone minimal age hardening during its service life. Laboratory work conducted by Chipps et al. (2001) showed similar results.

In general, the addition of crumb rubber to HMA, and the proper design and field implementation of the AR-HMA, expands the working range of the HMA providing a;

1. Reduction of rutting at high temperatures;
2. Reduction of fatigue cracking at intermediate temperatures;
3. Reduction of thermal cracking; and
4. Minimizes the potential for age hardening.

Therefore, to provide evidence that the AR-HMA developed in this project could accomplish all of the above, an extensive laboratory testing program was developed. The laboratory program utilized the following HMA/asphalt tests;

- Superpave Shear Tester (SST);
- Asphalt Pavement Analyzer (APA);
- Binder Consistency: Viscosity-Temperature Relationship;
- Simple Performance Test (SPT) – Repeated Load; and
- Dynamic Modulus (E*).

Superpave Shear Tester

In 1987, SHRP began a 5 year, $50 million study to address and provide solutions to the performance problems of HMA pavements in the United States (FHWA-SA-95-003, 1995). As part of the study, the Superpave Shear Tester (SST) was developed to become the performance test used in the mix design process. The initial testing required a total of 6 different tests (*AASHTO M-003, Determining the Shear and Stiffness Behavior of Modified and Unmodified Hot Mix Asphalt in the Superpave Shear Test*). The tests included:

1. Uniaxial
2. Hydrostatic
3. Repeated Shear at Constant Stress Ratio (RSCSR)
4. Frequency Sweep at Constant Height (FSCH)
5. Simple Shear at Constant Height (SSCH)
6. Repeated Shear at Constant Height (RSCH)

The first two tests, as well as the Simple Shear, were mainly used for modeling purposes within the Superpave modeling program. However, test complexities associated with

industry use resulted in eliminating the first three tests. The test now only utilizes the SSCH, FSCH, and RSCH modes (AASHTO TP7-01).

The SSCH test evaluates the creep properties of the asphalt mix under at varying (low to moderate) temperatures. The FSCH test evaluates the shear stiffness of the asphalt mix at varying (low to high) temperatures. The RSCH test evaluates the asphalt mixes ability to resist permanent deformation (rutting) at high temperatures.

The development and selection of the Superpave Shear Tester (SST) by the SHRP researchers was based on the device having the capability of measuring properties under states of stress that are encountered within the entire rutting zone of the pavement, particularly near the surface. Since there are an infinite number of states of stress that could exist within the pavement, it would be impossible to truly simulate all of them considering the non-linear and viscous behavior of HMA. Realizing this (Sousa et al., 1993) the SHRP researchers concentrated on the most important aspects and simulative conditions of the HMA behavior.

The following summary of factors which significantly affect the behavior of HMA was taken from the SHRP research product entitled, *Accelerated Performance-Related Tests for Asphalt-Aggregate Mixes and Their Use in Mix Design and Analysis Systems, SHRP-A-417.*

1. Specimen Geometry: a) A six inch by 2 inch specimen can easily be obtained from any pavement section by coring, or from any typical compaction method; b) the state of stress is relatively uniform for the loads applied; c) the magnitude of loads needed to be applied can easily be achieved by the use of normal hydraulic equipment.
2. Rotation of Principle Axis: The test set-up permits the controlled rotation of principal axes of strain and stress which represent the conditions that impact rutting.
3. Repetitively Applied Loads: Work by the SHRP researchers has indicated that to accurately capture the rutting phenomena, repetitive loads are required. This type of loading is needed given the viscous nature of the binder (load frequency dependent) and also granular nature of the aggregate (aggregates behave differently under static and dynamic loading).
4. Dilation: As discussed earlier, the dilation plays an important role in the rutting behavior of HMA. The SST constrains the dilation, and by doing so, confining stresses are developed. It is in part due to the development of these confining stresses that a mix derives most of its stability against rutting. The SST allows this by implying a constant height on the specimen while under going a shear stress. In the constant height regime, the development of axial stresses (confining stress in the SST) is fully dependent on the dilatency characteristics of the HMA. A vertical LVDT is positioned on the specimen to measure the dilation. This in turn props the axial actuator to either create a compressive or tensile force on the sample, depending on the volume change characteristic of the specimen. In this configuration, the HMA will either resist permanent deformation by relying on

the high binder stiffness to minimize shear strains or the aggregate structure stability developed by the axial stresses from the dilation. In the constant height test, these two mechanisms are free to fully develop their relative contribution to the resistance of permanent deformation.

Figure 2 is an illustration of the SST device with an asphalt sample ready for testing.

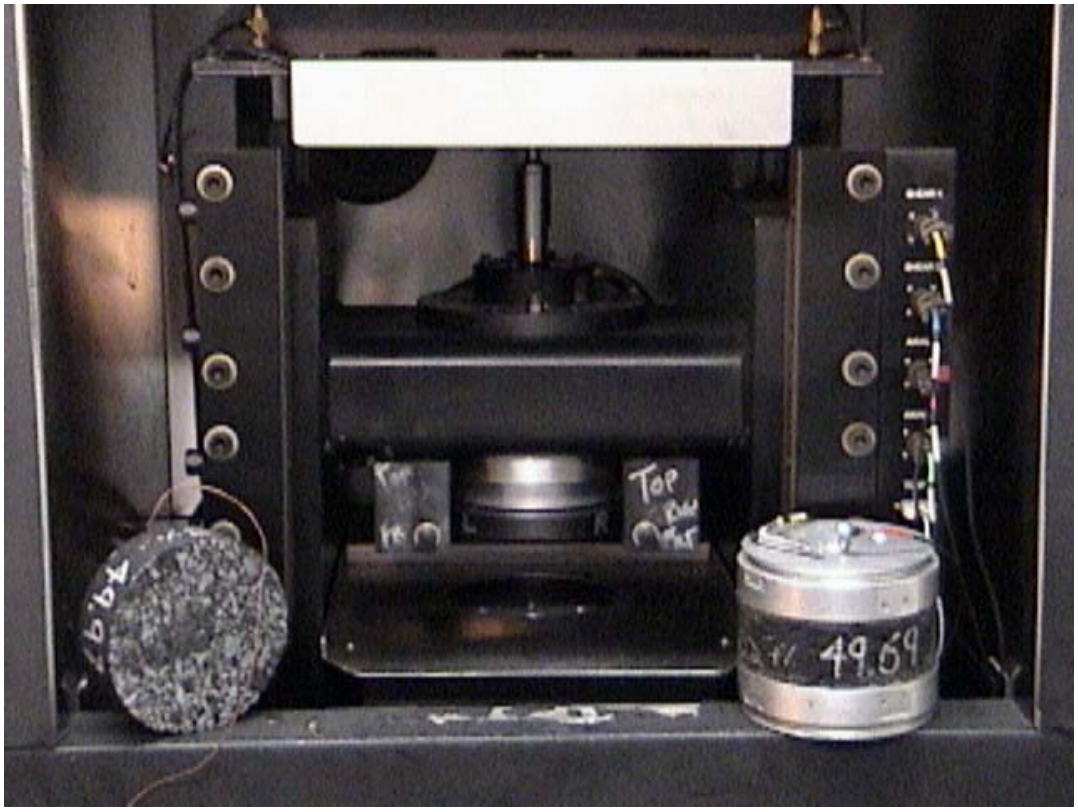

Figure 2 – Superpave Shear Tester (SST) at the Rutgers Asphalt/Pavement Laboratory

Asphalt Pavement Analyzer (APA)

The APA is a second-generation loaded wheel tester (Figure 3 and Figure 4). It has the capability of testing compacted brick or pill samples under various environmental conditions in both rutting (high temperature permanent deformation) and fatigue (low temperature cracking). The device can also be linked to a computer and data acquisition system so the user can measure the rutting of the HMA for each load cycle.

Figure 3 – Asphalt Pavement Analyzer

The moving wheel load is applied at a rate of about one cycle per second to a ¾ inch pressurized hose that rests atop the HMA samples. This simulates (on a small scale) the traffic loading that typically occurs in the field. However, as to date, there have been no successful attempts at directly comparing the results of the APA to actual rutting in the field. Therefore, the major use of the device is as a comparative tool for mixture selection (i.e. one would select the mix that ruts the least from the APA testing).

The APA is typically run at a test temperature of 64^{o}C. The samples are conditioned under this temperature for minimum of 4 hours prior to testing. The loading configurations typically used within the APA are a wheel load of 100 lbs and a hose pressure of 100 psi, although some other researchers have had success with increased loads and pressures (Williams and Prowell, 1999). Both the APA User's

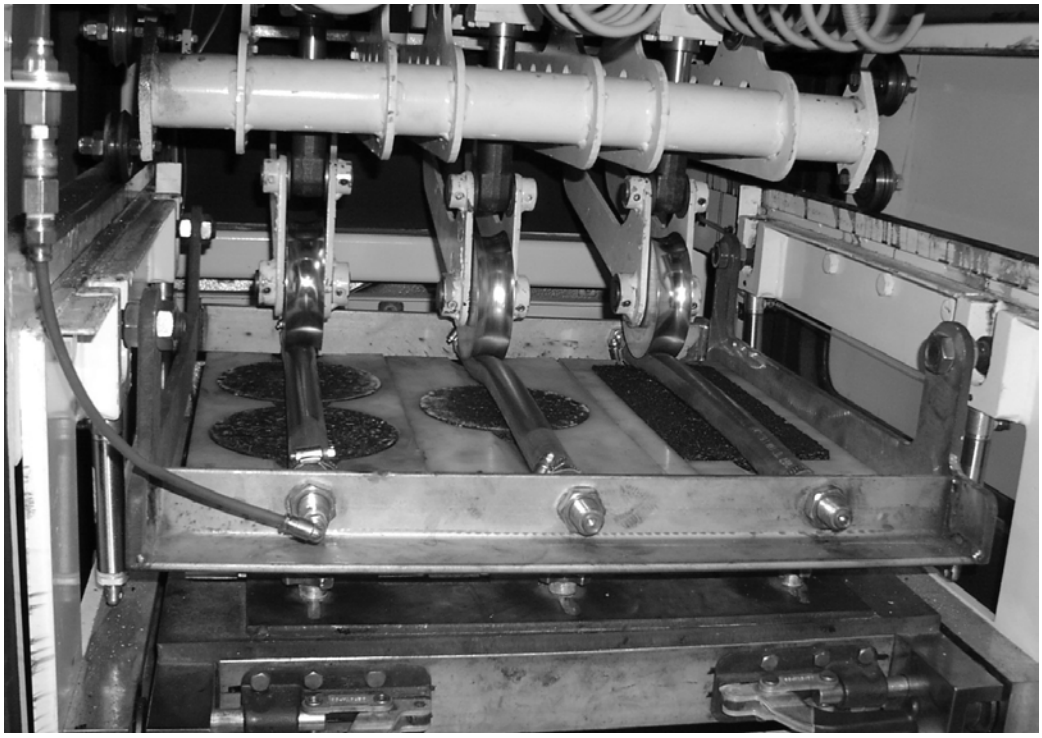

Figure 4 – Looking Inside the APA

Group (2000) and the National Center for Asphalt Technology (Kandhal and Cooley, 2002) have recommended using 100 psi hose pressure with 100 lbs wheel load. Once conditioned, the samples under-go a 25 cycle seating load. Once the 25 cycles have completed, the initial rut depths are measured. Testing then usually continues until a minimum of 8,000 cycles are completed. The difference between the initial and final rut depth measurements is calculated as the APA rut depth.

Binder Consistency Test – Viscosity Temperature Relationship

Experience by Witczak et al. (2000) has shown that conventional/standard asphalt binder consistency testing, such as the Brookfield Rotational Viscometer, can be used as a general guide for the material's performance and potential for age hardening. The testing procedure uses 4 test temperatures in the range of 200 to 350^{o}F. The viscosity measurements are used to obtain a viscosity (η) – temperature (T_R) relationship from the following regression equation:

$$\log\log\eta = A_i + VTS_i \log T_R \qquad (1)$$

where,

η = viscosity in centi-Poise (cP)
T_R = test temperature in Rankine
A_i = intercept of the regression equation
VTS_i = slope of the regression equation, called the Viscosity Temperature Susceptibility parameter

In general, a larger (more negative) slope value indicates the asphalt binder viscosity is more susceptible to change due to changes in temperature. An asphalt binder that is less susceptible to change will tend to have a greater working temperature range. The A_i and VTS_i parameters are currently used for both the Witczak Dynamic Modulus Predictive equation and asphalt aging models in the 2002 Mechanistic Design Guide.

Dynamic Modulus (E*)

Some of the following discussion of the dynamic modulus test was taken from Kaloush et al. (2002).

For linear elastic materials, such as hot mix asphalt, the stress to strain relationship under a continuous sinusoidal loading is defined by a complex number called the complex modulus (ASTM D3497). The complex modulus has a real and an imaginary part that defines the elastic and viscous behavior of the linear, visco-elastic material. The absolute value of the complex modulus is called the dynamic modulus. Mathematically, the dynamic modulus is defined as the maximum (peak) dynamic stress (σ_o) divided by the peak recoverable axial strain (ε_o), as shown as equation (2).

$$E^* = \frac{\sigma_O}{\varepsilon_O} \qquad (2)$$

The dynamic modulus testing of asphalt materials is commonly conducted on unconfined cylindrical specimens (Figure 5) having a height to diameter ratio equal to 1.5 and uses a uniaxially applied sinusoidal (haversine) stress pattern (Figure 6). Under this loading regime, the sinusoidal stress at any given time, t, can be defined as:

$$\sigma_t = \sigma_O \sin(\omega t) \qquad (3)$$

where,

σ_O = peak dynamic stress amplitude;
ω = angular frequency in radian per second; and
t = time (second)

The resultant dynamic strain at any given time is given by:

$$\varepsilon_t = \varepsilon_O \sin(\omega t - \phi) \qquad (4)$$

where,

ε_O = recoverable strain (in/in)
ϕ = phase lag or angle (degrees)

Figure 5 – HMA Sample Instrumented for the Dynamic Modulus Test

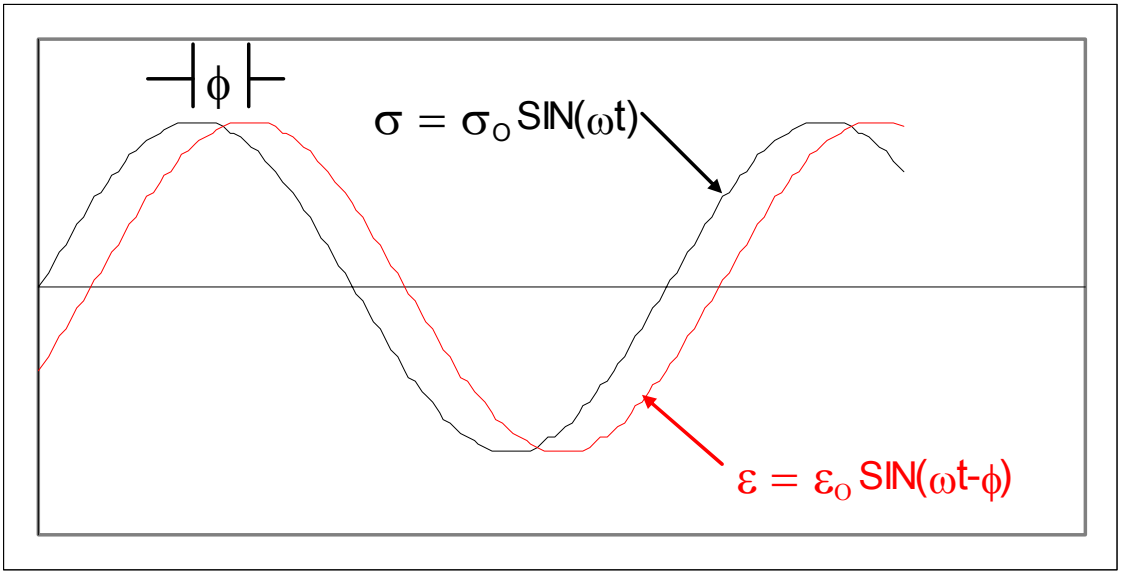

Figure 6 – Sinusoidal Stress Wave Form Applied During the Dynamic Modulus Test

The phase angle is simply the angle at which the ε_O lags σ_O and is an indicator of the viscous or elastic properties of the material being evaluated. For pure elastic material, $\phi = 0^o$. This condition would occur at very low temperatures for asphalt materials. For pure viscous materials, $\phi = 90^o$. This condition would occur at very high temperatures for asphalt materials.

The dynamic modulus test protocol utilizes 5 test temperatures (10, 40, 70, 100, and 130^{o}F) and 6 loading frequencies (25, 10, 5, 1, 0.5, and 0.1 Hz). This provides an evaluation of the material's stiffness over a wide range of temperature (low to high) and loading (fast to slow) conditions. The loading is conducted within a strain range of 50 to 150 micro-strains to ensure the material properties are within a linear-elastic state.

The dynamic modulus parameters are also used as a means of evaluating the rutting potential of the HMA materials. Research by Witczak et al. (2002) has shown that the use of the dynamic modulus divided by the sin of the phase angle, $E^*/\sin\phi$, was a good indicator of rutting susceptibility. The greater the parameter, the less susceptible the asphalt material was to rutting. The value is determined at the test temperature of 130^{o}F and a loading frequency of 5 Hz.

Dynamic Repeated Load - Permanent Deformation Test

One of the more traditional means of evaluating the rutting potential of asphalt materials is to subject a specimen to a repeated dynamic load for several thousand repetitions and measure the cumulative permanent deformation. This approach was first used by Monismith et al. (1975) in the 1970's using uniaxial compression tests. Later research conducted by Witczak et al. (2002) used test temperatures of 100 and 130^{o}F and loading stresses of 10, 20,and 30 psi for an unconfined specimen. The approach by Witczak et al. (2002) has since been adopted as a potential test procedure to determine rut susceptible asphalt mixes after the Superpave mix design is complete.

Figure 7 shows the typical relationship between the total cumulative plastic strain (permanent) and the number of loading cycles. The cumulative plastic strain is generally divided into three zones; primary, secondary, and tertiary. In the primary zone, the permanent deformation occurs rapidly, mostly due to compaction of air voids. The permanent strain decreases to a rate which remains constant in the secondary zone. Finally, the rate of permanent strain again increases and accumulates rapidly in the tertiary zone. The starting point, or loading cycle number, at which the tertiary flow occurs is referred to as the flow number.

One of the main advantages of using the repeated load permanent deformation test is that the parameters derived from the data can be used to "material-specific" calibrate the HMA rutting model that is included in the 2002 Mechanistic Pavement Design Guide.

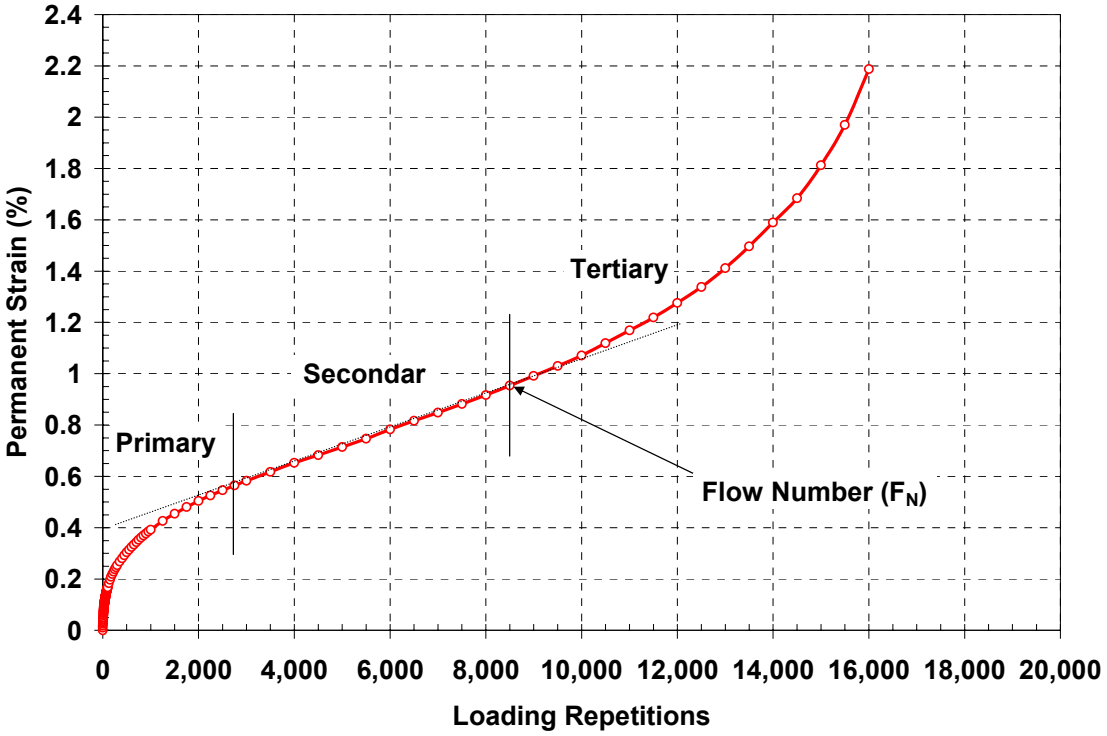

Figure 7 – Typical Relationship Between Total Cumulative Permanent Deformation and Number of Loading Cycles

TEST RESULTS

Superpave Shear Tester (SST)

The testing conducted in the SST involved Simple Shear, Frequency Sweep, and Repeated Shear at Constant Height. The tests were conducted at the following test temperatures:

- Simple Shear at Constant Height (SSCH): 4, 20, and 40°C
- Frequency Sweep at Constant Height (FSCH): 4, 20, 40, and 64°C
- Repeated Shear at Constant Height (RSCH): 64°C

All results are an average of triplicate samples. Individual sample results for the SST testing are located in Appendix A (SSCH), Appendix B (FSCH) and Appendix C (RSCH).

Simple Shear at Constant Height (SSCH)

SSCH Test Background

The SSCH test is a shear-loaded creep test. The specimen is loaded at a stress rate of 70 kPa/sec until a pre-determined creep load is obtained. The creep load is based on the

temperature for which it is tested. The creep loads used in this study conform to those recommended in AASHTO TP7-01 Test Procedure B, and are; 345 ± 5 kPa for 4°C, 105 ± 5 kPa for 20°C, and 35 ± 5 kPa for 40°C. The creep load is applied for 10 seconds and then the load is reduced to zero at a rate of 25 kPa/sec. Once the stress reaches zero, the shear strain is measured for another 10 seconds. The test is complete after these final 10 seconds at zero stress.

AASHTO TP7-01, Test Procedure B, recommends the calculation of the maximum shear strain that occurs during the test and also the permanent shear strain at the end of the test. Therefore, these two parameters were used in the evaluation of the HMA. However, one other parameter was also evaluated from the SSCH test, called the SSCH creep slope.

To determine the SSCH creep slope, the data from the creep load portion of the SSCH test is extrapolated and used as an evaluation parameter. The data focuses on the shear strain that occurs only when the creep load is constant. The results for each sample for the particular temperature tested is plotted along side one another for analysis. This type of analysis is similar to the creep compliance test. Once isolated, the slope of the SSCH creep curve is determined by using a linear regression relationship. Although the SSCH creep curves are not a straight line, by fixing the linear regression to the origin, only one regression constant is determined and can be used for a direct comparison. The R^2 value (coefficient of correlation) for each of the regressions is typically greater than 0.85, indicating that even by using the fixed linear regression, a good correlation is able to be achieved.

The SSCH is not commonly used for this type of analysis; however, the creep performance of the mix would surely be changed if some type of modifier has been applied to the asphalt binder. Work conducted by Buncher et al. (2000) recommended using the SSCH to estimate a mixture's susceptibility to permanent deformation since the test measures the mixes ability to resist shear strain. Lytton et al (1993) also used the creep compliance test to predict fatigue-cracking and low-temperature cracking. So, although the SSCH and the creep compliance test are performed differently, the creep information from both tests can be an important indicator of performance.

SSCH Test Results

The SSCH test procedure was conducted at 4, 20, and 40°C to evaluate the creep properties of the baseline and AR-HMA mixes. The SSCH curves are shown as Figure 8, 9, and 10 for 4, 20, and 40°C, respectively. At lower temperatures, longer life materials will achieve higher creep strains. Higher creep strains at low temperatures are needed to ensure that flexibility is maintained. Materials with high stiffness (low flexibility) at low temperatures will be susceptible to cracking at low temperatures. In contrast, at higher temperatures, HMA materials need to be able resist creep (lower creep strains) to aid in minimizing permanent deformations due to traffic loading.

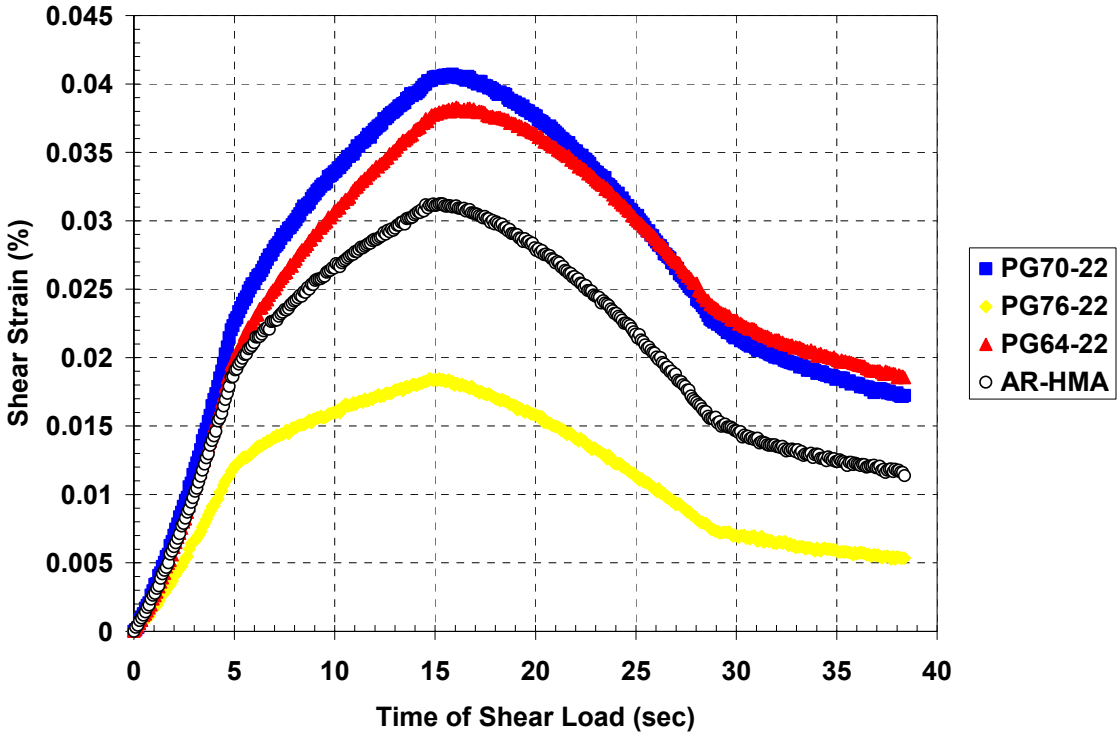

Figure 8 – SSCH Test Results Conducted at a Test Temperature of 4°C

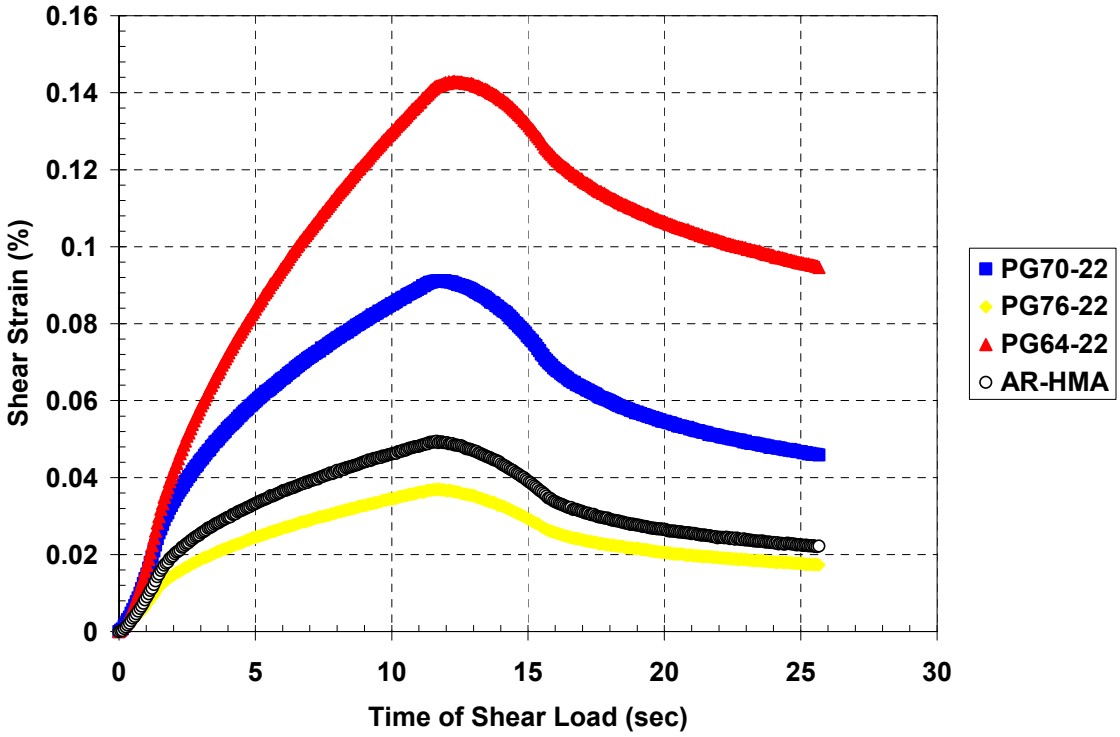

Figure 9 – SSCH Test Results Conducted at a Test Temperature of 20°C

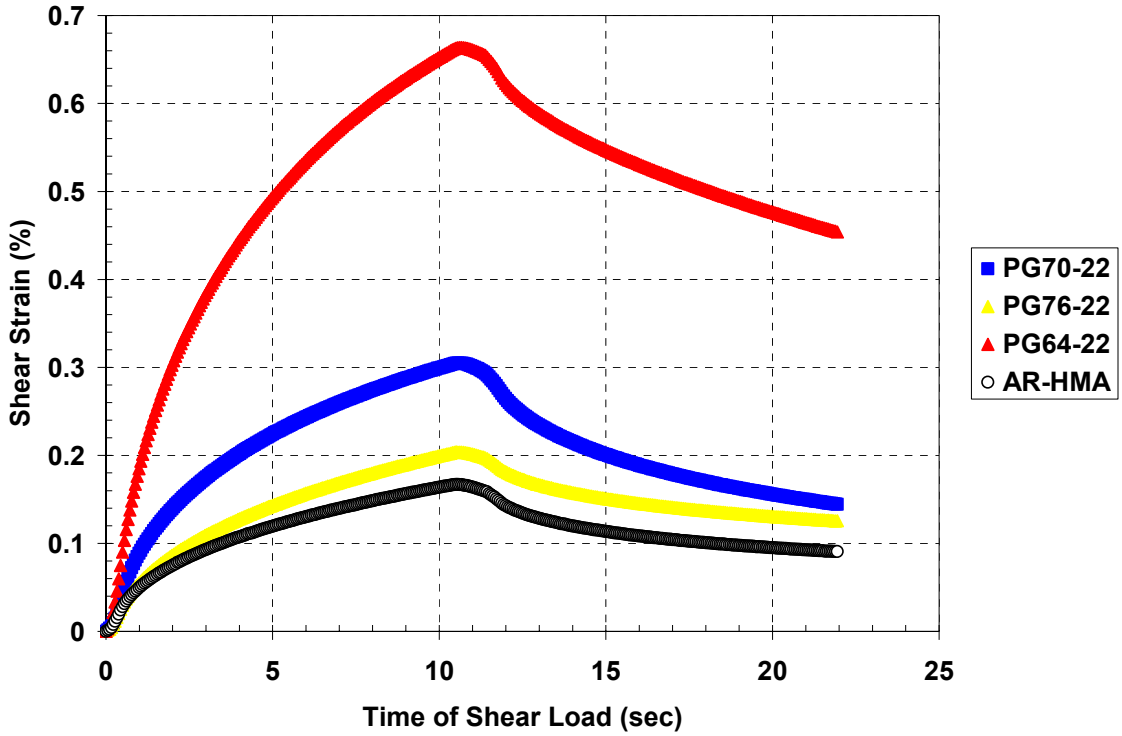

Figure 10 – SSCH Test Results Conducted at a Test Temperature of 40°C

The SSCH test results conducted at 4°C indicate that the AR-HMA material allows for greater creep straining than the PG76-22, however, both the PG64-22 and the PG70-22 were able to obtain larger creep strains at 4°C. Meanwhile, at the high temperature of 40°C, the AR-HMA material obtained the lowest creep strain. Therefore, based on the SSCH curves, the AR-HMA was able to provide flexibility at low temperatures while minimizing creep strain at the higher test temperature.

Three parameters are typically used to further compare the SSCH test results;
1) Maximum creep strain (ε_{MAX}), 2) Permanent creep strain (ε_{PERM}), and 3) Creep slope. The maximum creep strain is largest amount of creep strain obtained during the test. The permanent creep strain is the remaining creep strain in the sample after the creep load has been released. The creep slope is the slope of the creep strain vs time plot when isolating the strain produced by the creep load. In the SSCH test, the load is ramped up to obtain a constant load. Therefore, not all of the strain is due to a constant load. In addition, to only evaluate the strain associated with a constant load, the creep strain pertaining to only the time at which the applied load is constant is isolated for analysis. Figure 11, 12 and 13 show the isolated creep slope curves for the 4, 20, and 40°C test temperatures, respectively. Table 2 summarizes the data for the maximum creep strain, permanent creep strain and the creep slope.

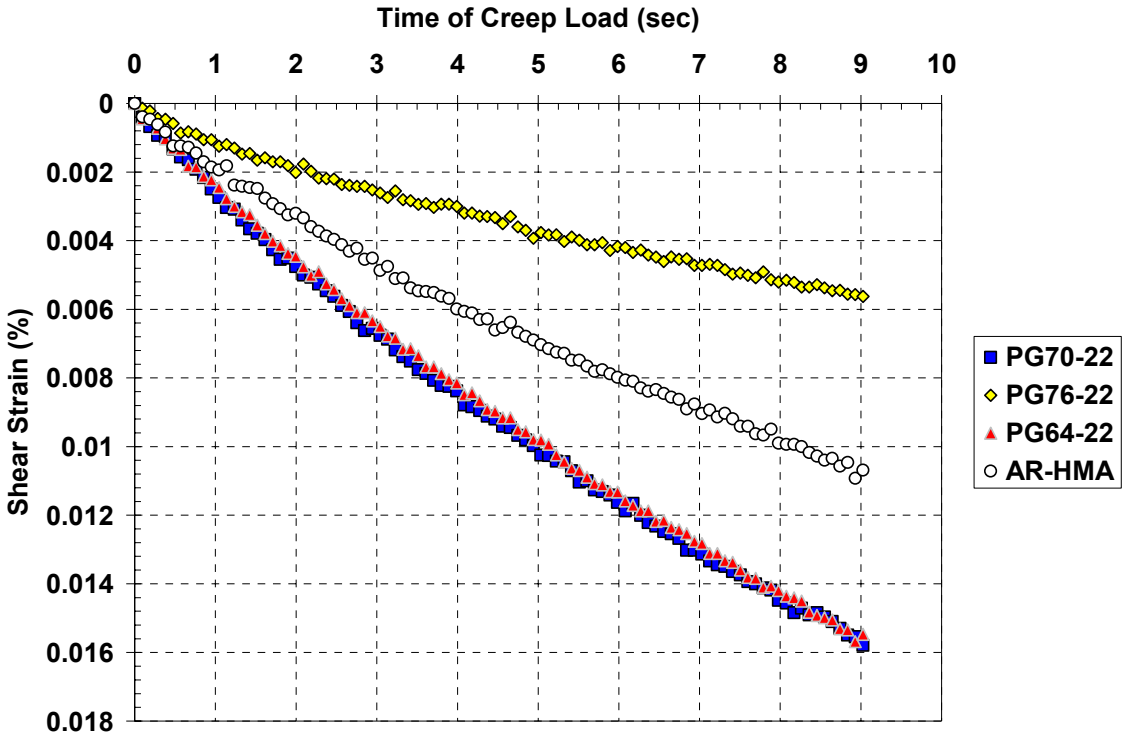

Figure 11 – SSCH Creep Slope Plots for 4°C

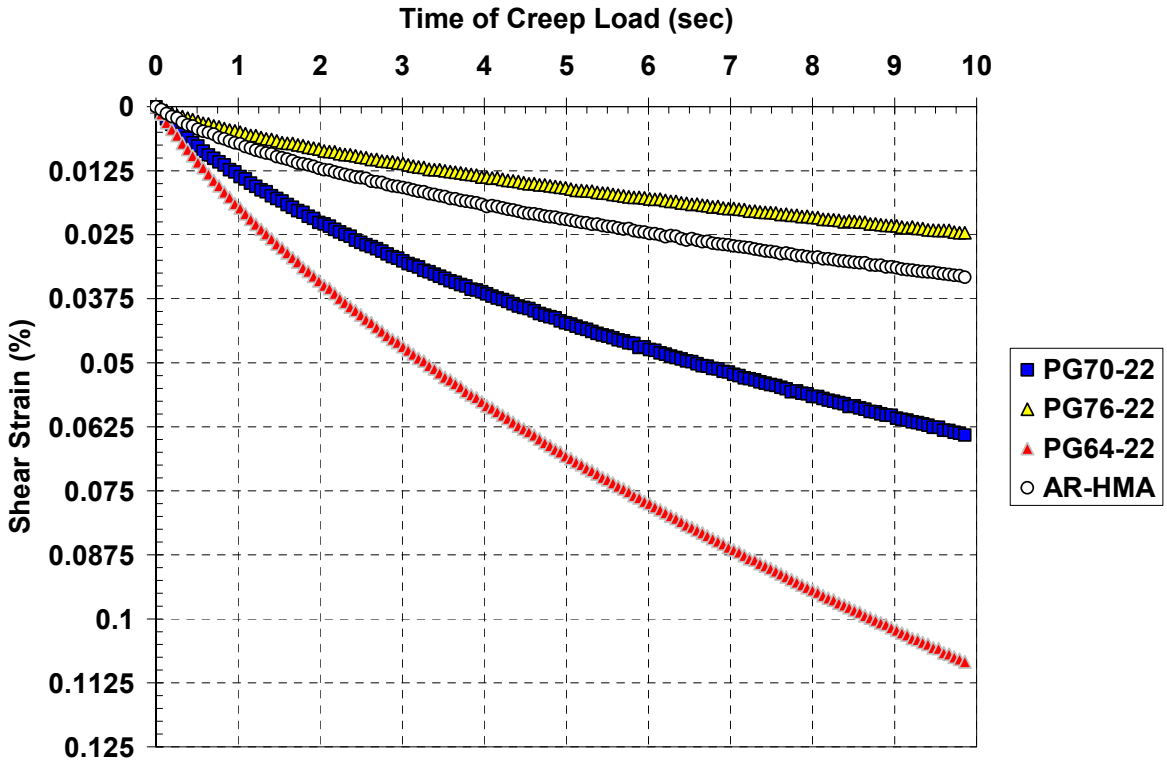

Figure 12 – SSCH Creep Slope Plots for 20°C

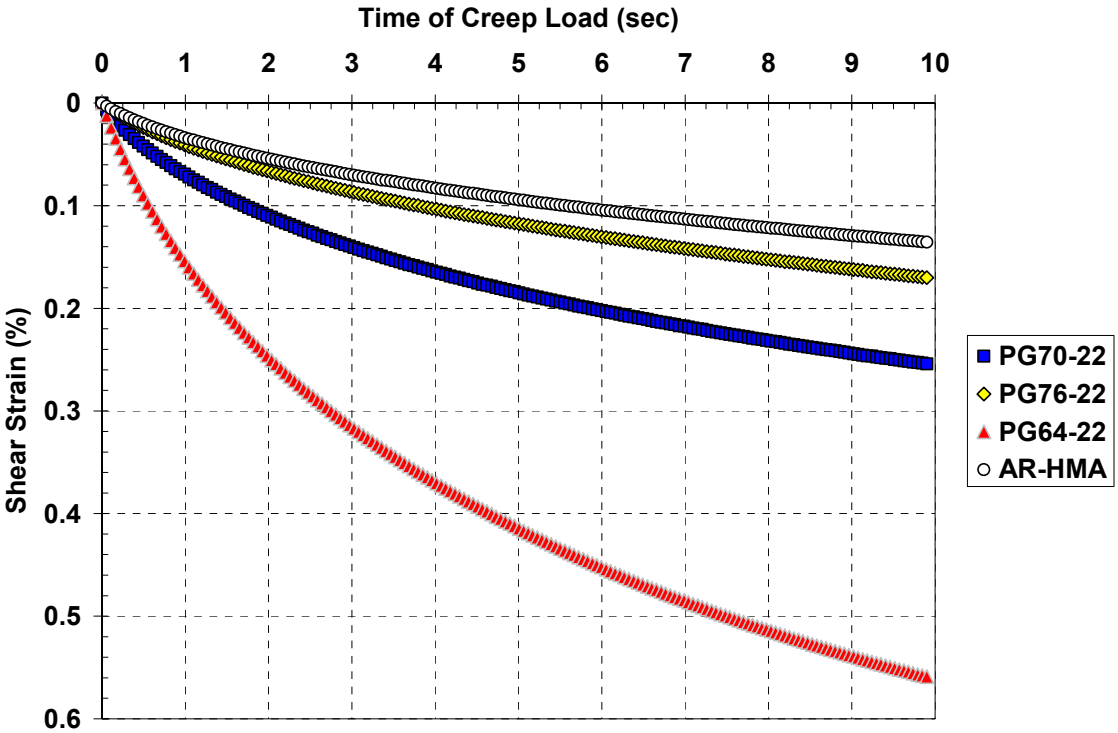

Figure 13 – SSCH Creep Slope Plots for 40°C

Table 2 – SSCH Test Results

Material Type	Temperature (°C)	ε_{MAX} (%)	ε_{PERM} (%)	Creep Slope (%/sec)
PG64-22	4	0.0383	0.0185	0.0019
PG70-22		0.407	0.0172	0.0019
PG76-22		0.185	0.0054	0.0007
AR-HMA		0.0313	0.0114	0.0013
PG64-22	20	0.143	0.0946	0.0123
PG70-22		0.0911	0.0459	0.0074
PG76-22		0.0371	0.0173	0.0028
AR-HMA		0.0495	0.0222	0.0039
PG64-22	40	0.6636	0.454	0.0692
PG70-22		0.3051	0.1446	0.0311
PG76-22		0.204	0.1256	0.0202
AR-HMA		0.167	0.0907	0.0162

In analyzing the results in Table 2, the better performing materials will have larger ε_{MAX} and creep slopes at 4°C and have smaller ε_{MAX} and creep slopes at 40°C. Both the PG64-22 and PG70-22 performed equally well at 4°C, although the AR-HMA was comparable. Meanwhile, the AR-HMA performed the best at 40°C with the PG76-22 being somewhat comparable to the AR-HMA.

Summary of the SSCH Test Results

The Simple Shear at Constant Height measures the creep performance of the HMA material. For an HMA material to provide a long-life pavement system, the creep properties of the HMA should behave in a manner to resist the temperature dependent distress. For example, at low temperature, the HMA material should allow creep to occur so as not to promote cracking. However, at high temperature, the HMA material should limit the amount of creep to aid in resisting permanent deformation.

The SSCH test results indicate that the AR-HMA allows for creep to develop at lower test temperatures, comparable to the PG64-22 and PG70-22 and more than the PG76-22. The AR-HMA also limits the amount of creep at high temperatures, lower than that of the PG76-22 and much lower than the PG64-22 and PG70-22.

Evaluation of Age Hardening

Simple Shear Results

Work conducted by Bell et al. (1994) has shown that curing the compacted asphalt sample in an oven for eight days at 85°C models field aging for:

- 9 years of dry-freeze weather, or
- 18 years of wet-no freeze weather

This procedure is termed Long-Term Oven Aging (LTOA) and is commonly performed to evaluate an asphalt's tendency to develop age hardening. The natural aging of the asphalt increases the potential for cracking since the material becomes more brittle.

To evaluate the potential for age hardening, the creep properties from the Superpave Shear Tester's Simple Shear test were determined for the LTOA samples and compared to the STOA samples. A test temperature of 4°C was used since the potential for cracking is more common at lower temperatures. The results of the Simple Shear tests are shown in Figures 14 to 17.

The results clearly indicate a decrease in the creep deformation in the PG64-22 and PG70-22 samples. There is also a decrease in the creep deformation for the PG76-22 sample, but not as severe as the other baseline mixes. The results also show that there is no decrease in creep deformation for the AR-HMA sample, indicating that the material did not undergo age hardening as severe as the other mixes.

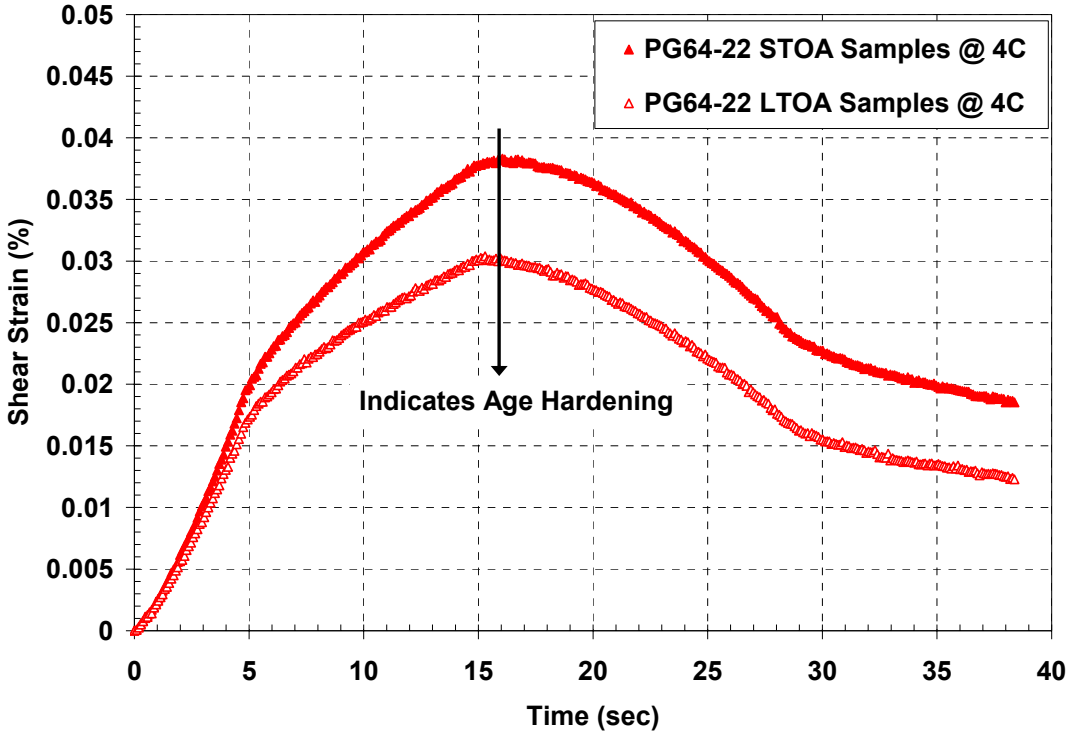

Figure 14 – Simple Shear Results for Aged (LTOA) and Unaged (STOA) PG64-22 Samples

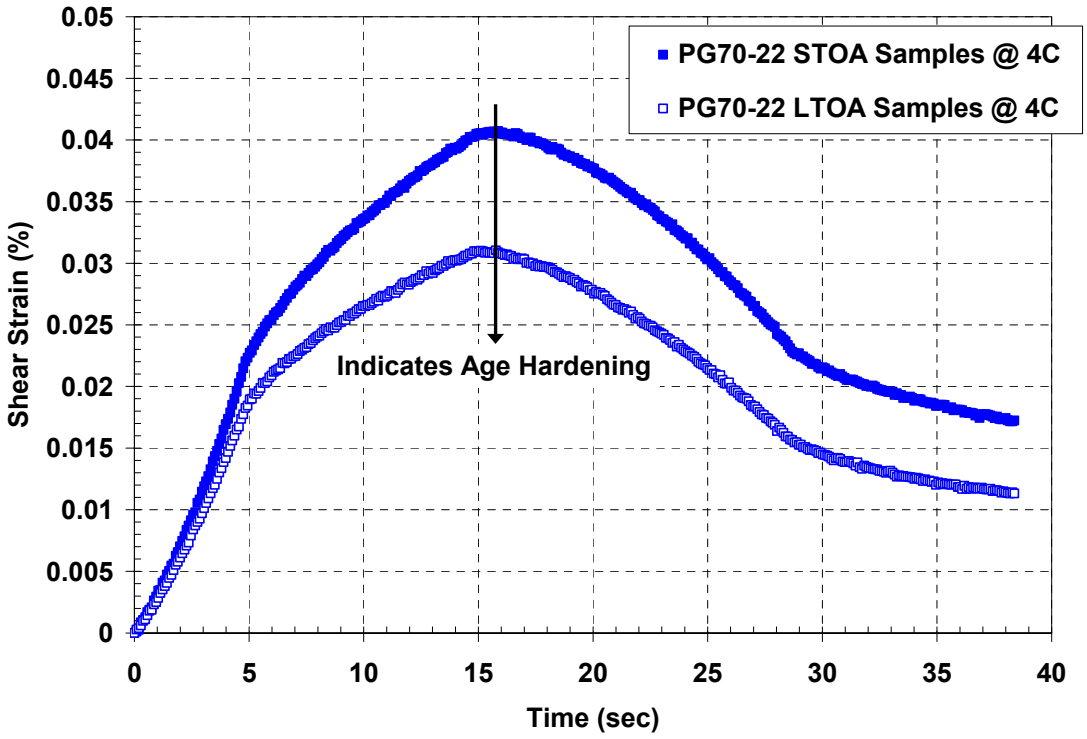

Figure 15 - Simple Shear Results for Aged (LTOA) and Unaged (STOA) PG70-22 Samples

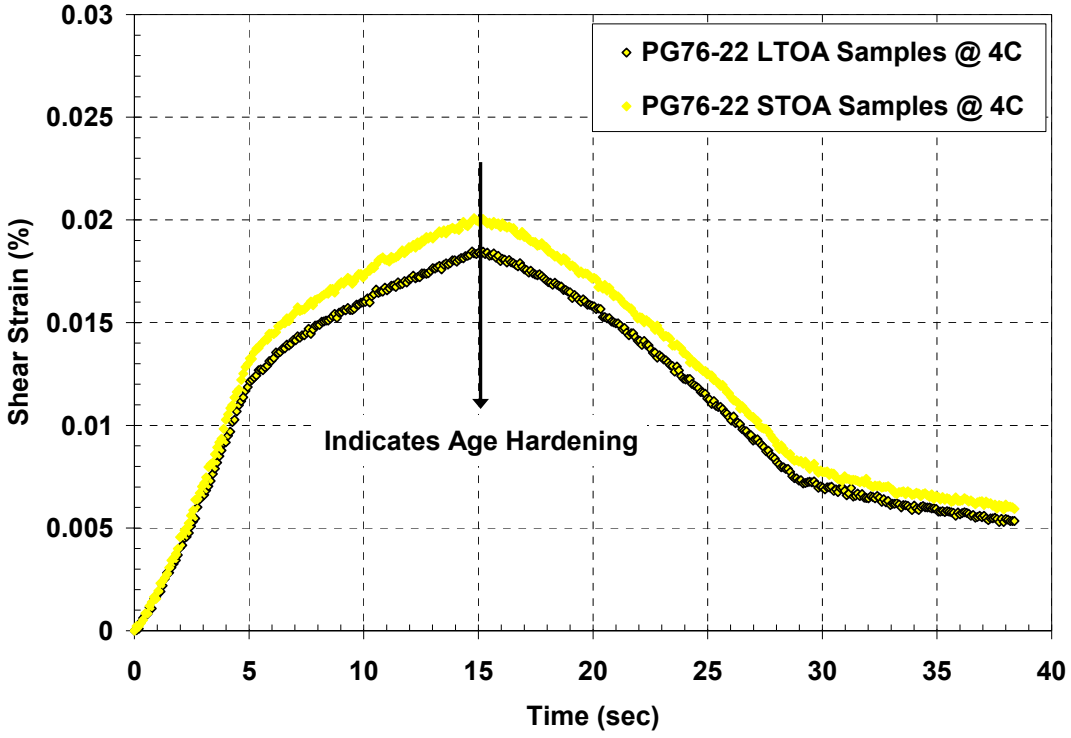

Figure 16 - Simple Shear Results for Aged (LTOA) and Unaged (STOA) PG76-22 Samples

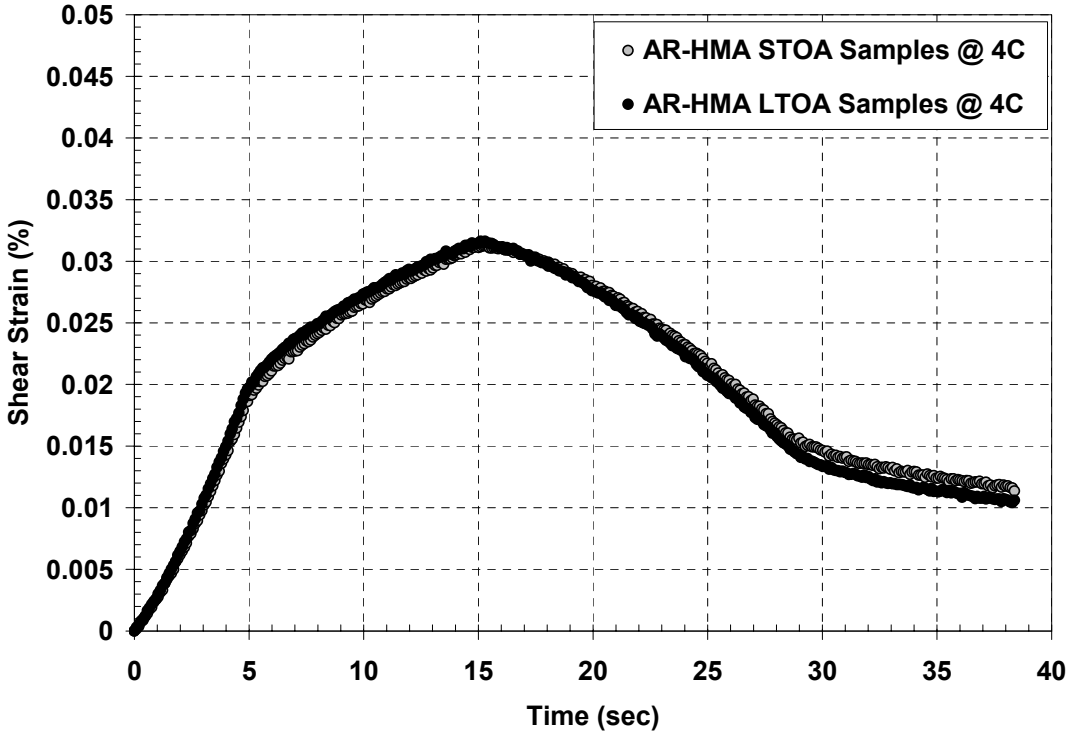

Figure 17 - Simple Shear Results for Aged (LTOA) and Unaged (STOA) AR-HMA Samples

Table 3 shows the results of the maximum shear strain of the LTOA and STOA samples. It also includes the % of LTOA to STOA. The lower the value, the more hardened the material was due to the laboratory aging. The table clearly shows the effect of aging on the PG64-22 and PG70-22 mixes.

Table 3 – Maximum Shear Strain Ratio (MSSR) for LTOA and STOA Simple Shear Samples

	Maximum Shear Strain (%)		
Mix Type	LTOA	STOA	MSSR
PG64-22	0.03	0.038	79.3 %
PG70-22	0.031	0.041	76.3 %
PG76-22	0.02	0.018	91.9 %
AR-HMA	0.032	0.031	101.1 %

Frequency Sweep at Constant Height (FSCH)

Background of FSCH

The FSCH test procedure was conducted at 4, 20, 40, and 64°C. At each test temperature, a strain-controlled sinusoidal wave-form is applied at a loading rate of 10, 5, 2, 1, 0.5, 0.2, 0.1, 0.05, 0.02, and 0.01 Hz. The sample is loaded to achieve a shear strain of 100 micro-strain. From this, the dynamic shear modulus and the phase angle are determined.

Mathematically, the dynamic shear modulus is defined as the maximum (peak) dynamic shear stress (τ_o) divided by the peak recoverable shear strain (γ_o), as shown as equation (5).

$$G^* = \frac{\tau_O}{\gamma_O} \quad (5)$$

Under this loading regime, the sinusoidal shear stress at any given time, t, can be defined as:

$$\tau_t = \tau_O \sin(\omega t) \quad (6)$$

where,

τ_O = peak dynamic shear stress amplitude;
ω = angular frequency in radian per second; and
t = time (second)

The resultant dynamic shear strain at any time is given by:

$$\gamma_t = \gamma_O \sin(\omega t - \phi) \quad (7)$$

where,

γ_O = recoverable strain (in/in)
ϕ = phase lag or angle (degrees)

The phase angle is simply the angle at which the γ_O lags τ_O and is an indicator of the viscous or elastic properties of the material being evaluated. For pure elastic material, $\phi = 0^o$. This condition would occur at very low temperatures for asphalt materials. For pure viscous materials, $\phi = 90^o$. This condition would occur at very high temperatures for asphalt materials.

Both the dynamic shear modulus (G*) and the phase angle (ϕ) can be used to evaluate the performance of the HMA material at different test temperatures. For example, when comparing the performance at low temperatures, an engineer would prefer an HMA material to obtain a lower G* and a higher ϕ. This would be an indication of lower stiffness. Lower stiffness at low temperatures would aid in minimizing fatigue cracking. Meanwhile, when comparing materials at high temperatures, an engineer would prefer that the HMA material obtain a higher G* and a lower ϕ. This would indicate a stiffer material. A stiffer HMA at high temperatures would aid in resisting permanent deformation.

After the sample has been tested over a range of temperatures, a master stiffness curve can be developed. The master stiffness curve of HMA allows for the comparison of visco-elastic materials when testing has been conducted using different loading frequencies and temperatures. The master curve can be constructed using the time-temperature superposition principle. This principle suggests that the temperature and loading frequency of visco-elastic materials are interchangeable.

The data from the FSCH tests can be "shifted" relative to the time of the frequency, so that the various curves can be aligned to form a single "master curve" (Pellinen, 2001). The shifting is theoretically allowed because the HMA material will act differently under the loading frequency and temperature. What actually occurs is that a G* at a temperature of 40°C and a loading frequency of 5 Hz may equal the G* at a temperature of 20°C and a loading frequency of 0.5 Hz. An example of this from work conducted at RAPL is shown as Figure 18.

Figure 18 shows the results of FSCH tests conducted at 20, 40, 52, and 64°C on a coarse Superpave mix with a PG64-22 asphalt binder. As can be seen from the figure, the same shear modulus (G*) value can be achieved at different temperatures and at different frequencies. The G* value of 4,000 psi was marked on the figure. This value for temperatures of 40, 52, and 64°C corresponds to approximate loading frequencies of 0.065, 1, and 5.5 Hz, respectively.

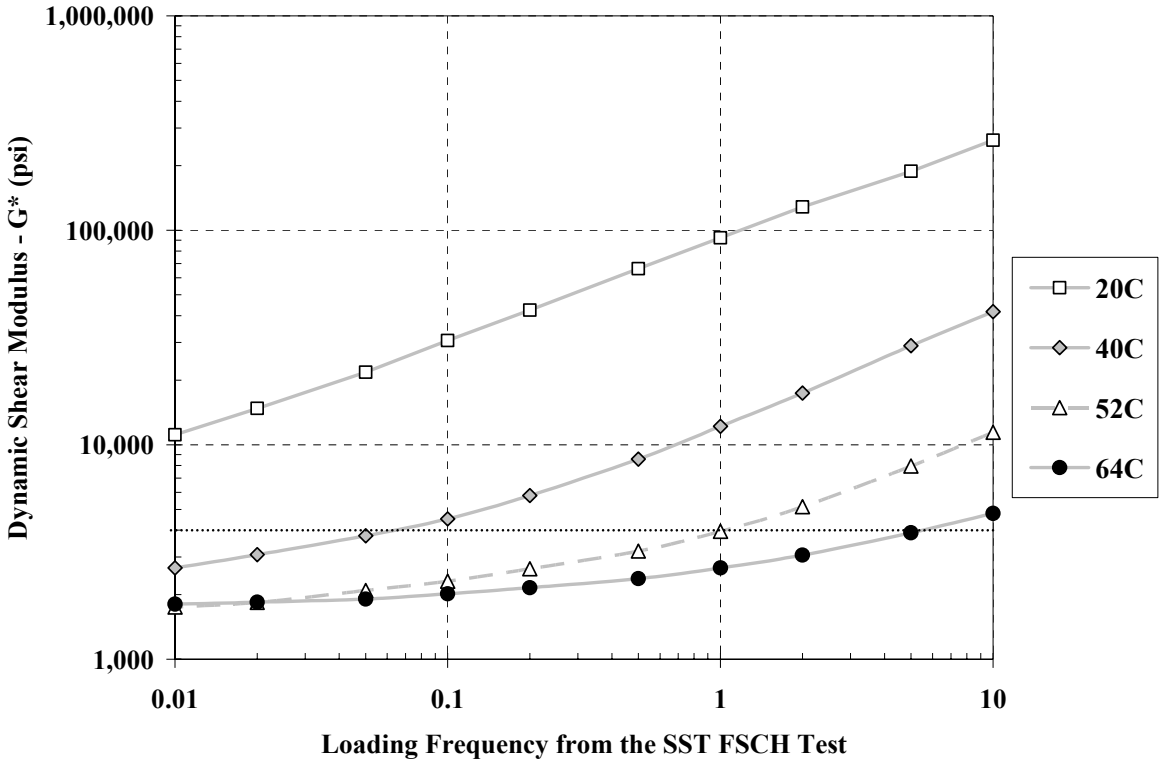

Figure 18 – FSCH Results from Testing Conducted at RAPL

The "shifting" of the curves necessitates the determination of a "shifting factor". The shift factor, a(T), defines the required shift at a given temperature (i.e. a constant by which the frequency must be multiplied or divided by to get an increased or reduced frequency (t_r) for the master curve (equation 8).

$$t_r = \frac{t}{a(T)} \quad \text{or} \quad t\left[a(T)\right] \tag{8}$$

The master curve can be developed using any arbitrarily selected reference temperature to which all of the data are fitted. For a more detailed explanation of the time-temperature superposition principle, refer to Painter and Coleman (1997).

A new method for developing master curves of HMA mixtures was utilized in this report. This method was developed at the University of Maryland (Pellinen, 1999). In this method, the master curves are constructed by fitting a sigmoidal function to the measured dynamic modulus test data using a non-linear least squares regression procedure. The shifting factors, a(T), are solved using the VTS shifting technique developed by Andrei et al. (1999). The formulation of the VTS shifting is based on the viscosity and temperature relationship. For unaged binders, the viscosity at the temperature of interest can be determined from the viscosity temperature relationship discussed earlier. The determination of the shifting factors using the VTS approach is shown in equation (9).

$$\log a(T) = C\left(10^{A+VTS[\log(T_R)]} - 10^{A+VTS[\log(T_R)_O]}\right) \quad (9)$$

where,

C = constant
T_R = temperature, °Rankine
$(T_R)_O$ = reference temperature, °Rankine
A = regression intercept, and
VTS = regression slope of the Viscosity Temperature Susceptibility

The fitting function for the master curve construction is defined by equation (10).

$$y = \delta + \frac{\alpha}{1 + \exp^{(\beta - \gamma x)}} \quad (10)$$

where,

y = criterion variable (predicted value of modulus)
δ = location parameter for y (minimum value for modulus)
α = range of possible values to be added to the minimum modulus
β/γ = location parameter for the x corresponding to y = d + a/2
x = predictor variable (loading frequency)

The master curve is then constructed using the Solver Function in the Excel spreadsheet. Figure 19 illustrates the master curve developed based on the data in Figure 18 when shifted to 52°C.

FSCH Test Results

The test results for the FSCH conducted at 4, 20, 40, and 64°C are shown in Figure 20. The results are the average of triplicate samples. Individual sample results can be found in Appendix A.

The test results shown in Figure 20 indicate the following:

- The AR-HMA samples tested at 4°C had the lowest stiffness at the highest loading frequencies. This is important because at low temperatures and high loading frequencies (faster vehicle speeds), the asphalt pavement is susceptible to cracking. Having a less stiff HMA at this condition will aid in minimizing the potential for cracking.
- The AR-HMA had the highest stiffness at the highest test temperatures, especially when comparing the low frequencies. Permanent deformation of HMA pavements is most common at high temperature and low vehicle speeds (or low loading frequency). Therefore, to ensure that an HMA material will aid in minimizing rutting, the material should provide a higher stiffness at high temperatures and low loading frequencies. It is even more impressive to see how much additional shear stiffness at high temperatures is provided when adding

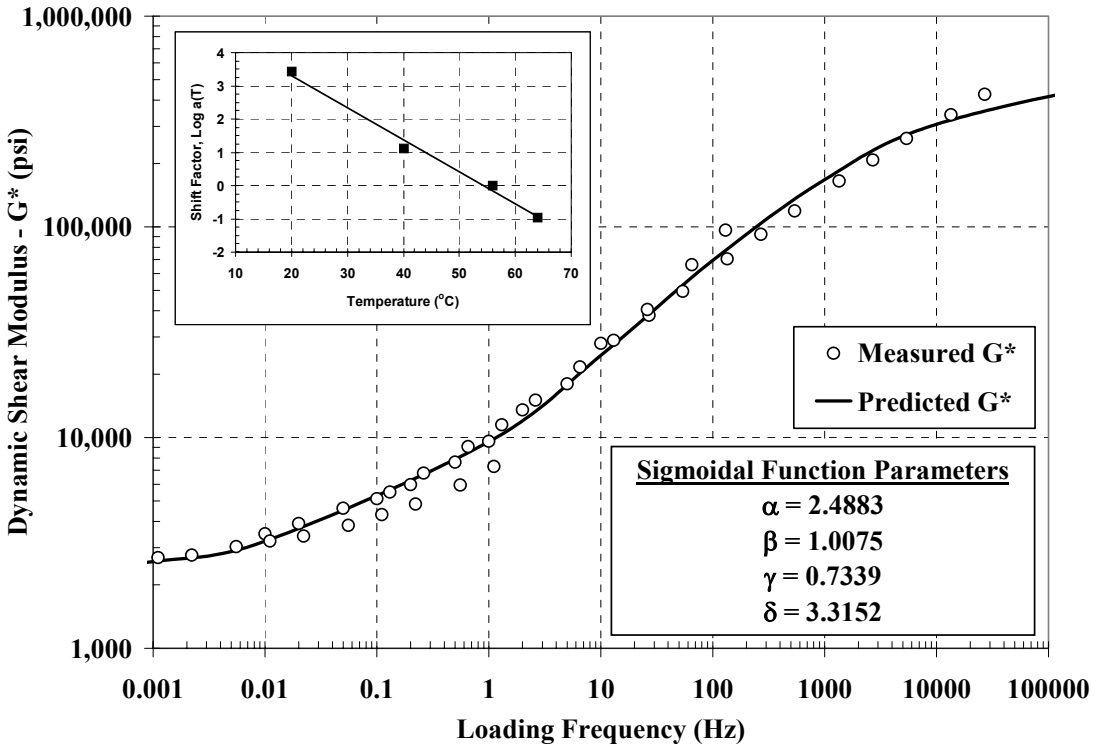

Figure 19 – Master Curve Developed from Testing Conducted at RAPL

crumb rubber to the baseline PG64-22. At 40°C, the shear modulus at 0.01 Hz is 5,469 and 1,556 psi for the AR-HMA and the PG64-22, respectively. In fact, even at 64°C, the AR-HMA is still able to achieve a higher shear modulus than the PG64-22 at 40°C.

Master Stiffness Curves from FSCH

Master stiffness curves were developed from the FSCH data using the procedure defined by Pellinen (1998). The plots from the master curves are shown in Figure 21. The curves indicate that the AR-HMA has a higher stiffness at high temperatures and a lower stiffness at low temperatures. The wide working temperature range of the AR-HMA would provide a rut resistant HMA pavement in high temperatures, but yet a crack resistant HMA pavement in low temperatures.

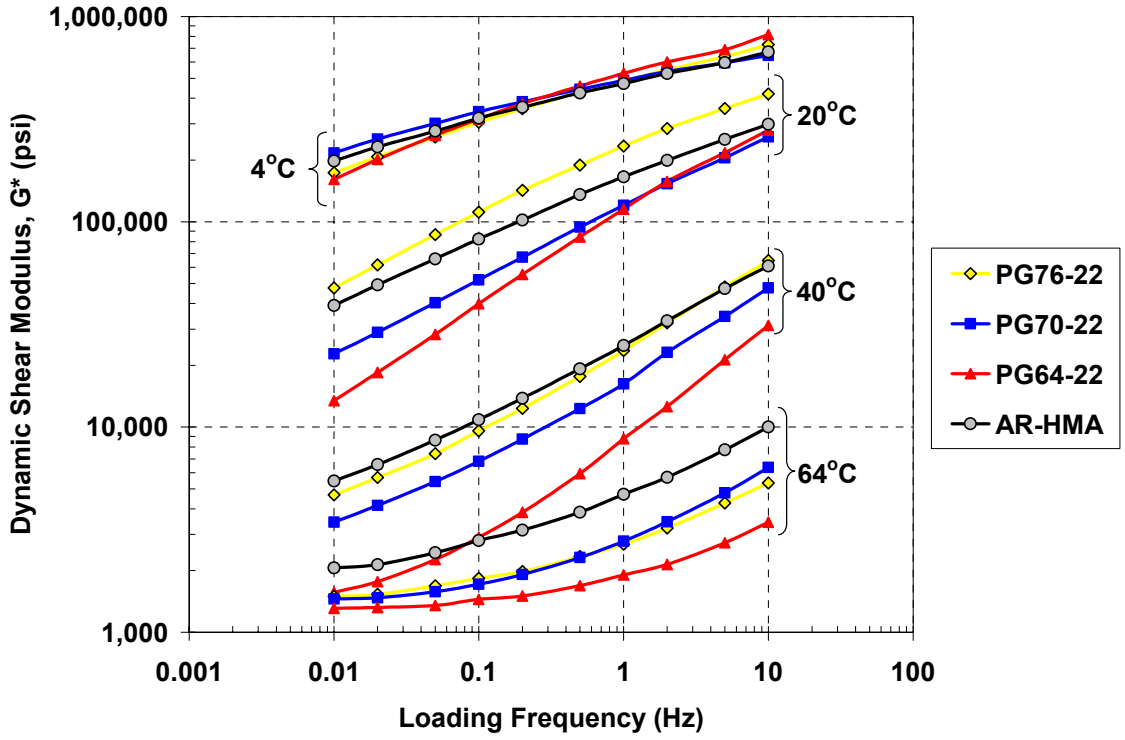

Figure 20 – Frequency Sweep at Constant Height (FSCH) Test Results

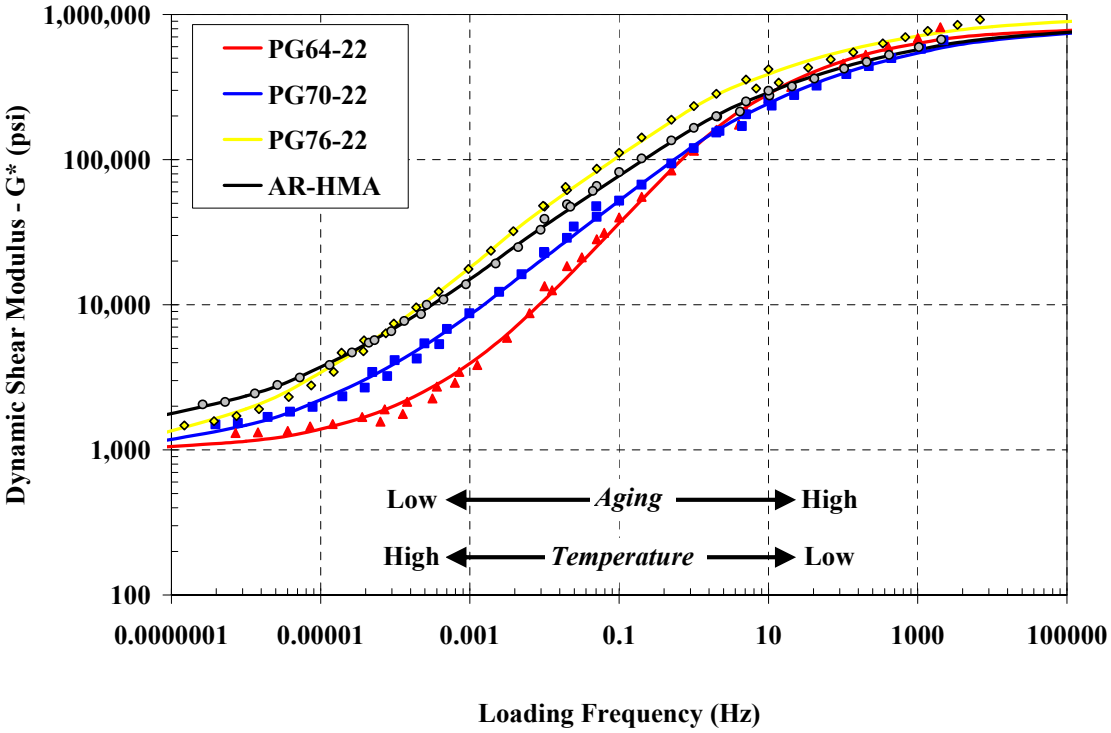

Figure 21 – Master Shear Stiffness Curves from the FSCH Test

Rutting Parameter from FSCH

The rutting parameter of the HMA, defined as G*/sinϕ from the FSCH test data, is similar to G*/sinδ (rutting parameter) of PG graded asphalt binder. It is a measure of HMA stiffness at high pavement temperatures (40 and 64°C) at a slow rate of loading (0.1 cycle/second). Higher values of G*/sinϕ indicate an increased stiffness of HMA mixtures and, therefore, increased resistance to rutting. G* is the complex modulus and ϕ is the phase angle when HMA is tested under dynamic loading. HMA material will better resist rutting with a higher the shear stiffness (G*). It will also better resist rutting if the material behaves more elastic at higher temperatures. The level of elasticity can be evaluated by observing the phase angle. The lower the phase angle, closer to zero, the more elastic the material behavior. The larger the phase angle, closer to 90 degrees, the more viscous the material behavior. Therefore, HMA materials with higher G* and lower ϕ will be more rut resistant.

The results of the rutting parameter evaluation are shown in Figure 22 for the test temperatures of 40 and 64°C. As the asphalt binder performance grade increases for the baseline samples, the rutting parameter also increases. The PG64-22 has the lowest rutting parameter for each test temperature, while the PG76-22 has the highest rutting parameter when only comparing the baseline mixes. The AR-HMA had the highest rutting parameter for all test temperatures when comparing all mixes.

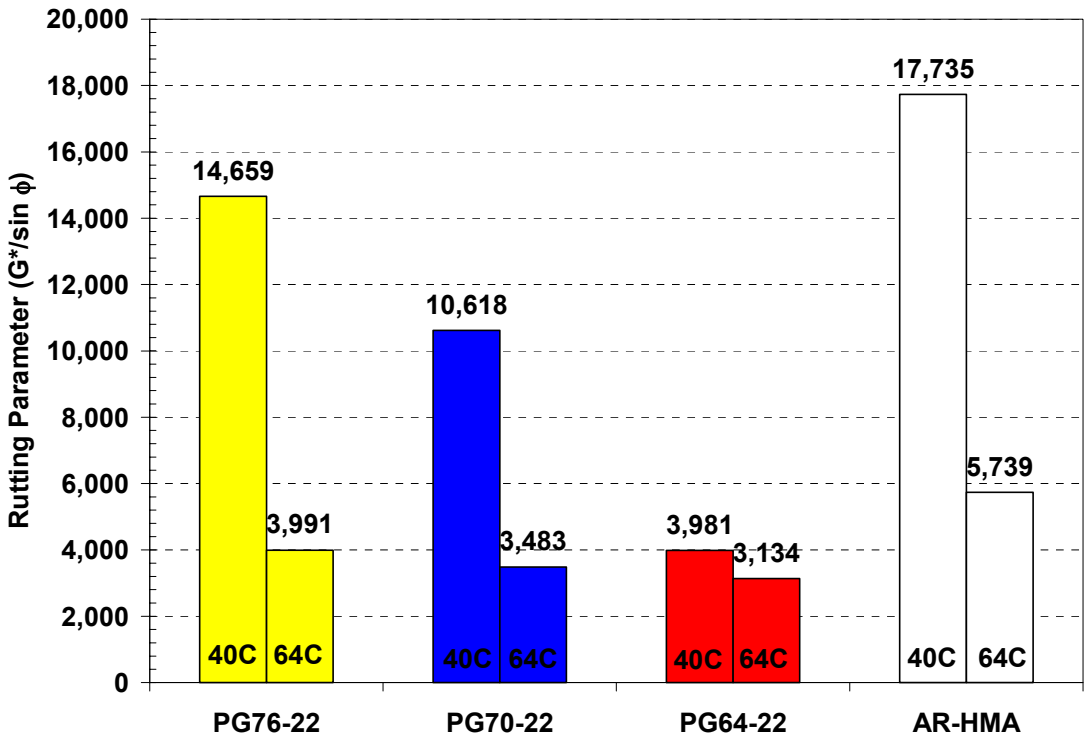

Figure 22 – Rutting Parameter Results from the FSCH Test

Summary of FSCH Test Results

Frequency Sweep at Constant Height (FSCH) tests were conducted at 4, 20, 40, and 64°C. A review of the test results indicates that;

- At elevated test temperatures, the AR-HMA samples obtained the highest shear modulus (stiffness). In fact, the AR-HMA samples obtained a larger shear modulus at the 64°C test temperature than the PG64-22 at the 40°C test temperature when compared at low loading frequencies. Higher shear modulus at high pavement temperatures would provide more resistance to rutting.
- The rutting susceptibility can also be evaluated by comparing the rutting parameter determined at a low loading frequency. The results from Figure 18, which were determined at a loading frequency of 0.1 Hz, shows that the AR-HMA had the highest rutting parameter value. This would indicate that the AR-HMA is more rut resistant than the other baseline mixes. When comparing the baseline mixes, the rutting parameter decreases as the high temperature performance number decreases.
- At the 4°C test temperature, the AR-HMA had the lowest shear modulus (stiffness) at the highest loading frequency. By obtaining lower stiffness at low temperatures, the HMA will be less prone to fatigue cracking at lower temperatures.
- The development of the master stiffness curve shows that the AR-HMA has highest stiffness at the low loading frequencies (corresponding to high temperatures) and lowest stiffness at the high loading frequencies (corresponding to low temperatures). This essentially shows the expanded working temperature range of the AR-HMA material when compared to the baseline mixes.

Repeated Shear at Constant Height (RSCH)

Background of RSCH Test

The RSCH test involves applying a repeated haversine shear stress of 10 psi a sample that has the dimensions of 150 mm in diameter and 50 mm in height. The applied load has a duration of 0.1 seconds, with an unload time of 0.6 seconds. An axial load is applied to the sample during the test to ensure a constant height is obtained at all times. The test procedure followed for this test was AASHTO TP7-01, Test Procedure C. The HMA sample is tested at a test temperature that corresponds to local pavement temperatures.

For this study, samples were tested at the high temperature performance grade used for New Jersey (64°C). The shear stress is applied to the sample for 5,000 loading cycles, or until the sample reaches 5% permanent shear strain. Work conducted by a number of researchers (Harvey et al., 1994; Monismith et al., 2000; Witzcak et al., 2002) has indicated the RSCH to be an excellent tool in determining rut susceptible HMA mixes. For this study, the test was expanded to 6,000 cycles. The parameter used for evaluation from the test is the % permanent shear strain that has occurred at 5,000 loading cycles.

RSCH Test Results

The results for the RSCH tests are shown in Figure 23. The results show that the AR-HMA sample obtained the lowest amount of permanent deformation (1.46 %), while the PG64-22 obtained the largest. The AR-HMA showed similar results to the PG76-22, which obtained a permanent shear strain of 1.66% after 5,000 loading cycles. The results are also shown in tabular format (Table 4).

The test results indicate that AR-HMA is more rut resistant than the PG64-22 and the PG70-22. The AR-HMA is statistically equal to the PG76-22 when comparing the RSCH permanent shear strain.

Table 4 – Permanent Shear Strain at 5,000 Loading Cycles from the RSCH Test

Sample Type	Permanent Shear Strain (%)
PG64-22	5.65 %
PG70-22	2.24 %
PG76-22	1.66 %
AR-HMA	1.46 %

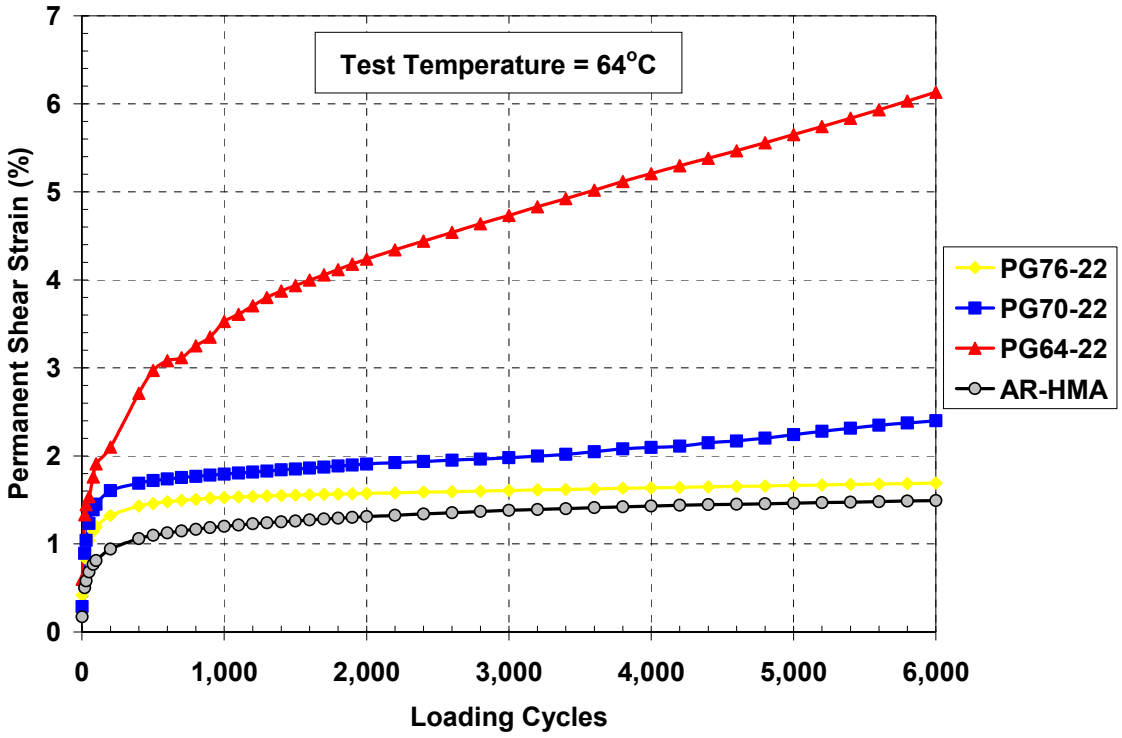

Figure 23 – Accumulated Permanent Shear Strain from the RSCH Test

Binder Consistency Testing – Rotational Viscometer

Viscosity-Temperature relationships were developed for each asphalt binder used in the study. The viscosity-temperature relationship defines how the asphalt binder viscosity changes with the change in temperature. Four test temperatures within the range of 200 to 350°F were used to develop the relationship defined in equation (1). The comparison between the baseline asphalt binders and the AR-HMA asphalt binder is shown in Figure 24 and Table 5. Again, it should be noted that the AR-HMA asphalt binder was produced by adding 20% crumb rubber (#30 (-) mesh) by total weight of the PG64-22 asphalt binder. The crumb rubber and PG64-22 were blended for approximately one hour prior to testing.

Table 5 – Viscosity-Temperature Susceptibility (VTS) Evaluation

Asphalt Binder Type	Original (Tank Aged)		Plant Aged (Theoretical)	
	VTS	A	VTS	A
PG64-22	-3.47	10.371	-3.411	10.248
PG70-22	-3.405	10.209	-3.347	10.09
PG76-22	-2.986	9.061	-2.935	8.96
AR-HMA	-2.444	7.569	-2.402	7.494

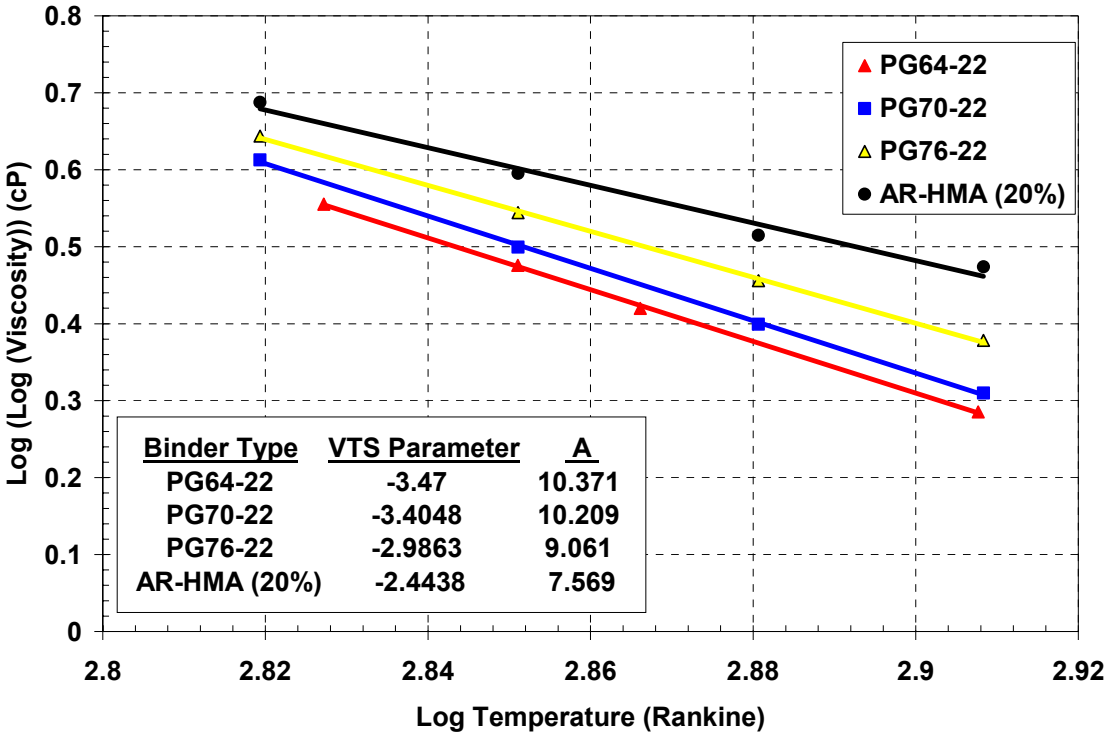

Figure 24 – Viscosity-Temperature Susceptibility Test Results

The VTS relationships developed were for the original binder properties (i.e. not aged, simulates in the tank prior to mixing). The relationship developed by Mirza and Witczak (1997), called the Mix/Lay-Down Model, was used to convert the original binder viscosity values to viscosities that are associated with plant aging (Equation 10). During the mixing and the transportation to the field location, the asphalt binder in the HMA undergoes what is termed Short-Termed Aging. This is high temperature associated aging of the asphalt binder that occurs for all HMA prior to placement. The viscosity properties at this condition (called time = 0) is important since this is the time at which the loading on the HMA begins.

$$\log\log(\eta_{t=0}) = a_0 + a_1 \log\log(\eta_{org}) \qquad (10)$$

where,

$a_0 = 0.054405 + 0.004082$ x (*code*)
$a_1 = 0.972035 + 0.010886$ x (*code*)
code = hardening resistance (0 for average); Table 6 for recommended values

Table 6 – Recommended Code Values for the Mix/Lay-Down Model

Mix/Lay-Down Hardening Resistance	Expected Hardening Resistance Values	Code Value
Excellent to Good	HR < 1.030	-1
Average	1.030 < HR < 1.075	0
Fair	1.075 < HR < 1.100	1
Poor	HR > 1.100	2

A code value of zero was used for all binders tested. The Plant Aged viscosity properties were used to develop the master stiffness curves (from both the FSCH and the Dynamic Modulus).

Dynamic Modulus (E*)

In order to utilize the upcoming 2002 AASHTO Mechanistic Design Guide, the dynamic modulus of the HMA is required. The dynamic modulus describes the stress to strain (stiffness) properties of an HMA material loaded under a sinusoidal waveform. The stiffness of the HMA pavement is dependent on both the vehicle speed and the pavement temperature. Therefore, to provide a comprehensive assessment of the HMA stiffness, the dynamic modulus is tested at wide range of temperatures (10, 40, 70, 100, and 130^{o}F) and loading frequencies (25, 10, 5, 1, 0.5, and 0.1 Hz). After the testing has been completed, once again a master stiffness curve can be generated using the procedure outlined by Pellinen (1998).

The results of the dynamic modulus testing are shown in Figures 25 and 26. All five test temperatures were not able to be put on the same chart because of the large amount of overlapping data. The results from Figure 21 show that the AR-HMA samples achieved the lowest stiffness at the 10°F test temperature. A lower stiffness at low temperatures will help to minimize low temperature cracking. Meanwhile, the AR-HMA samples at the 130°F test temperature produced dynamic modulus results that were statistically equal to the PG76-22, which were the highest obtained. The high modulus values at the high test temperatures would indicate that the AR-HMA would provide an HMA material that is more rut resistant than either the PG70-22 or PG64-22, and as rut resistant as the PG76-22.

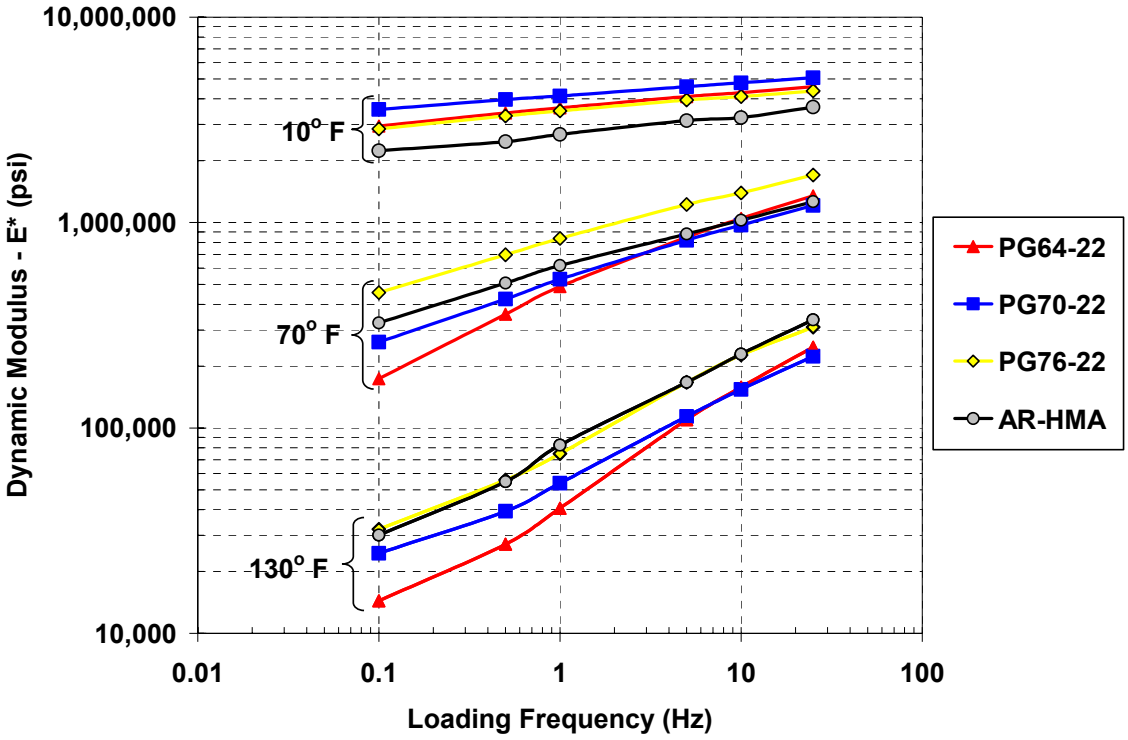

Figure 25 – Dynamic Modulus Results for 10, 70, and 130°F

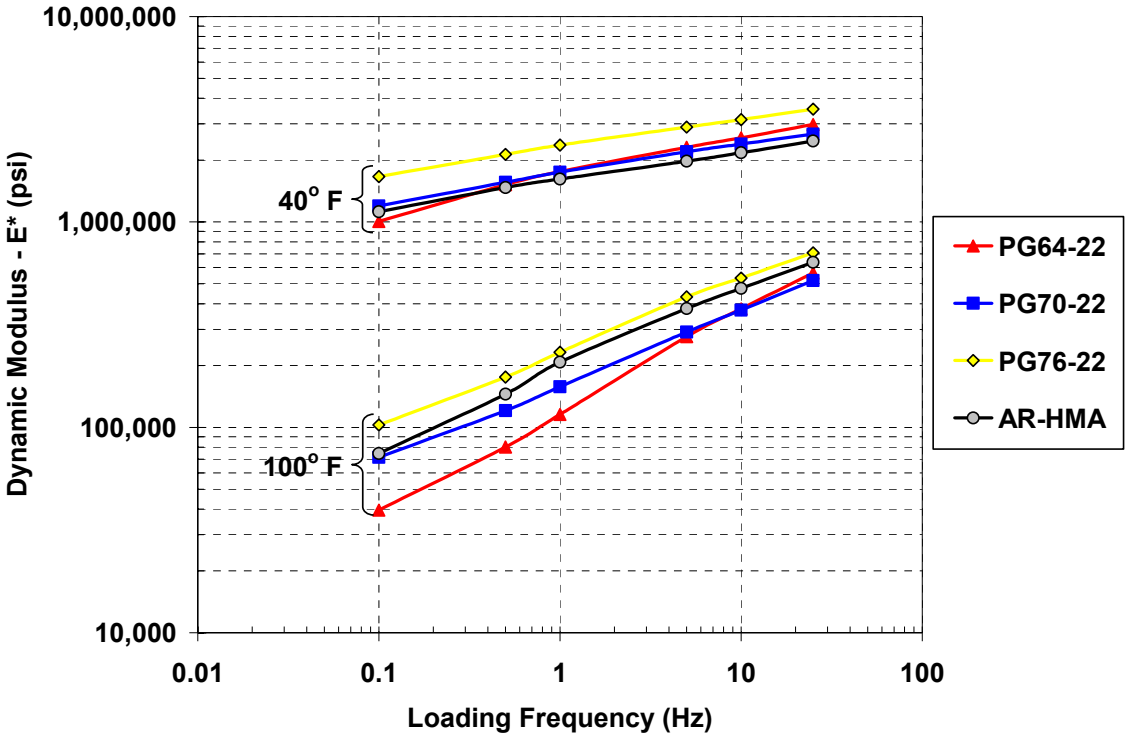

Figure 26 – Dynamic Modulus Results for 40 and 100°F

Master Stiffness curves were also generated from the dynamic modulus data. The master stiffness curves are shown in Figure 27. Similar to the FSCH master curves, the AR-HMA showed the lowest stiffness at the highest loading frequencies (low temperatures). However, when comparing the lower frequency range, the AR-HMA was comparable to the PG70-22 and lower than the PG76-22 even though the actual E* measured was comparable to the PG76-22 and larger than the PG70-22. The difference between the master curves and the actual data is the method in developing the master curves themselves.

To evaluate how the method of shifting the dynamic modulus affects the stiffness master curve, another shifting procedure was examined. In the Arrhenius Equation, defined by Painter and Coleman (1997), the relaxation processes below the glass transition temperature, T_g, in amorphous polymers involve local motions. The glass transition temperature is the temperature at which the asphalt binder's behavior transitions from an amorphous liquid to a glassy solid. The Arrhenius equation describes the relationship between the rate constants and temperature. The Activation Energy, ΔE_a, describes the barrier that molecules must cross in order to react upon colliding (Pellinen et al., 2004). Below the T_g the shift factors can be described the by the Arrhenius Equation (Equation 11).

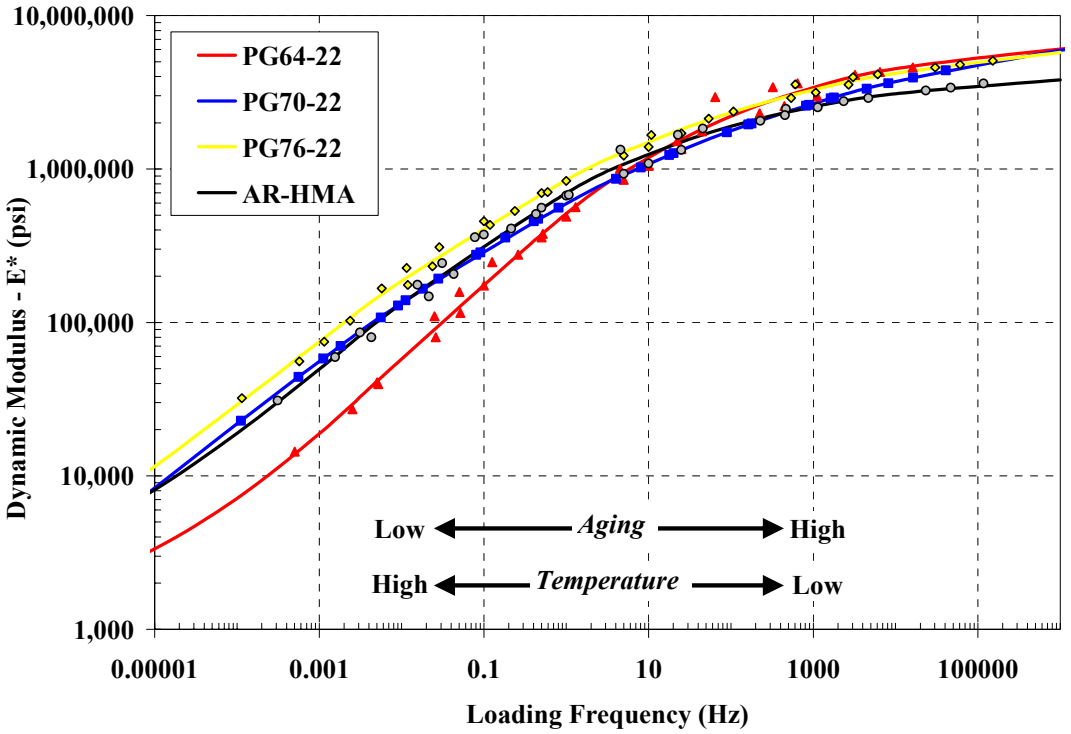

Figure 27 – Master Stiffness Curves Generated from E* Data Using the VTS Method

$$\log a(T) = \frac{\Delta E_A}{2.303R}\left(\frac{1}{T} - \frac{1}{T_O}\right) \qquad (11)$$

where,

$a(T)$ = horizontal shift factor for $T < T_g$,
ΔE_a = apparent activation energy,
R = universal gas constant = 8.314 J/^{o}K-mol,
T = temperature, ^{o}K, and
T_O = reference temperature, ^{o}K.

The new master stiffness curve, constructed using the Arrhenius Equation and an assumed activation energy of 204 kJ/mol (Pellinen et al. (2004), is shown as Figure 28. The results now show that the AR-HMA is comparable to the PG76-22 at the low loading frequencies (high temperatures), while still having the lowest stiffness at the highest loading frequencies (low temperatures). The Arrhenius-shifted master curve provides a better representation to the actual test data. Recent work by Pellinen et al., (2004) has indicated that Arrhenius Equation may provide a better means of shifting. Unfortunately, the VTS method will most likely be used in the upcoming 2002 Mechanistic Pavement Design Method. The downfall in using the VTS method for the stiffness master curve, based on the data generated in this study, is that the design software will interpret the AR-HMA stiffness being less than the PG76-22 and similar to the PG70-22 at high

temperatures. Therefore, the rutting of the AR-HMA will most likely be similar to that of the PG70-22 and not closer to the PG76-22, which is actually the case.

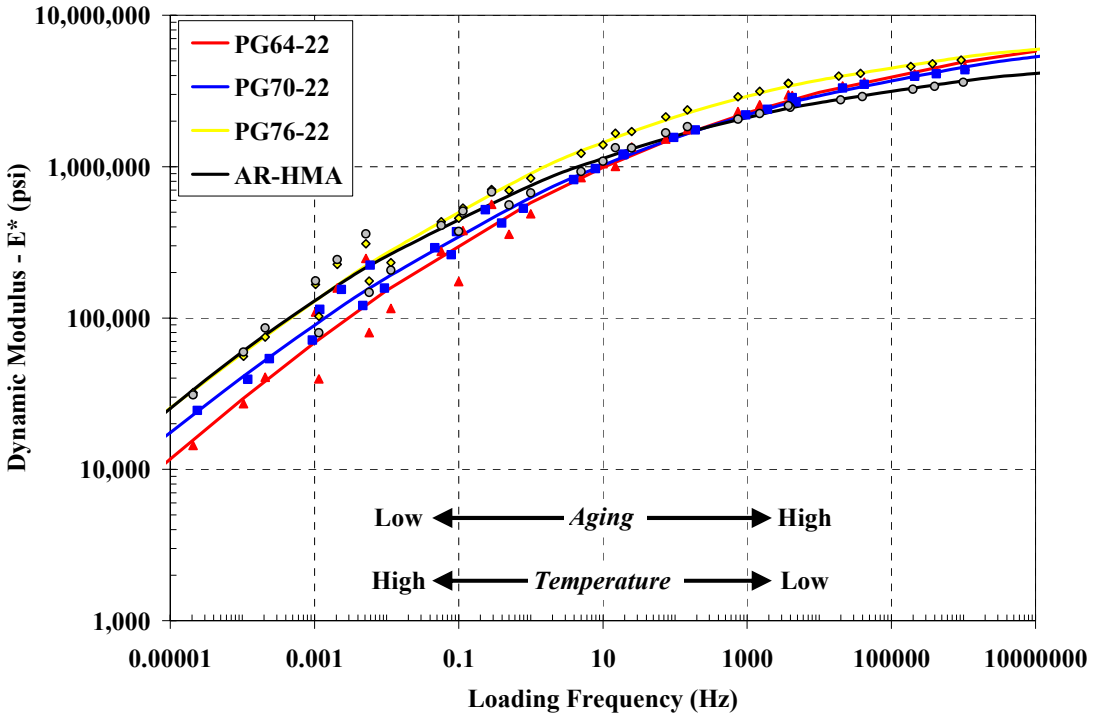

Figure 28 – Master Stiffness Curves Generated from E* Data Using the Arrhenius Equation

Dynamic Modulus Parameter for Rut Susceptibility

As mentioned earlier, the (E*/sin ϕ) stiffness parameter calculated from the dynamic modulus test has been selected as a candidate for the Simple Performance Test (SPT) to predict rut susceptible mixes. The (E*/sin ϕ) is determined using the same concept as the rutting parameter for the FSCH test. The (E*/sin ϕ) is to be calculated at the 130°F test temperature and a loading frequency of 5 Hz (Witczak et al., 2002). The larger the E*/sin ϕ, the lower the rutting potential. Table 7 shows the calculated values of the E*/sin ϕ at a test temperature of 130°F and a loading frequency of 5 Hz. The results show that the AR-HMA had the highest value, indicating that it had the lowest potential for rutting when compared to the other baseline mixes.

Table 7 – E*/sin ϕ for Mixes Tested at 130°F and 5 Hz

Material Type	E*/sin ϕ
PG64-22	201,901
PG70-22	249,283
PG76-22	324,756
AR-HMA	433,579

Dynamic Repeated Load – Permanent Deformation Test

The dynamic repeated load test was conducted to determine the HMA's susceptibility to rutting. As stated earlier, the results from the NCHRP 465 Final Report (Witczak et al., 2002) have indicated that the Flow Number from the Repeated Load Permanent Deformation Test showed excellent correlation to rutting in the field. For comparison purposes, the material that has the highest Flow Number (FN) will have the lowest permanent deformation in the field.

The Flow Number results from the Repeated Load Permanent Deformation test are shown in Table 8. The results in the table are the average of two tests. The actual permanent deformation curves are shown in the Appendix.

Table 8 – Flow Number of Mixes Tested Under Repeated Load

Material Type	Flow Number (FN)	Air Voids (%)
PG64-22	1,538	3.7 %
PG70-22	5,253	3.7 %
PG76-22	17,817	4.1 %
AR-HMA	14,530	4.8 %

The results from Table 8 show that the PG76-22 obtained the highest Flow Number from the testing, with the AR-HMA mix having the second highest. However, it should be noted that the compacted air voids of the AR-HMA was almost 0.7% higher than the PG76-22. Typically, the higher the air voids, the more permanent deformation the mix would sustain. Therefore, if the air voids of the AR-HMA were closer to the PG76-22, a better comparison may have occurred.

CONCLUSIONS

An asphalt rubber mix design was conducted using a 12.5mm Superpave aggregate gradation. The #30 (-) mesh crumb rubber was added to a PG64-22 asphalt binder and allowed to blend for approximately 1 hour prior to mixing. A number of different samples were compacted to provide a performance evaluation of the asphalt rubber mix. The asphalt rubber mix was compared to a PG64-22, PG70-22, and a PG76-22 hot mix asphalt using the identical aggregate gradation. The performance testing included 1) Binder Consistency Testing (Viscosity-Temperature Susceptibility), 2) Superpave Shear Tester – Simple Shear, 3) Superpave Shear Tester – Frequency Sweep, 4) Superpave Shear Tester – Repeated Shear, 5) Dynamic Modulus, and 6) Simple Performance Test – Repeated Load Permanent Deformation. Based on the performance testing, the following conclusions were drawn:

- The Binder Consistency testing showed that the AR-HMA binder had the lowest Viscosity-Temperature Susceptibility slope. This would indicate that the material is less prone to viscosity change due to temperature change. This would aid in increasing the working temperature range of the asphalt.
- The Simple Shear tests conducted in the Superpave Shear Tester indicate that the AR-HMA was comparable with the PG64-22 and PG70-22 at low temperatures, with the PG76-22 having the lowest creep strain. It is important for asphalt materials to exhibit creep at low temperatures to minimize the potential for low temperature cracking. At high temperatures, the AR-HMA obtained the lowest creep strain. By minimizing creep at high temperatures, the asphalt can resist permanent deformation.
- The Frequency Sweep tests conducted in the Superpave Shear Tester indicate that the AR-HMA had the lowest stiffness at higher loading frequencies at 4^{o}C. By obtaining lower stiffness' at low temperatures, the asphalt will be able to resist low temperature cracking due to brittleness. At the 64^{o}C test temperature, the AR-HMA obtained the largest stiffness. The AR-HMA shear stiffness at 64^{o}C was even higher than the PG64-22 at 40^{o}C. The increased stiffness at high temperatures will aid in resisting permanent deformation.
- The Repeated Shear tests conducted in the Superpave Shear Tester concluded that the AR-HMA obtained the lowest overall permanent shear strain. Research has shown that asphalt materials that obtain lower permanent shear strains in the Repeated Shear test will obtain lower permanent deformation (rutting) in the field.
- The Dynamic Modulus test results very clearly demonstrated the increased working temperature range of the AR-HMA mix over the baseline mixes. The AR-HMA obtained the lowest stiffness at the 10^{o}F test temperature, but also obtained a comparable stiffness to the PG76-22 at the 130^{o}F test temperature.
- The Repeated Load Permanent Deformation test results using the Simple Performance set-up showed that the AR-HMA obtained a Flow Number greater than the PG64-22 and PG70-22 mixes, however, the AR-HMA was slightly lower than the PG76-22 mix. Research has shown that the materials that obtain larger Flow Number's would be less rut susceptible. Therefore, the AR-HMA would be less rut susceptible than the PG64-22 and PG70-22 mixes, but slightly more rut susceptible than the PG76-22. The AR-HMA's larger Flow Number may have been attributed to the higher compacted air voids (4.8% for the AR-HMA to 4.1% for the PG76-22).
- The performance testing showed that overall the AR-HMA mix is a material that will perform very well under both cold and warm temperatures. The additional 1.0% of asphalt binder in the AR-HMA mix, when compared to the baseline mixes, should also provide additional fatigue resistance. Preliminary Beam Fatigue tests, not included in this study and only tested at a tensile strain of 500 μs, indicate that the AR-HMA mix has better fatigue properties (Figure 29). Therefore, an asphalt mix that can better resist low temperature cracking, better resist high temperature permanent deformation, and also have better fatigue resistance properties, will ultimately have a longer service life.

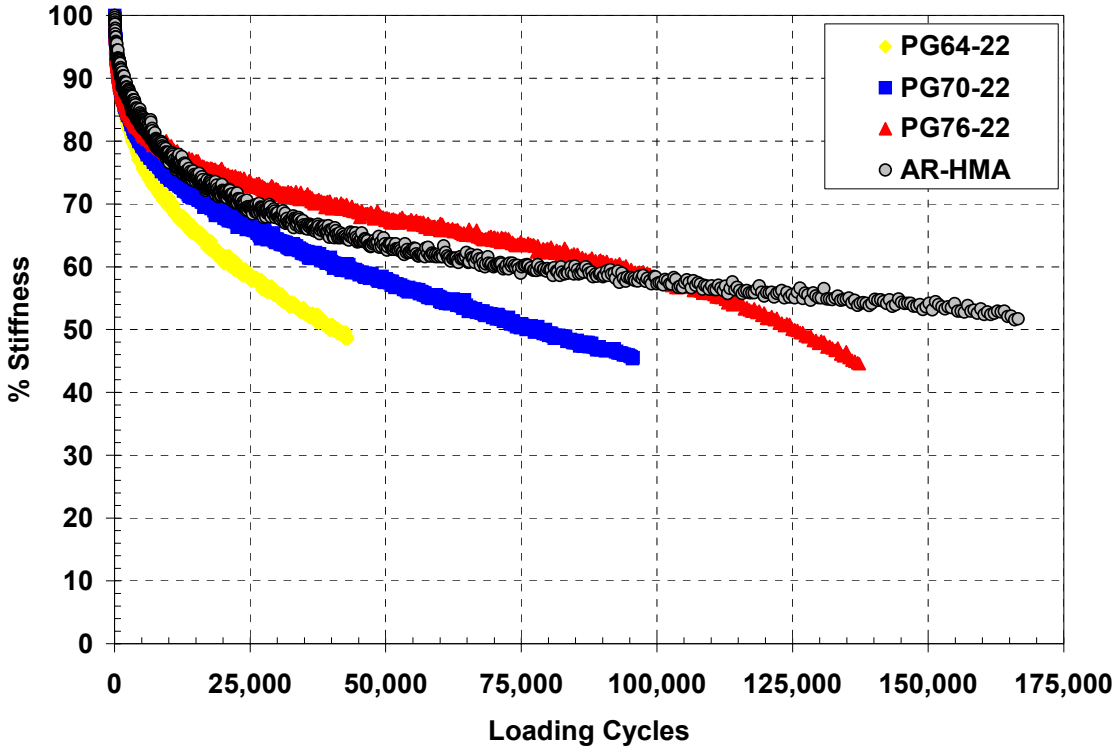

Figure 29 – Flexural Beam Fatigue Testing of Baseline and AR-HMA Samples

RELATED REFERENCES

Andrei, D. Witczak, M.W., and Mirza, M.W., 1999, Development of a Revised Predictive Model for the Dynamic (Complex) Modulus of Asphalt Mixtures", Development of the 2002 Guide for the Design of New and Rehabilitation Pavement Structures – NCHRP 1-37A, Interim Team Technical Report, Department of Civil Engineering, University of Maryland, College Park, MD.

APA Users Group Meeting Minutes. Jackson, Mississippi. September 26-27, 2000.

American Association of State Highway and Transportation Officials (AASHTO), *Test Method for Determining the Permanent Shear Strain and Stiffness of Asphalt Mixtures Using the Superpave Shear Tester (SST), AASHTO TP7-01*, AASHTO Provisional Standards, pp. 146 – 156.

Bahia, H.U., and Davies, R., 1994, "Effect of Crumb Rubber Modifiers (CRM) on Performance Related Properties of Asphalt Binders.", *Journal of the Association of Asphalt Paving Technologies*, Vol. 63, 1994, pp. 414 – 441.

Bell, C., Wieder, A., and Fellin, M., *Laboratory Aging of Asphalt-Aggregate Mixtures: Field Validation*. SHRP-A-390, Strategic Highway Research Program Report, National Research Council, Washington D.C., 1994.

Brown, D.R., Jared, D., Jones, C., and Watson, D., 1997, "Georgia's Experience with Crumb Rubber in Hot-Mix Asphalt.", In *Transportation Research Record 1583*, TRB, National Research Council, Washington D.C., pp. 45 – 51.

Buncher, M., Peterson, R., Walker, D., Turner, P., and Anderson, M., 2000, "Laboratory Process for Comprehensive Evaluation of Mixture Properties.", Paper Submitted for Presentation at the 2000 Transportation Research Board Annual Meeting.

Chipps, J.F., Davison, R.R., Estakhri, C.K., and Glover, C.J., 2001, "Field Tests and Economic Analysis of High-Cure Crumb-Rubber Modified Asphalt Binders in Dense-Graded Mixes.", Presented at the 80th Annual Meeting of the Transportation Research Board, Washington, D.C.

Gopal, V.T., Sebally, P., and Epps, J., 2002, "Effect of Crumb Rubber Particle Size and Content on the Low Temperature Rheological Properties of Binders.", Presented at the 81th Annual Meeting of the Transportation Research Board, Washington, D.C.

Harvey, J., Lee, T., Sousa, J.B., Pak, J., and Monismith, C.L., 1994, "Evaluation of Fatigue Stiffness and Permanent Deformation Properties of Several Modified and Conventional Field Mixes Using SHRP-A-003A Equipment.", Paper Accepted and Presented at the TRB 1994 Annual Meeting.

Harvey, J. and Tsai, B., 1997, "Long-Term Oven-Aging Effects on Fatigue and Initial Stiffness of Asphalt Concrete.", In *Transportation Research Record 1590*, TRB, National Research Council, Washington D.C., pp. 89 – 98.

Kaloush, K., Witczak, M.W., and Way, G., 2002, *Performance Evaluation of Arizona Asphalt Rubber Mixtures using Advanced Dynamic Material Characterization Tests*, College of Engineering and Applied Sciences, Department of Civil and Environmental Engineering, Arizona State University, pp. 240.

Kandhal, P. and Cooley, L., 2002, "Evaluation of Permanent Deformation of Asphalt Mixtures Using Loaded Wheel Tester.", NCAT Report No. 2002-08, 13 pp.

Kim, S., Loh, S., Zhai, H., and Bahia, H., 2001, "Advanced Characterization of Crumb Rubber Modified Asphalts Using Protocols Developed for Complex Binders.", Presented at the 80th Annual Meeting of the Transportation Research Board, Washington, D.C.

Monismith, C.L., Hicks, R.G., and Finn, F.N., *Accelerated Performance-Related Tests for Asphalt-Aggregate Mixes and Their Use in Mix Design and Analysis Systems*, SHRP-A-417, Strategic Highway Research Program Report, National Research Council, Washington, D.C., 1994.

Monismith, C.L., Harvey, J.T., Long, F., and Weissman, S., 2000, "Tests to Evaluate the Stiffness Permanent Deformation Characteristics of Asphalt/Binder-Aggregate Mixes.", Technical Memorandum: TM-UCB PRC-2000-1, 86 pp.

Painter, P.C. and Coleman, M.M, 1997, *Fundamentals of Polymer Science – An Introductory Text*, Technomic Publishing Co. Inc., Lancaster, P.A.

Pellinen, T., 1998, *The Assessment of Validity of Using Different Shifting Equations to Construct a Master Curve of HMA*, Department of Civil Engineering, University of Maryland at College Park, MD.

Pellinen, T., 2001, *Investigation of the Use of Dynamic Modulus as an Indicator of Hot Mix Asphalt Performance,* A Dissertation Presented in Partial Fulfillment of the Requirements for the Degree Doctor of Philosophy, Arizona State University, 803 pp.

Pellinen, T., Witczak, M.W., and Bonaquist, R., 2004, "Asphalt Mix Master Curve Construction Using Sigmoidal Fitting Function with Non-Linear Least Squares Optimization", *Recent Advances in Materials Characterization and Modeling of Pavement Systems, Geotechnical Special Publication No. 123*, American Society of Civil Engineering, pp. 83 – 101.

Raad, L., Saboundjian, S., and Minassian, G., 2001, "Field Aging Effects ofn the Fatigue of Asphalt Concrete and Asphalt-Rubber Concrete.", Presented at the 80th Annual Meeting of the Transportation Research Board, Washington, D.C.

Takallou, H.B., Bahia, H.U., Perdomo, D., and Schwartz, R., 1997, "Use of Superpave Technology and Construction of Rubberized Asphalt Mixtures.", In *Transportation Research Record 1583,* TRB, National Research Council, Washington D.C., pp. 71 – 81.

West, R., Page, G.C., Veilleux, J.G., and Choubane, B., 1998, "Effect of Tire Rubber Grinding Method on Asphalt-Rubber Binder Characteristics.", In *Transportation Research Record 1638*, TRB, National Research Council, Washington D.C., pp. 134 – 140.

Williams, C. and Prowell, B., 1999, "Comparison of Laboratory Wheel-Tracking Test Results to WesTrack Performance.", Presented at the 78th Annual Meeting of the Transportation Research Board, Washington, D.C.

Witczak, M.W., K.E. Kaloush, T. Pellinen, M. El-Basyouny, and H. Von Quintus, 2002, *Simple Performance Test for Superpave Mix Design, NCHRP Report 465*, Transportation Research Board, National Research Council, Washington, D.C., 105 pp.

APPENDIX A – SUPERPAVE SHEAR TESTER

SIMPLE SHEAR TESTS – Short Term Oven Aged

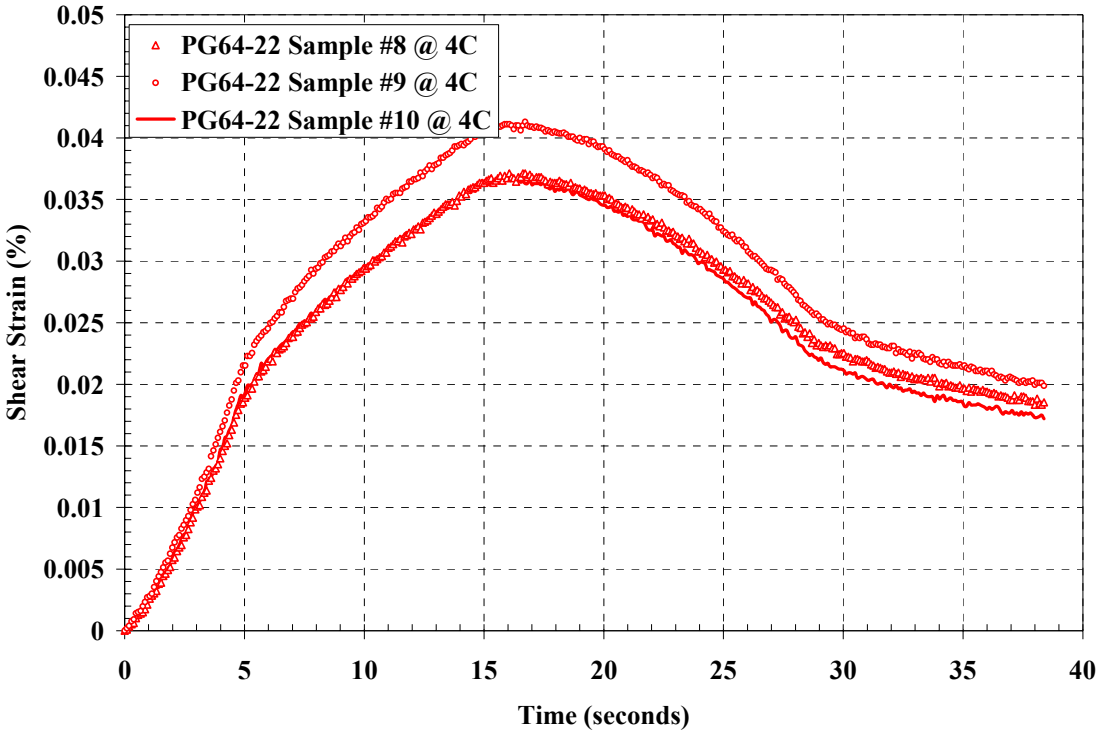

Figure A.1 – Simple Shear Results for PG64-22 at 4°C

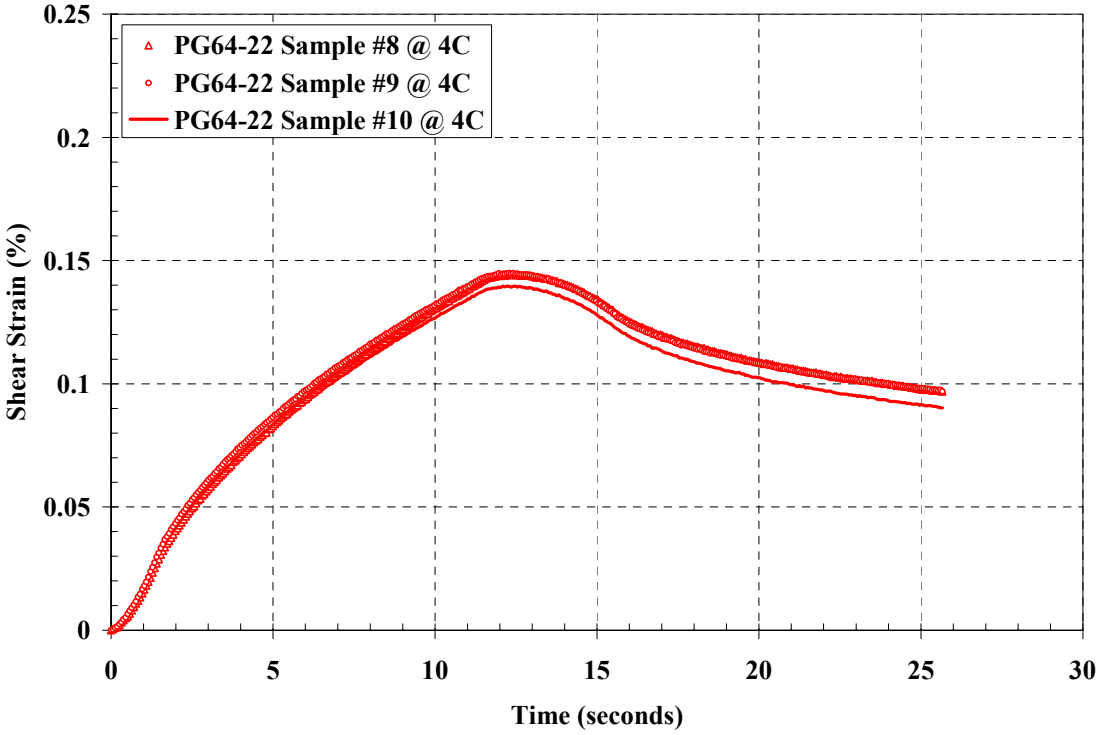

Figure A.2 – Simple Shear Results for PG64-22 at 20°C

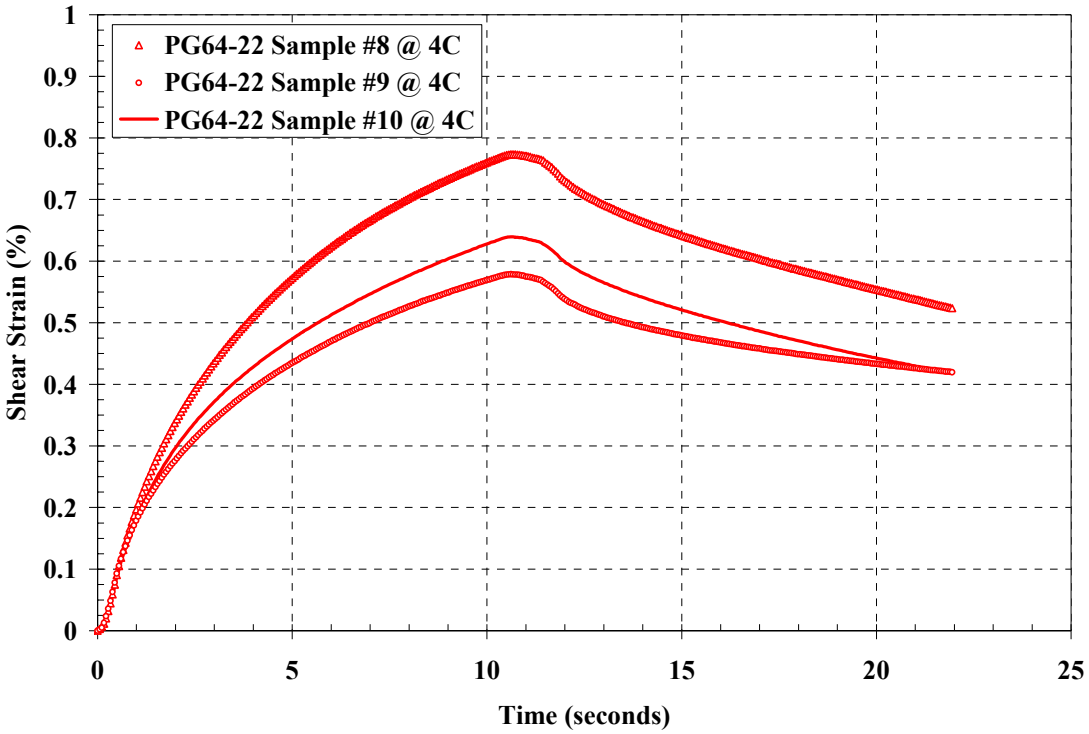

Figure A.3 – Simple Shear Results for PG64-22 at 40°C

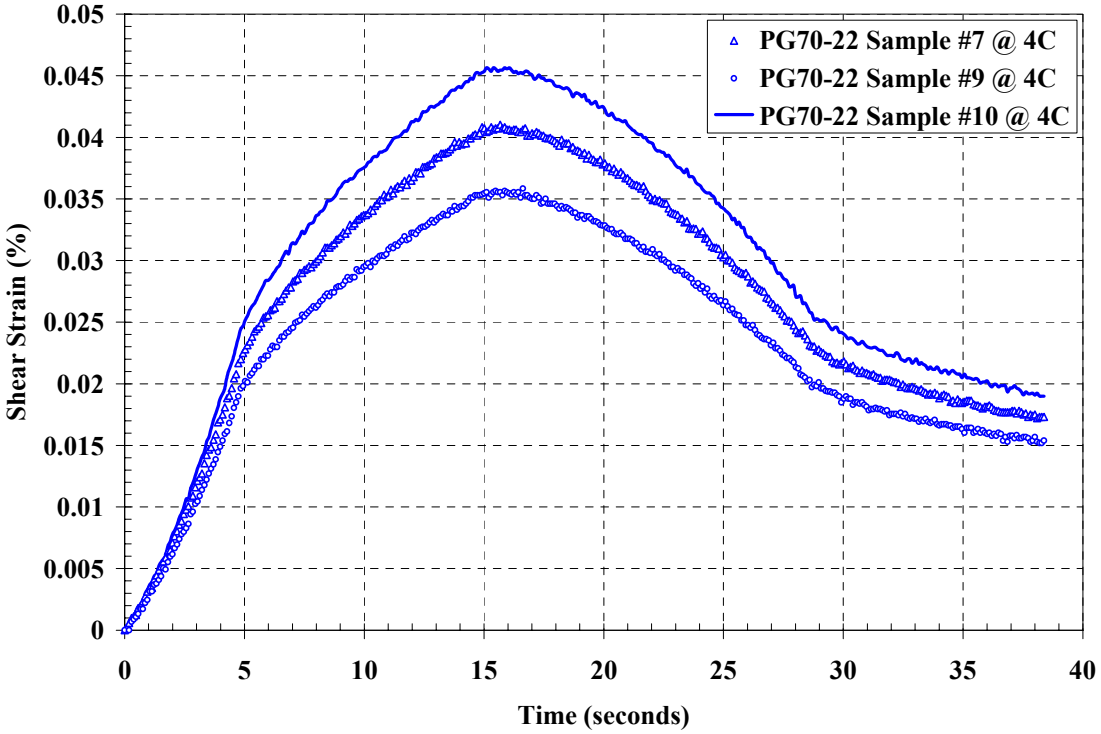

Figure A.4 – Simple Shear Results for PG70-22 at 4°C

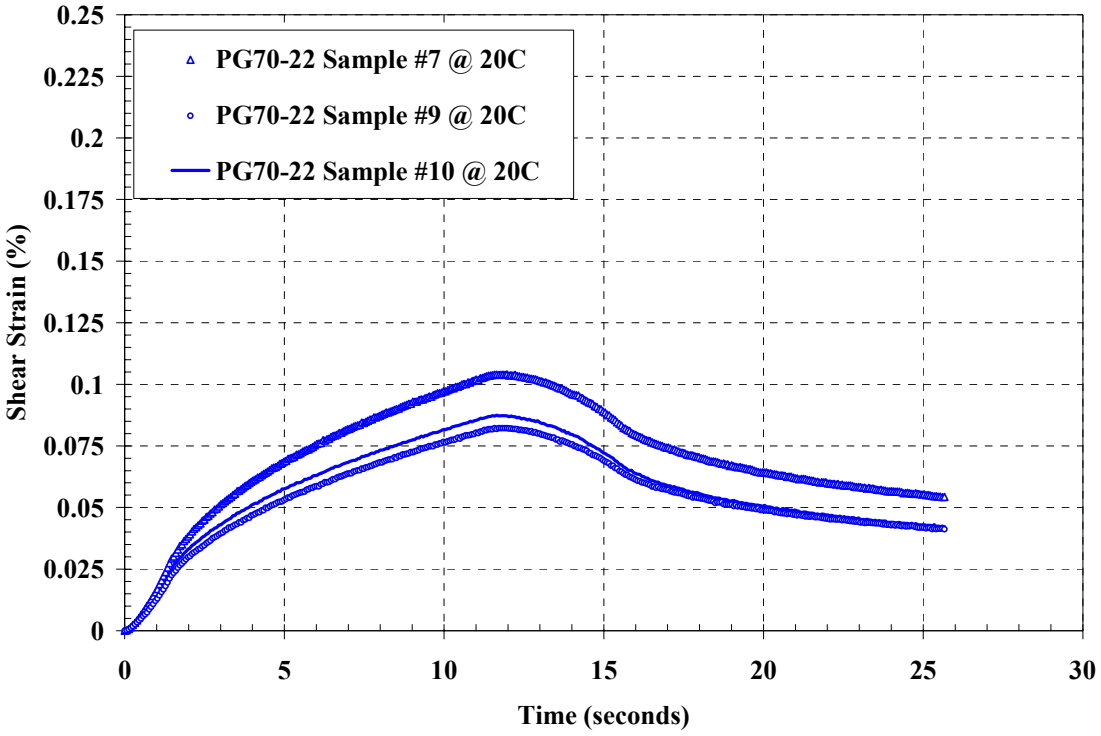

Figure A.5 – Simple Shear Results for PG70-22 at 20°C

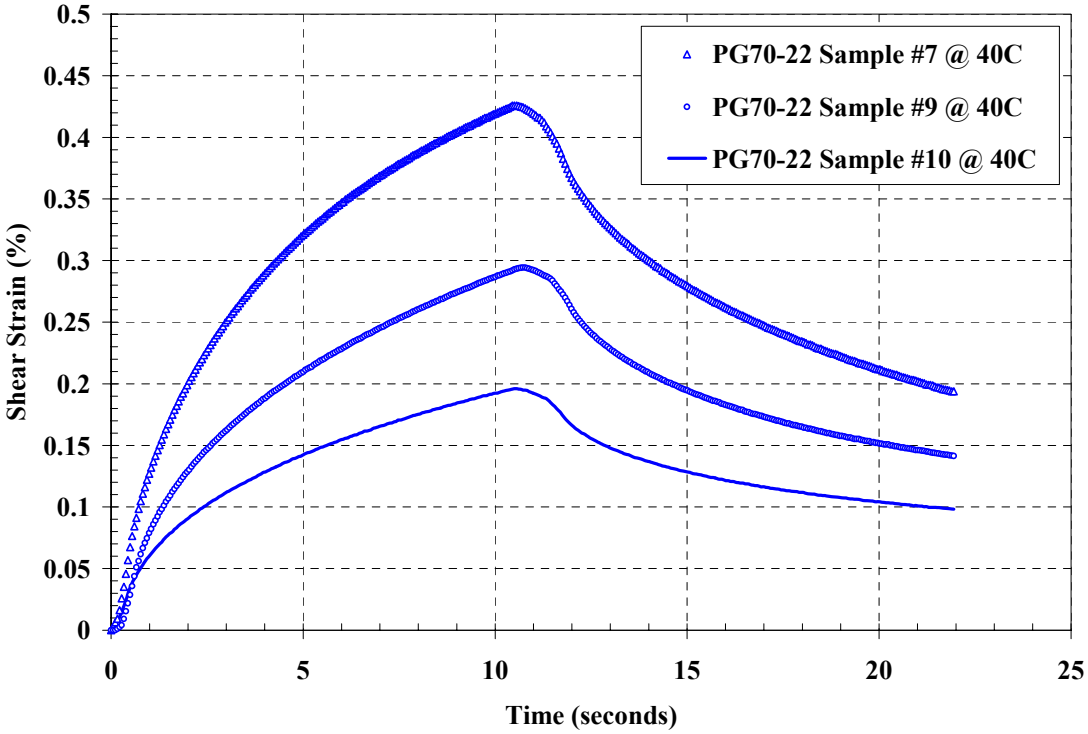

Figure A.6 – Simple Shear Results for PG70-22 at 40°C

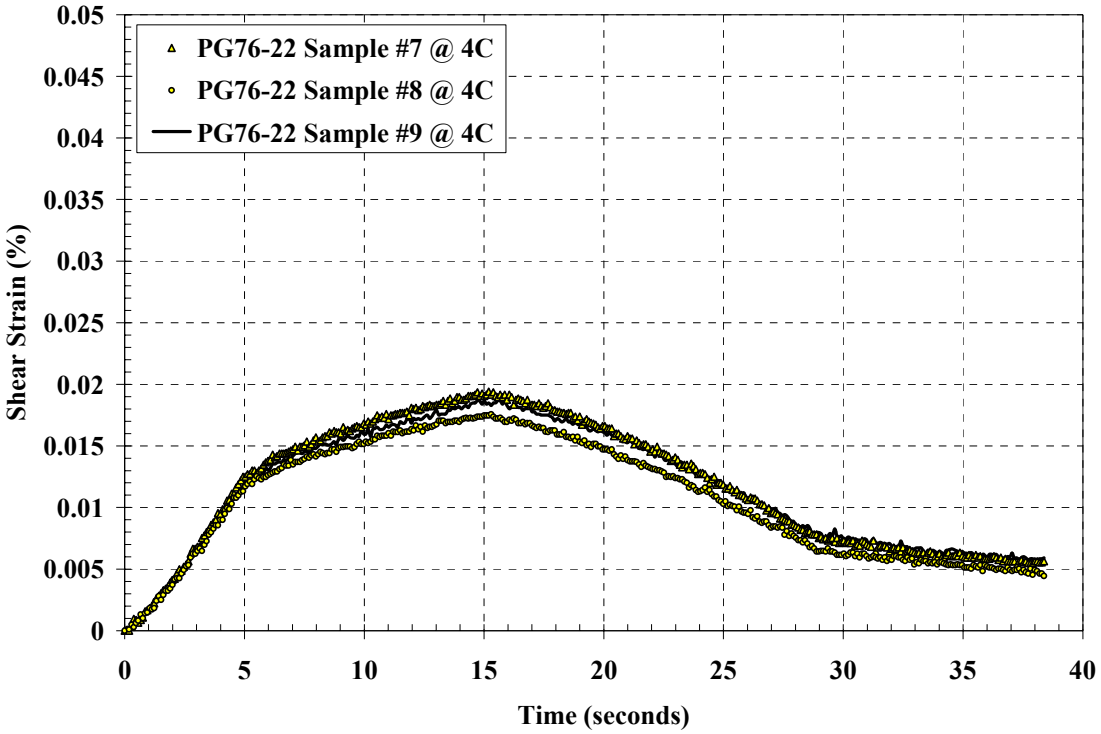

Figure A.7 – Simple Shear Results for PG76-22 at 4°C

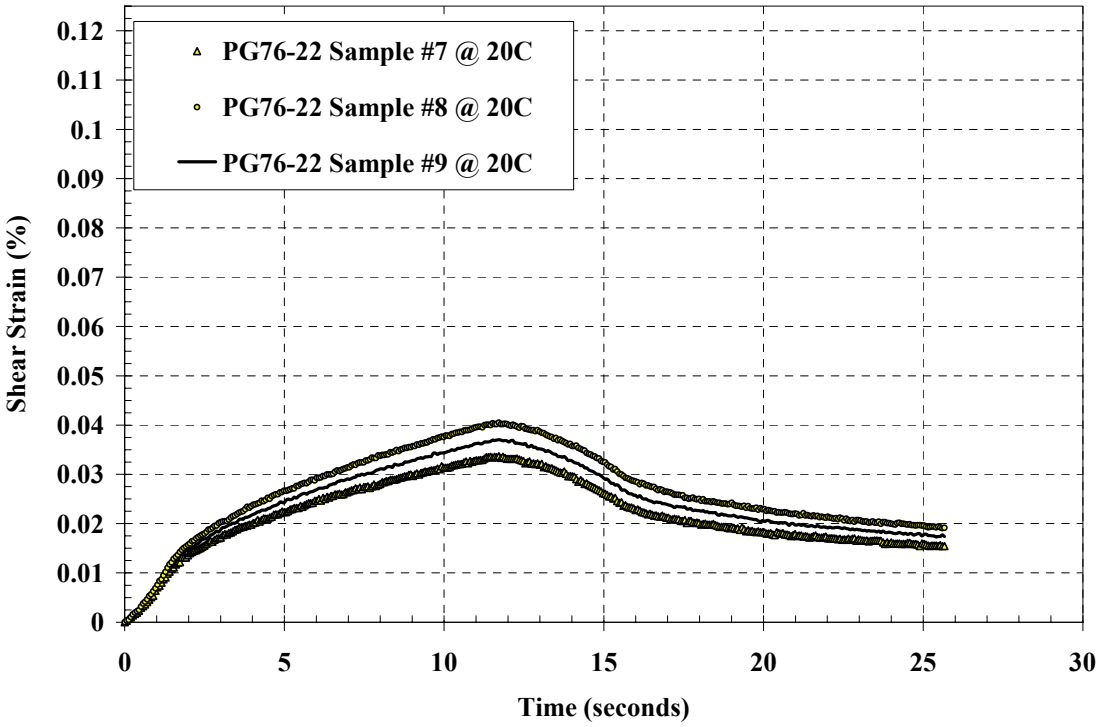

Figure A.8 – Simple Shear Results for PG76-22 at 20°C

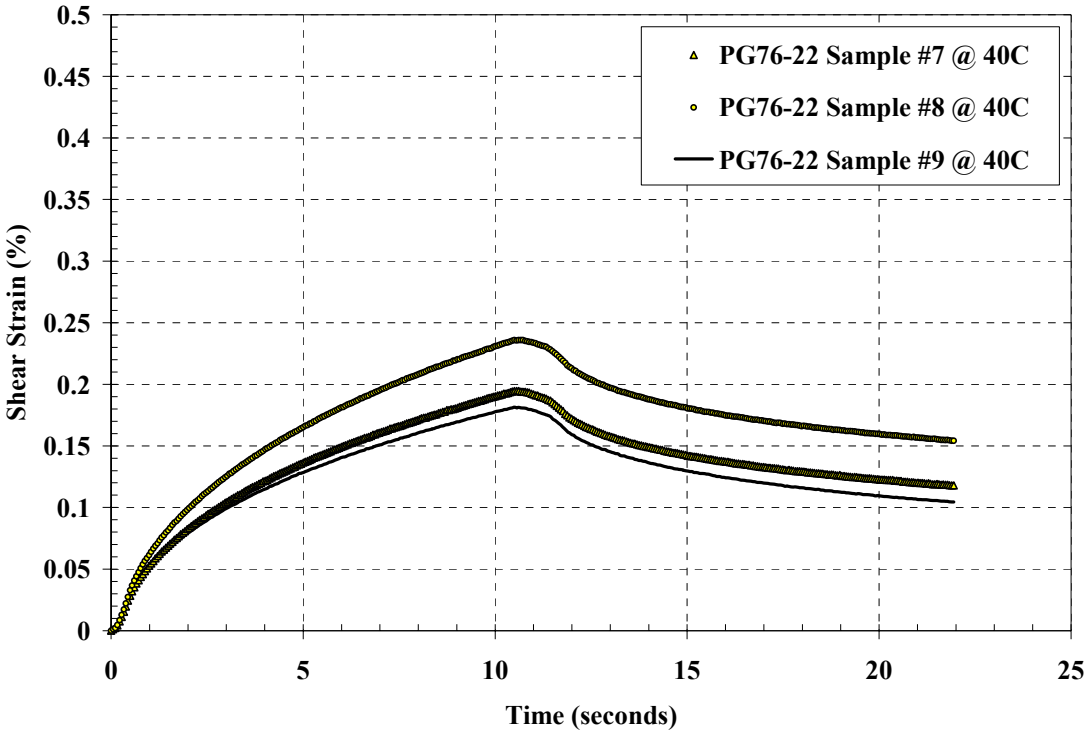

Figure A.9 – Simple Shear Results for PG76-22 at 40°C

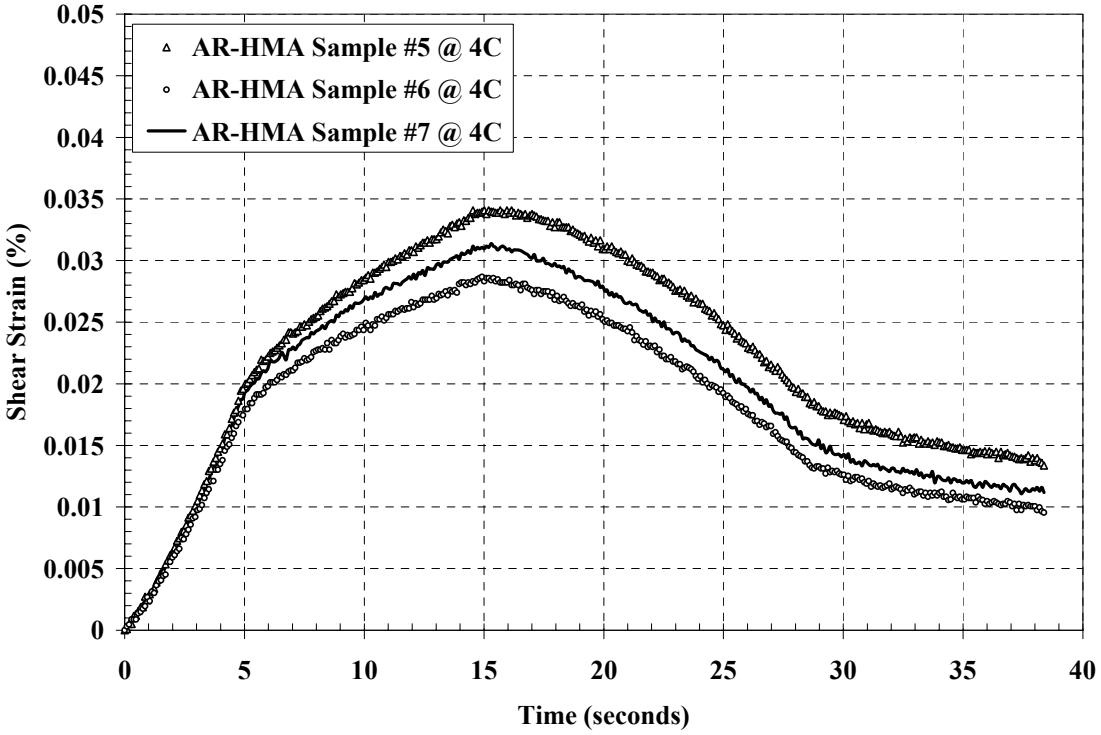

Figure A.10 – Simple Shear Results for AR-HMA at 4°C

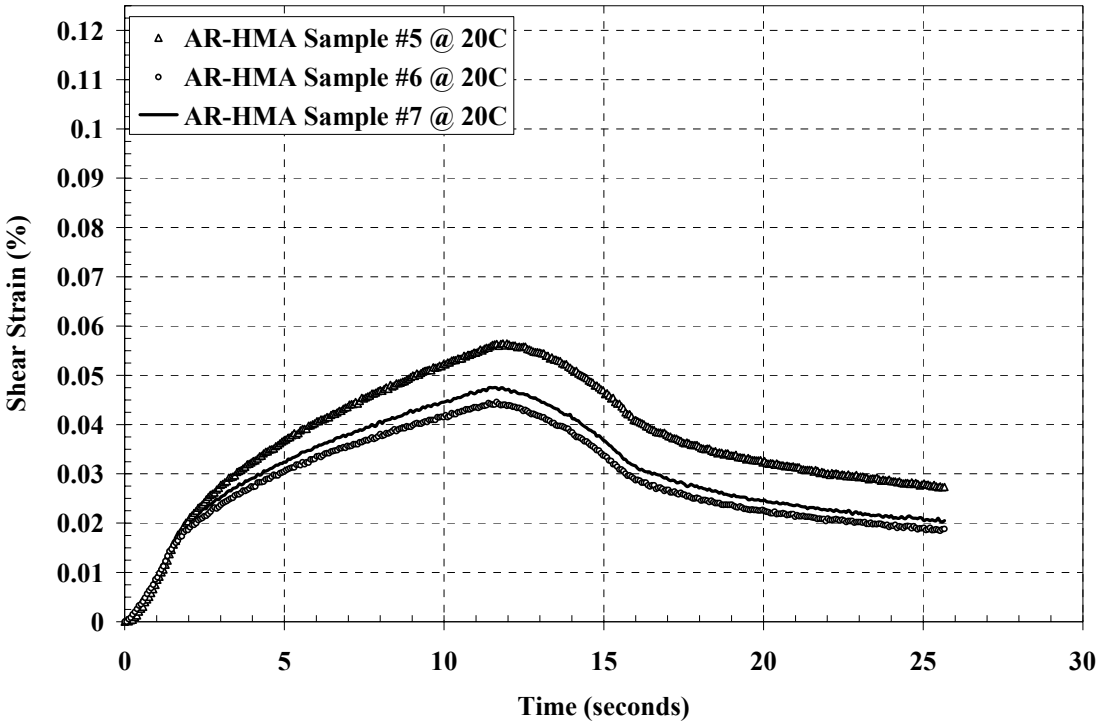

Figure A.11 – Simple Shear Results for AR-HMA at 20°C

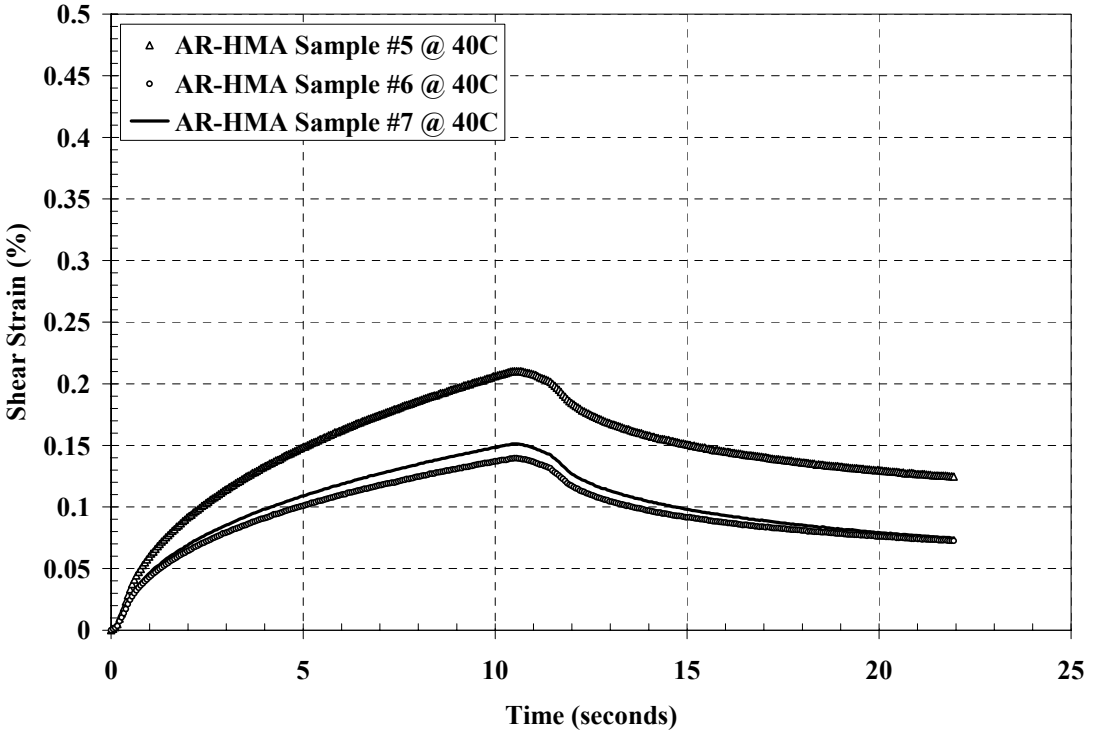

Figure A.12 – Simple Shear Results for AR-HMA at 40°C

SIMPLE SHEAR TESTS – Long Term Oven Aged

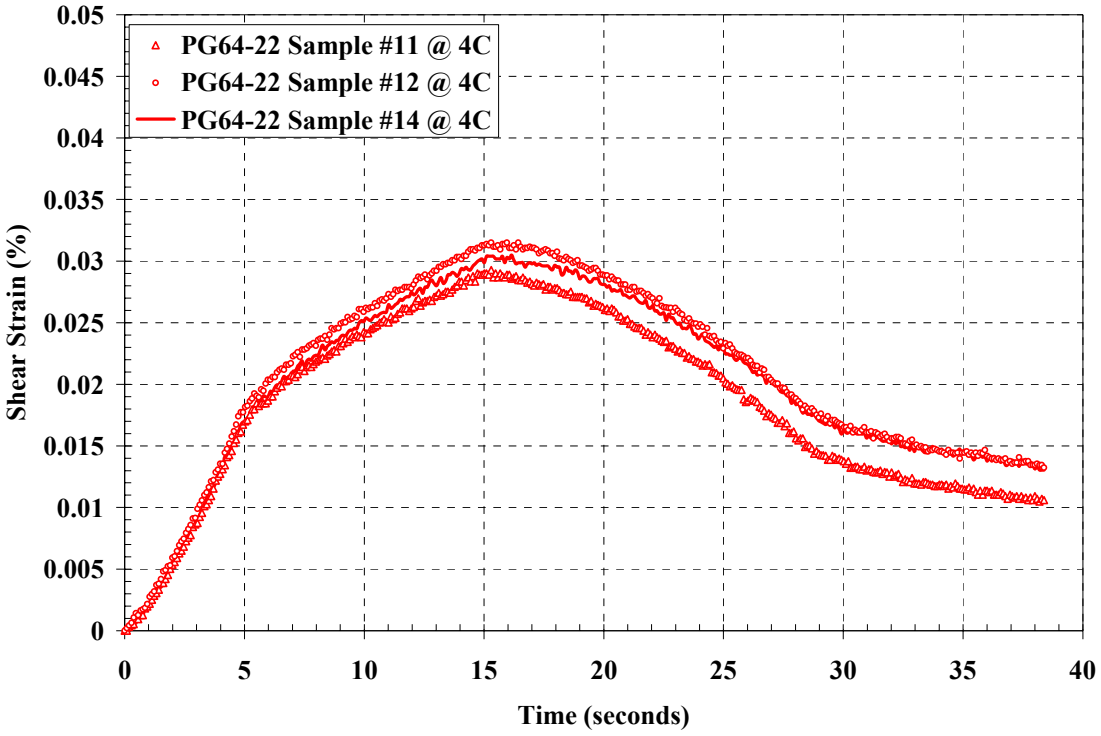

Figure A.13 – Simple Shear Results for PG64-22 at 4°C (Laboratory Aged)

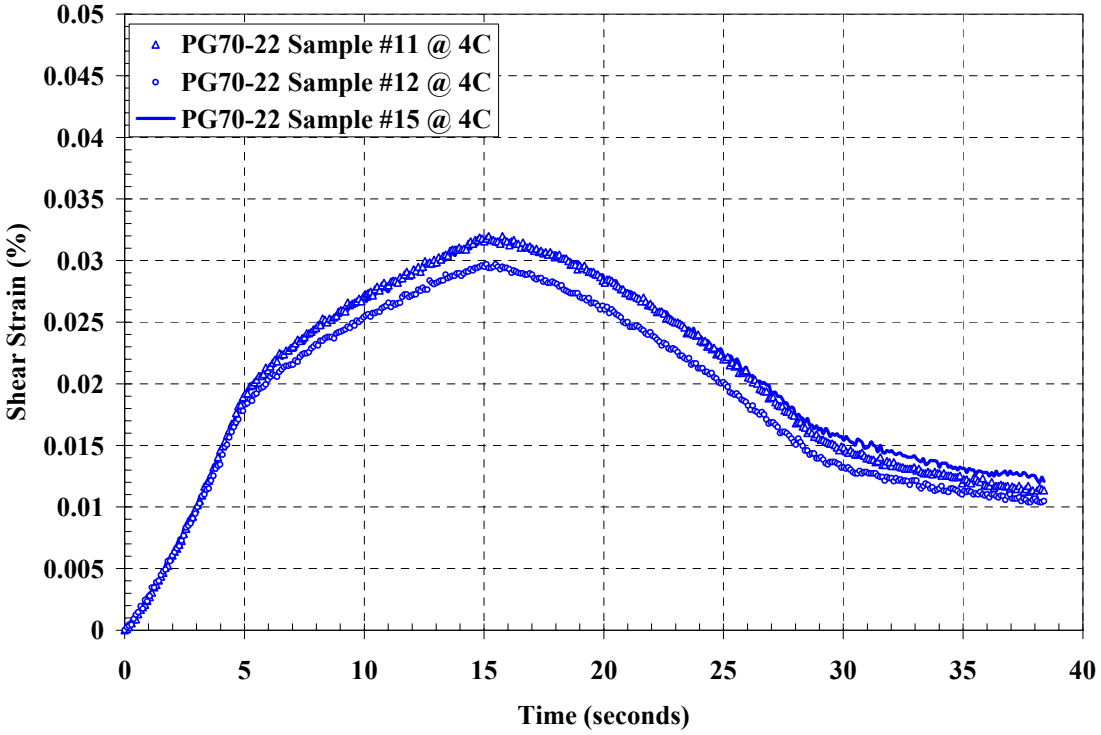

Figure A.14 – Simple Shear Results for PG70-22 at 4°C (Laboratory Aged)

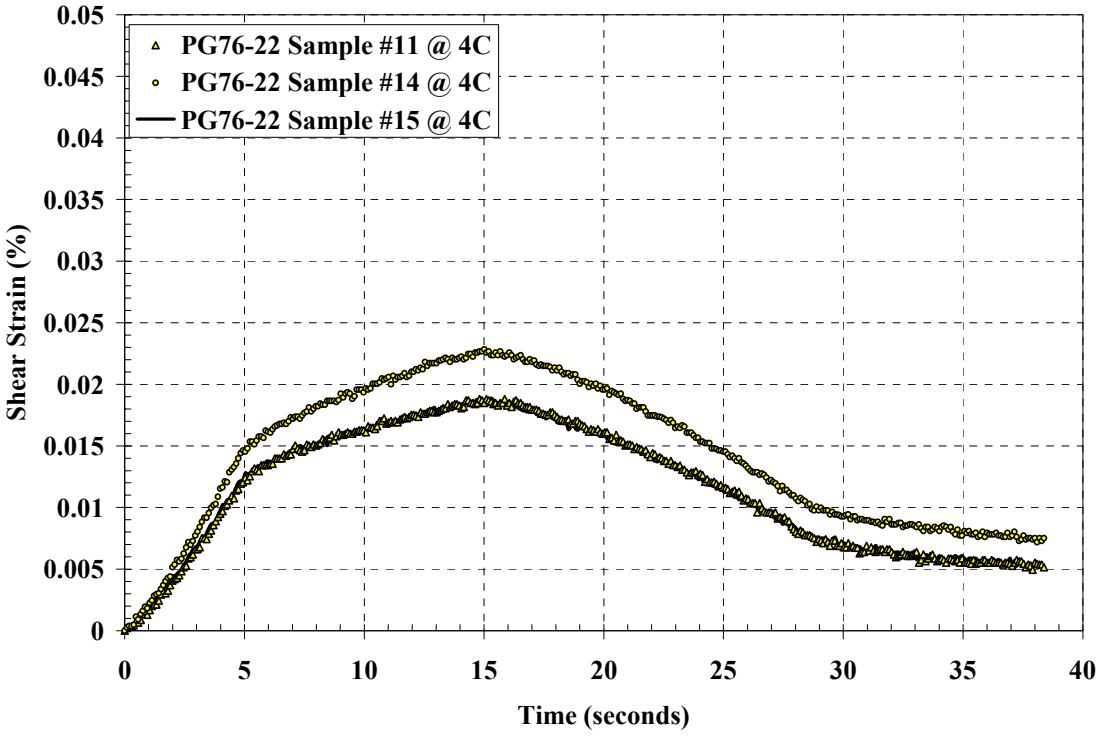

Figure A.15 – Simple Shear Results for PG76-22 at 4°C (Laboratory Aged)

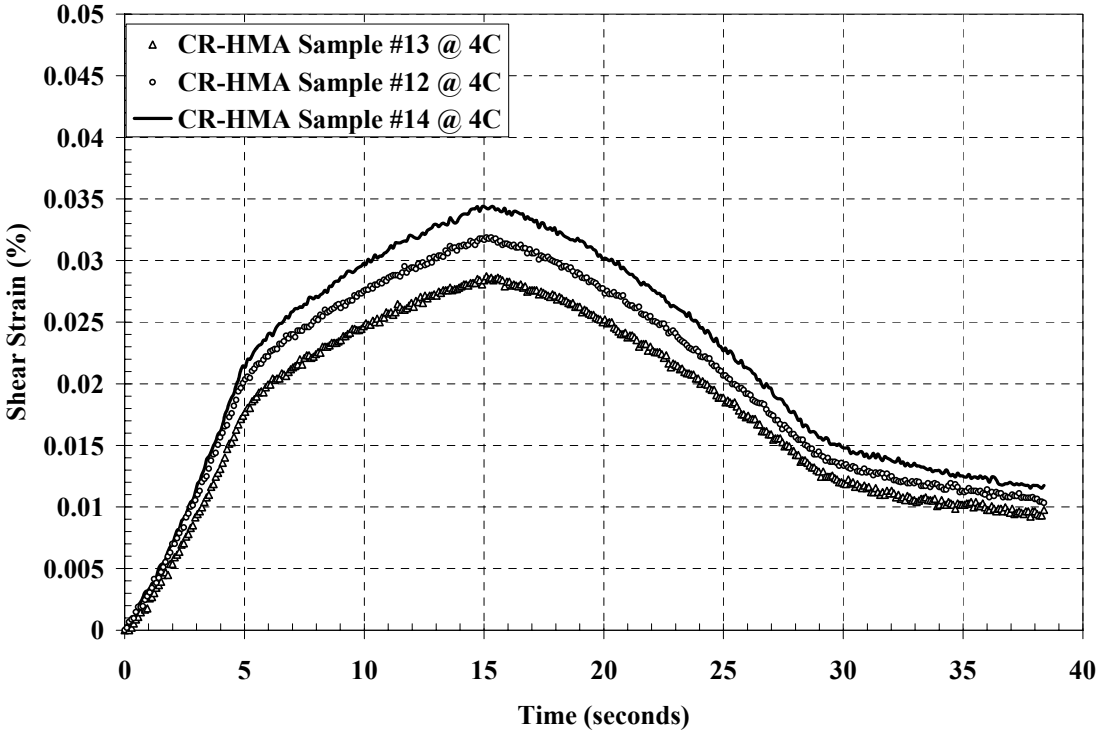

Figure A.16 – Simple Shear Results for AR-HMA at 4°C (Laboratory Aged)

APPENDIX B – SUPERPAVE SHEAR TESTER

FREQUENCY SWEEP

PG64-22 Dynamic Shear Modulus (G*) Test Results (Average of 3 Samples)

Temp = 4C

Frequency Hz	G* PSI	Std Dev G* PSI	COV G* (%)	Phase Angle (ϕ) Degrees	Std Dev (ϕ) Degrees	COV (ϕ) (%)
10	816,393	97,719	11.97	15	0.70	4.74
5	689,631	42,649	6.18	15	0.73	4.83
2	599,841	37,514	6.25	16	0.38	2.34
1	528,610	31,138	5.89	18	0.41	2.34
0.5	458,813	29,776	6.49	19	0.69	3.53
0.2	376,446	25,645	6.81	22	0.68	3.08
0.1	317,104	20,938	6.60	24	0.73	2.98
0.05	263,951	16,210	6.14	27	0.65	2.45
0.02	201,535	9,664	4.80	30	0.68	2.26
0.01	160,896	7,365	4.58	32	0.32	1.00

Temp = 20C

Frequency Hz	G* PSI	Std Dev G* PSI	COV G* (%)	Phase Angle (ϕ) Degrees	Std Dev (ϕ) Degrees	COV (ϕ) (%)
10	279,814	18,313	6.54	31	0.76	2.46
5	216,997	11,721	5.40	34	0.84	2.47
2	157,117	8,573	5.46	38	1.05	2.77
1	115,268	4,636	4.02	40	1.13	2.83
0.5	84,307	3,919	4.65	43	1.07	2.49
0.2	55,377	2,485	4.49	45	0.44	0.98
0.1	39,916	1,594	3.99	46	0.09	0.20
0.05	28,268	926	3.27	48	0.52	1.08
0.02	18,464	724	3.92	48	0.30	0.63
0.01	13,424	460	3.42	48	1.18	2.48

Temp = 40C

Frequency Hz	G* PSI	Std Dev G* PSI	COV G* (%)	Phase Angle (ϕ) Degrees	Std Dev (ϕ) Degrees	COV (ϕ) (%)
10	31,315	2,360	7.54	57	0.65	1.13
5	21,280	1,405	6.60	57	0.17	0.30
2	12,588	831	6.60	56	0.66	1.19
1	8,767	625	7.13	55	0.71	1.30
0.5	5,931	373	6.28	55	0.46	0.85
0.2	3,842	212	5.51	50	0.40	0.80
0.1	2,902	196	6.76	47	0.90	1.92
0.05	2,264	115	5.07	42	1.16	2.75
0.02	1,767	162	9.14	40	2.88	7.25
0.01	1,566	92	5.88	34	1.47	4.34

Temp = 64C

Frequency Hz	G* PSI	Std Dev G* PSI	COV G* (%)	Phase Angle (ϕ) Degrees	Std Dev (ϕ) Degrees	COV (ϕ) (%)
10	3,444	228	6.62	51	1.75	3.43
5	2,732	150	5.50	44	2.81	6.36
2	2,143	164	7.64	37	3.65	9.77
1	1,903	127	6.69	33	3.12	9.31
0.5	1,689	128	7.60	30	2.59	8.55
0.2	1,505	53	3.53	27	3.68	13.50
0.1	1,449	77	5.33	24	2.38	9.82
0.05	1,352	73	5.43	22	0.38	1.72
0.02	1,323	50	3.80	22	2.25	10.18
0.01	1,309	32	2.43	20	3.21	16.28

PG70-22 Dynamic Shear Modulus (G*) Test Results (Average of 3 Samples)

Temp = 4C

Frequency Hz	G* PSI	Std Dev G* PSI	COV G* (%)	Phase Angle (ϕ) Degrees	Std Dev (ϕ) Degrees	COV (ϕ) (%)
10	729,583	74,231	10.17	14	1.12	8.00
5	637,751	65,081	10.20	15	0.77	5.08
2	550,128	59,222	10.77	16	0.76	4.67
1	485,613	54,175	11.16	17	0.78	4.53
0.5	427,208	51,391	12.03	18	0.77	4.18
0.2	355,436	44,668	12.57	20	0.81	3.99
0.1	305,684	41,422	13.55	22	1.22	5.59
0.05	258,907	36,848	14.23	23	1.08	4.71
0.02	207,506	30,653	14.77	25	1.45	5.69
0.01	173,206	27,340	15.78	27	1.21	4.47

Temp = 20C

Frequency Hz	G* PSI	Std Dev G* PSI	COV G* (%)	Phase Angle (ϕ) Degrees	Std Dev (ϕ) Degrees	COV (ϕ) (%)
10	259,324	15,851	6.11	28	1.31	4.68
5	204,987	13,984	6.82	30	1.27	4.31
2	153,454	11,589	7.55	32	1.23	3.88
1	120,246	11,596	9.64	33	1.59	4.79
0.5	94,167	9,403	9.99	35	1.17	3.38
0.2	67,271	8,574	12.75	36	1.17	3.25
0.1	52,137	7,011	13.45	37	0.65	1.77
0.05	40,395	6,344	15.70	37	1.45	3.89
0.02	28,927	4,601	15.91	37	1.22	3.25
0.01	22,726	3,797	16.71	37	0.74	2.00

Temp = 40C

Frequency Hz	G* PSI	Std Dev G* PSI	COV G* (%)	Phase Angle (ϕ) Degrees	Std Dev (ϕ) Degrees	COV (ϕ) (%)
10	47,632	5,434	11.41	46	0.86	1.85
5	34,578	4,185	12.10	45	0.42	0.93
2	23,122	2,219	9.60	46	0.19	0.41
1	16,210	1,875	11.57	45	0.55	1.24
0.5	12,296	1,341	10.91	44	0.72	1.66
0.2	8,732	880	10.08	42	0.48	1.14
0.1	6,807	562	8.26	40	0.12	0.30
0.05	5,422	473	8.72	39	0.48	1.25
0.02	4,152	386	9.30	37	0.45	1.21
0.01	3,440	432	12.56	34	1.71	4.96

Temp = 64C

Frequency Hz	G* PSI	Std Dev G* PSI	COV G* (%)	Phase Angle (ϕ) Degrees	Std Dev (ϕ) Degrees	COV (ϕ) (%)
10	5,343	1,917	35.88	46	4.48	9.84
5	4,262	1,258	29.51	41	4.01	9.89
2	3,224	697	21.61	37	4.74	12.82
1	2,685	436	16.23	34	4.68	13.60
0.5	2,340	242	10.34	31	6.86	21.88
0.2	1,979	88	4.43	29	6.12	21.46
0.1	1,832	61	3.33	27	6.28	22.99
0.05	1,685	85	5.04	26	4.94	18.98
0.02	1,531	138	8.99	24	5.95	24.62
0.01	1,496	138	9.25	23	5.91	25.87

PG76-22 Dynamic Shear Modulus (G*) Test Results (Average of 3 Samples)

Temp = 4C

Frequency Hz	G* PSI	Std Dev G* PSI	COV G* (%)	Phase Angle (ϕ) Degrees	Std Dev (ϕ) Degrees	COV (ϕ) (%)
10	646,604	32,696	5.06	11.8	1.15	9.77
5	594,675	46,226	7.77	11.9	0.74	6.22
2	539,266	46,848	8.69	12.1	0.87	7.18
1	488,935	39,402	8.06	12.7	1.05	8.24
0.5	442,078	36,830	8.33	13.8	1.05	7.64
0.2	384,221	35,876	9.34	15.4	1.08	7.00
0.1	343,452	35,242	10.26	16.8	1.09	6.52
0.05	301,498	29,898	9.92	17.8	0.63	3.55
0.02	253,414	25,402	10.02	20.3	0.80	3.94
0.01	216,301	21,680	10.02	22.4	0.64	2.87

Temp = 20C

Frequency Hz	G* PSI	Std Dev G* PSI	COV G* (%)	Phase Angle (ϕ) Degrees	Std Dev (ϕ) Degrees	COV (ϕ) (%)
10	419,379	24,591	5.86	23.0	1.38	6.00
5	356,299	17,081	4.79	23.9	0.37	1.53
2	284,845	14,364	5.04	25.5	1.04	4.07
1	233,602	11,234	4.81	27.8	1.03	3.72
0.5	188,845	9,651	5.11	29.5	0.93	3.14
0.2	142,254	6,785	4.77	31.8	1.63	5.13
0.1	111,374	5,210	4.68	33.7	1.04	3.09
0.05	86,589	4,228	4.88	35.6	1.07	3.00
0.02	61,586	2,939	4.77	36.9	0.98	2.65
0.01	47,571	2,576	5.41	38.2	0.72	1.88

Temp = 40C

Frequency Hz	G* PSI	Std Dev G* PSI	COV G* (%)	Phase Angle (ϕ) Degrees	Std Dev (ϕ) Degrees	COV (ϕ) (%)
10	64,807	10,456	16.13	44.6	2.91	6.52
5	48,163	8,070	16.76	45.1	2.35	5.21
2	32,146	4,857	15.11	44.7	1.24	2.77
1	23,561	4,307	18.28	44.3	1.65	3.73
0.5	17,631	3,148	17.85	43.2	0.91	2.11
0.2	12,325	2,219	18.00	41.7	0.33	0.79
0.1	9,594	1,615	16.83	40.9	0.80	1.96
0.05	7,418	1,184	15.96	38.8	1.82	4.68
0.02	5,682	804	14.14	38.5	2.75	7.14
0.01	4,677	503	10.76	35.9	3.15	8.76

Temp = 64C

Frequency Hz	G* PSI	Std Dev G* PSI	COV G* (%)	Phase Angle (ϕ) Degrees	Std Dev (ϕ) Degrees	COV (ϕ) (%)
10	6,365	1,069	16.79	50.7	2.83	5.57
5	4,783	685	14.32	45.9	3.06	6.67
2	3,453	399	11.55	41.3	3.30	7.99
1	2,781	187	6.73	38.0	2.48	6.53
0.5	2,316	98	4.21	35.2	1.32	3.76
0.2	1,912	76	4.00	31.3	2.02	6.46
0.1	1,715	80	4.67	29.5	1.10	3.72
0.05	1,576	55	3.49	26.9	2.12	7.88
0.02	1,473	75	5.11	25.8	1.97	7.62
0.01	1,454	128	8.78	24.1	3.25	13.49

AR-HMA Dynamic Shear Modulus (G*) Test Results (Average of 3 Samples)

Temp = 4C

Frequency Hz	G* PSI	Std Dev G* PSI	COV G* (%)	Phase Angle (ϕ) Degrees	Std Dev (ϕ) Degrees	COV (ϕ) (%)
10	671,791	50,811	7.56	15	0.55	3.77
5	595,966	23,604	3.96	14	1.02	7.23
2	527,184	24,563	4.66	14	1.61	11.13
1	471,327	21,779	4.62	16	0.63	4.05
0.5	423,981	16,798	3.96	16	1.52	9.34
0.2	361,577	15,530	4.30	18	1.87	10.48
0.1	319,760	18,799	5.88	19	1.70	8.99
0.05	276,821	19,226	6.95	20	1.89	9.30
0.02	231,798	18,551	8.00	22	2.54	11.46
0.01	197,786	19,062	9.64	24	2.64	11.22

Temp = 20C

Frequency Hz	G* PSI	Std Dev G* PSI	COV G* (%)	Phase Angle (ϕ) Degrees	Std Dev (ϕ) Degrees	COV (ϕ) (%)
10	298,556	8,946	3.00	25	0.91	3.68
5	251,723	7,669	3.05	25	1.73	6.82
2	199,233	5,170	2.59	27	1.65	6.08
1	165,630	3,465	2.09	28	1.60	5.78
0.5	135,667	4,897	3.61	29	1.66	5.72
0.2	102,031	6,103	5.98	31	2.17	7.06
0.1	82,322	5,896	7.16	32	2.28	7.18
0.05	65,931	5,999	9.10	33	2.45	7.47
0.02	49,268	5,412	10.99	33	1.96	5.87
0.01	39,069	4,570	11.70	35	2.76	7.98

Temp = 40C

Frequency Hz	G* PSI	Std Dev G* PSI	COV G* (%)	Phase Angle (ϕ) Degrees	Std Dev (ϕ) Degrees	COV (ϕ) (%)
10	60,917	5,442	8.93	40	2.35	5.86
5	47,315	4,815	10.18	41	2.61	6.43
2	32,886	3,734	11.35	40	2.03	5.02
1	24,970	3,329	13.33	40	2.26	5.65
0.5	19,234	2,942	15.29	40	1.83	4.60
0.2	13,810	2,321	16.81	39	1.66	4.28
0.1	10,864	1,830	16.84	38	1.92	5.07
0.05	8,637	1,583	18.33	37	1.81	4.89
0.02	6,568	1,237	18.83	35	1.03	2.92
0.01	5,469	1,081	19.76	34	1.48	4.33

Temp = 64C

Frequency Hz	G* PSI	Std Dev G* PSI	COV G* (%)	Phase Angle (ϕ) Degrees	Std Dev (ϕ) Degrees	COV (ϕ) (%)
10	10,014	3,169	31.65	45	3.10	6.81
5	7,746	2,479	32.00	42	3.14	7.55
2	5,697	1,539	27.02	38	4.66	12.32
1	4,699	1,124	23.93	35	4.61	13.02
0.5	3,846	872	22.67	35	3.52	10.16
0.2	3,151	606	19.24	31	3.50	11.25
0.1	2,797	532	19.03	29	3.52	12.06
0.05	2,443	416	17.05	27	3.73	13.79
0.02	2,136	340	15.94	26	2.19	8.40
0.01	2,060	296	14.37	25	2.30	9.37

APPENDIX C – SUPERPAVE SHEAR TESTER

REPEATED SHEAR

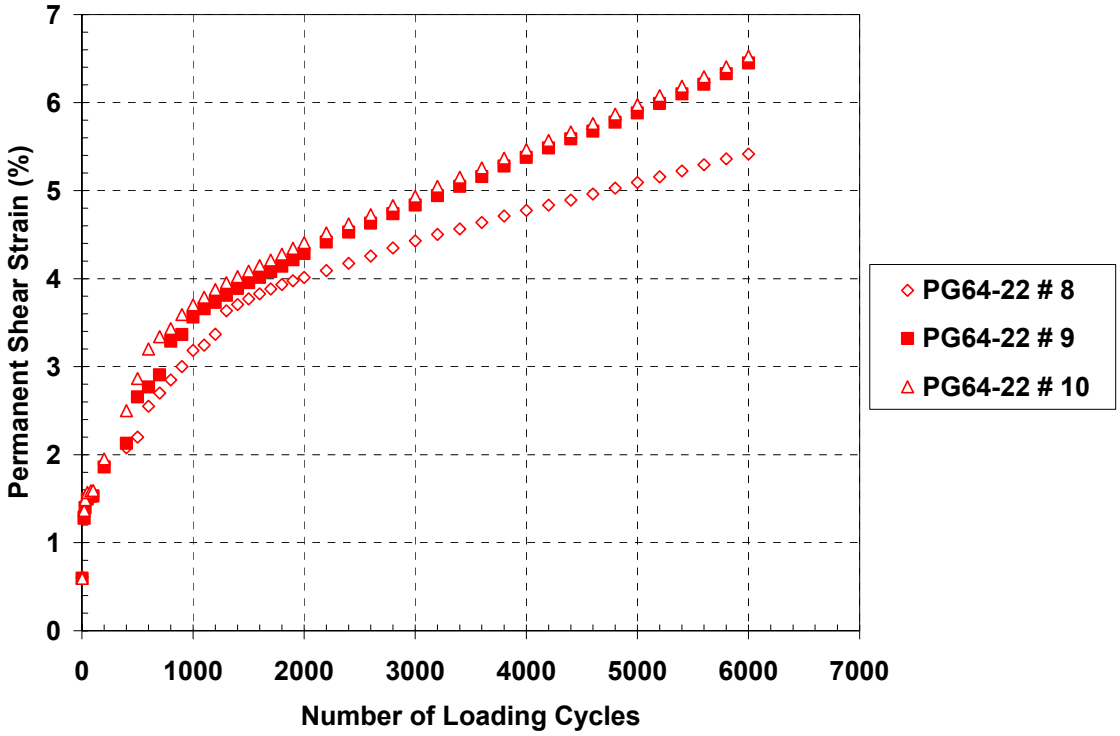

Figure C.1 – Repeated Shear Results for PG64-22 Samples

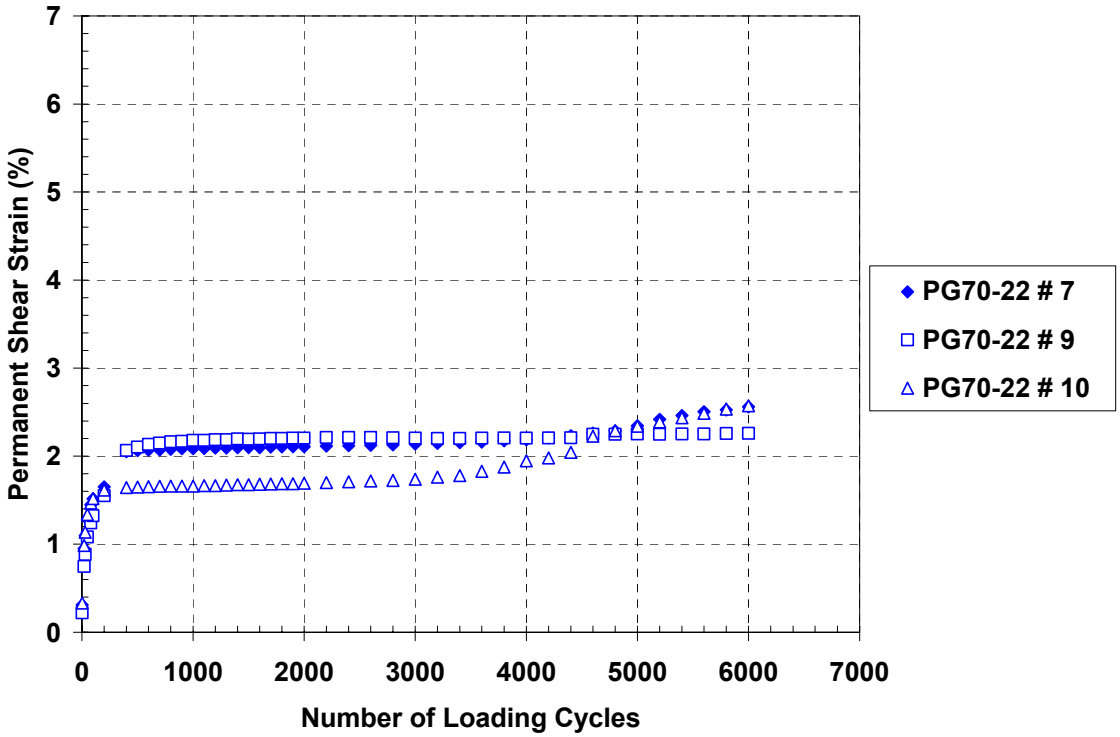

Figure C.2 – Repeated Shear Results for PG70-22 Samples

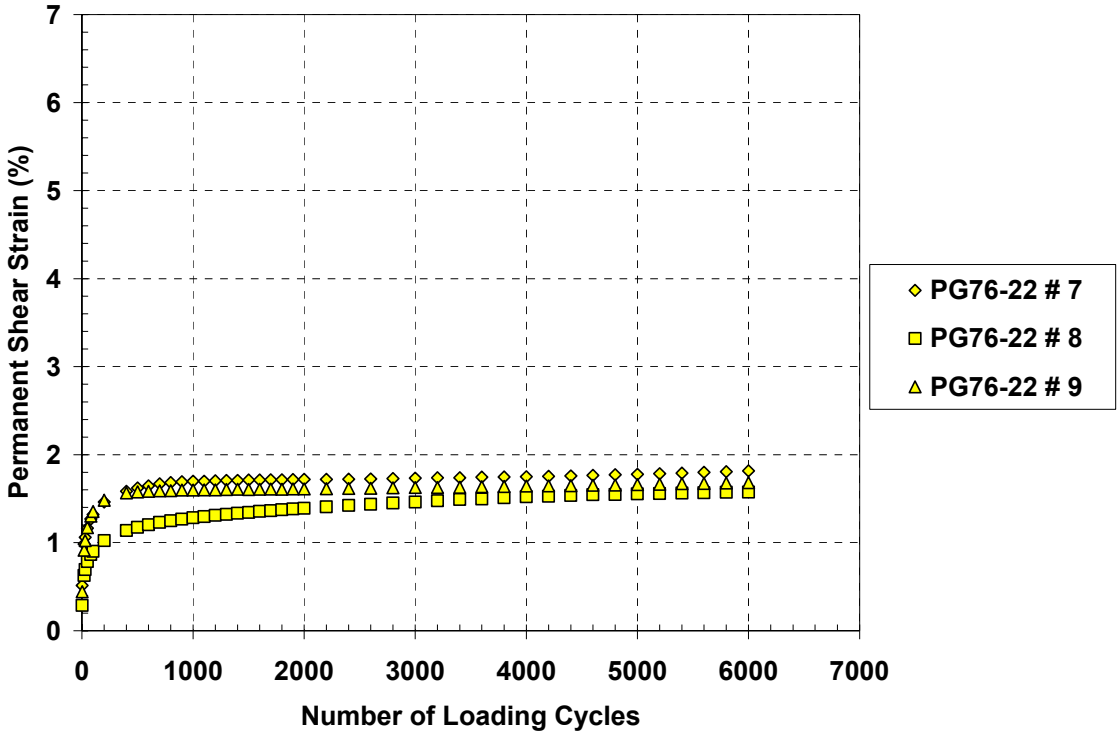

Figure C.3 – Repeated Shear Results for PG76-22 Samples

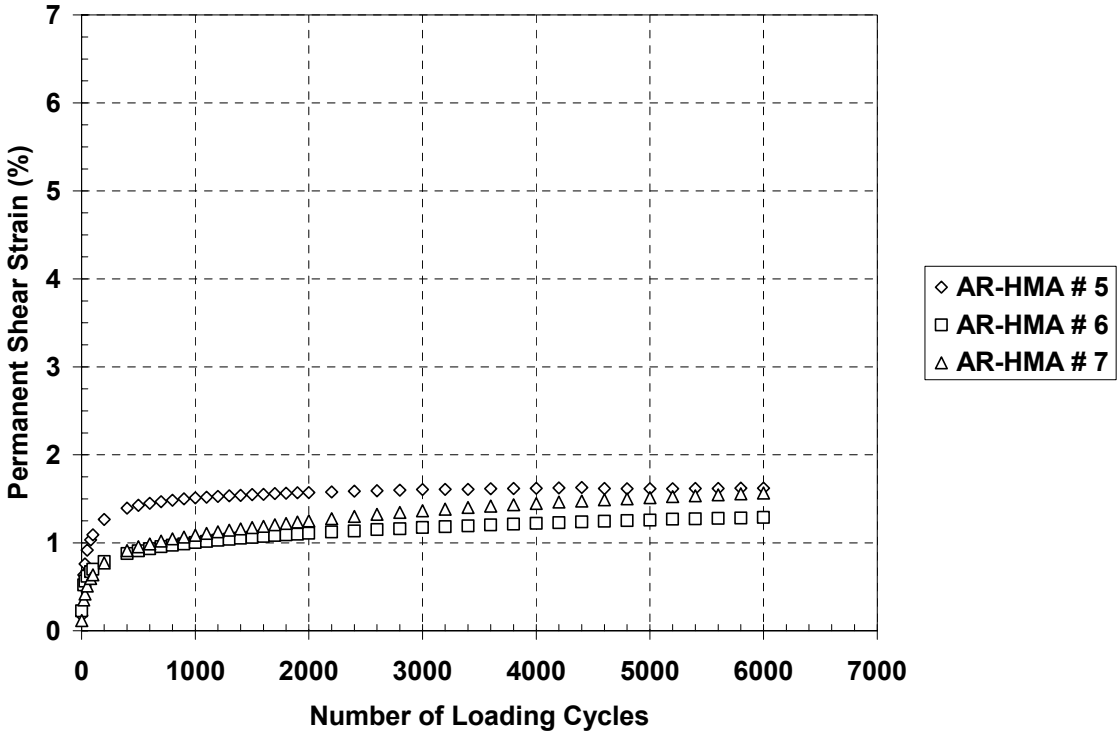

Figure C.4 – Repeated Shear Results for AR-HMA Samples

APPENDIX D – DYNAMIC MODULUS TEST RESULTS

PG64-22 Dynamic Modulus (E*) Test Results (Average of 3 Samples)

Temperature (F)	Loading Frequency (Hz)	Dynamic Modulus (psi)	E* Std Dev (psi)	E* COV (%)	Phase Angle (degrees)	ϕ Std Dev (degrees)	ϕ COV (%)
10.0	25	4,589,625	238,698	5.20	3.5	0.54	15.40
10.0	10	4,288,173	305,804	7.13	3.9	0.83	21.23
10.0	5	4,108,936	323,873	7.88	4.9	0.86	17.63
10.0	1	3,618,695	312,589	8.64	5.7	0.80	14.08
10.0	0.5	3,416,185	295,699	8.66	6.0	0.75	12.38
10.0	0.1	2,950,040	287,799	9.76	8.2	0.75	9.08

Temperature (F)	Loading Frequency (Hz)	Dynamic Modulus (psi)	E* Std Dev (psi)	E* COV (%)	Phase Angle (degrees)	ϕ Std Dev (degrees)	ϕ COV (%)
40.0	25	2,981,849	212,246	7.12	9.8	0.20	1.99
40.0	10	2,569,338	204,786	7.97	10.7	0.21	2.01
40.0	5	2,306,282	182,711	7.92	12.3	0.42	3.37
40.0	1	1,757,302	162,166	9.23	15.1	0.66	4.40
40.0	0.5	1,519,886	157,104	10.34	16.7	0.42	2.52
40.0	0.1	1,004,808	214,783	21.38	19.9	1.99	9.99

Temperature (F)	Loading Frequency (Hz)	Dynamic Modulus (psi)	E* Std Dev (psi)	E* COV (%)	Phase Angle (degrees)	ϕ Std Dev (degrees)	ϕ COV (%)
70.0	25	1,348,428	20,739	1.54	18.4	1.31	7.13
70.0	10	1,048,141	15,807	1.51	20.3	1.68	8.28
70.0	5	848,713	25,358	2.99	22.9	1.80	7.88
70.0	1	488,486	28,669	5.87	26.7	1.85	6.93
70.0	0.5	357,608	24,637	6.89	29.1	2.01	6.91
70.0	0.1	173,752	24,878	14.32	31.1	1.96	6.30

Temperature (F)	Loading Frequency (Hz)	Dynamic Modulus (psi)	E* Std Dev (psi)	E* COV (%)	Phase Angle (degrees)	ϕ Std Dev (degrees)	ϕ COV (%)
100.0	25	563,893	13,760	2.44	25.1	1.24	4.94
100.0	10	377,578	3,093	0.82	26.7	1.44	5.39
100.0	5	276,347	7,766	2.81	28.8	1.41	4.89
100.0	1	115,593	3,374	2.92	32.5	1.35	4.16
100.0	0.5	80,121	3,998	4.99	33.2	1.32	3.98
100.0	0.1	39,590	3,917	9.89	32.0	2.13	6.66

Temperature (F)	Loading Frequency (Hz)	Dynamic Modulus (psi)	E* Std Dev (psi)	E* COV (%)	Phase Angle (degrees)	ϕ Std Dev (degrees)	ϕ COV (%)
130.0	25	247,308	19,272	7.79	28.9	1.26	5.20
130.0	10	158,040	10,683	6.76	30.6	1.63	7.24
130.0	5	109,608	6,857	6.26	32.9	1.80	7.57
130.0	1	40,674	2,329	5.73	32.1	2.06	7.93
130.0	0.5	27,189	1,204	4.43	31.1	2.44	8.73
130.0	0.1	14,397	689	4.79	28.8	2.72	10.77

PG70-22 Dynamic Modulus (E*) Test Results (Average of 3 Samples)

Temperature (F)	Loading Frequency (Hz)	Dynamic Modulus (psi)	E* Std Dev (psi)	E* COV (%)	Phase Angle (degrees)	ϕ Std Dev (degrees)	ϕ COV (%)
10.6	25	4,557,385	487,771	9.63	3.2	0.20	6.28
10.6	10	4,308,318	536,312	11.20	3.5	0.27	7.68
10.6	5	4,126,204	459,809	10.03	4.4	0.33	7.46
10.6	1	3,719,102	482,359	11.67	4.8	0.41	8.58
10.6	0.5	3,567,783	429,458	10.83	5.0	0.35	7.04
10.6	0.1	3,195,670	353,297	9.95	6.4	0.34	5.24

Temperature (F)	Loading Frequency (Hz)	Dynamic Modulus (psi)	E* Std Dev (psi)	E* COV (%)	Phase Angle (degrees)	ϕ Std Dev (degrees)	ϕ COV (%)
38.6	25	2,675,979	217,774	8.14	8.8	0.72	8.18
38.6	10	2,393,081	145,583	6.08	9.4	0.27	2.84
38.6	5	2,195,473	115,755	5.27	10.7	0.24	2.23
38.6	1	1,745,791	136,746	7.83	12.2	0.40	3.32
38.6	0.5	1,559,293	125,187	8.03	13.0	0.51	3.95
38.6	0.1	1,196,751	90,210	7.54	15.8	0.36	2.27

Temperature (F)	Loading Frequency (Hz)	Dynamic Modulus (psi)	E* Std Dev (psi)	E* COV (%)	Phase Angle (degrees)	ϕ Std Dev (degrees)	ϕ COV (%)
71.5	25	1,210,818	38,865	3.21	18.0	0.71	3.94
71.5	10	971,175	52,589	5.41	19.0	0.70	3.67
71.5	5	819,808	40,533	4.94	20.7	1.03	4.96
71.5	1	529,955	27,221	5.14	23.5	1.61	6.87
71.5	0.5	423,598	22,930	5.41	25.1	1.41	5.62
71.5	0.1	262,014	16,040	6.12	27.2	1.41	5.18

Temperature (F)	Loading Frequency (Hz)	Dynamic Modulus (psi)	E* Std Dev (psi)	E* COV (%)	Phase Angle (degrees)	ϕ Std Dev (degrees)	ϕ COV (%)
101.4	25	519,172	24,305	4.68	24.4	0.86	3.53
101.4	10	371,756	21,154	5.69	26.2	0.84	3.20
101.4	5	290,804	21,381	7.35	27.4	0.99	3.61
101.4	1	157,605	14,766	9.37	28.1	0.76	2.72
101.4	0.5	120,734	12,347	10.23	28.4	0.43	1.51
101.4	0.1	71,529	8,462	11.83	27.0	0.26	0.98

Temperature (F)	Loading Frequency (Hz)	Dynamic Modulus (psi)	E* Std Dev (psi)	E* COV (%)	Phase Angle (degrees)	ϕ Std Dev (degrees)	ϕ COV (%)
128.9	25	223,592	16,027	7.17	27.7	1.12	4.02
128.9	10	154,095	12,623	8.19	26.2	1.12	4.28
128.9	5	113,818	11,090	9.74	27.2	1.20	4.43
128.9	1	53,863	5,083	9.44	26.8	1.47	5.08
128.9	0.5	39,320	3,762	9.57	25.1	1.42	4.97
128.9	0.1	24,515	2,213	9.03	22.9	0.83	3.63

PG76-22 Dynamic Modulus (E*) Test Results (Average of 3 Samples)

Temperature (F)	Loading Frequency (Hz)	Dynamic Modulus (psi)	E* Std Dev (psi)	E* COV (%)	Phase Angle (degrees)	ϕ Std Dev (degrees)	ϕ COV (%)
10.0	25	4,372,594	26,422	0.60	4.2	0.13	2.96
10.0	10	4,108,231	21,018	0.51	4.2	0.18	4.38
10.0	5	3,948,389	2,048	0.05	5.1	0.33	6.56
10.0	1	3,497,211	9,304	0.27	5.5	0.37	6.82
10.0	1	3,303,254	25,548	0.77	5.7	0.37	6.42
10.0	0	2,854,362	20,319	0.71	7.3	0.31	4.17

Temperature (F)	Loading Frequency (Hz)	Dynamic Modulus (psi)	E* Std Dev (psi)	E* COV (%)	Phase Angle (degrees)	ϕ Std Dev (degrees)	ϕ COV (%)
40.0	25.0	3,539,758	418,013	11.81	8.1	0.33	4.04
40.0	10.0	3,147,170	451,941	14.36	8.3	0.31	3.79
40.0	5.0	2,897,833	422,674	14.59	9.7	0.18	1.86
40.0	1.0	2,369,154	394,904	16.67	11.0	0.39	3.57
40.0	0.5	2,130,784	364,627	17.11	11.7	0.36	3.08
40.0	0.1	1,663,283	309,517	18.61	14.7	0.60	4.06

Temperature (F)	Loading Frequency (Hz)	Dynamic Modulus (psi)	E* Std Dev (psi)	E* COV (%)	Phase Angle (degrees)	ϕ Std Dev (degrees)	ϕ COV (%)
70.0	25.0	1,705,181	134,694	7.90	14.6	1.21	8.30
70.0	10.0	1,393,490	95,559	6.86	15.4	1.70	10.98
70.0	5.0	1,223,675	106,198	8.68	17.7	1.50	8.50
70.0	1.0	837,064	54,210	6.48	21.0	1.52	7.26
70.0	0.5	696,926	43,605	6.26	22.4	1.74	7.77
70.0	0.1	455,806	37,439	8.21	25.5	1.38	5.41

Temperature (F)	Loading Frequency (Hz)	Dynamic Modulus (psi)	E* Std Dev (psi)	E* COV (%)	Phase Angle (degrees)	ϕ Std Dev (degrees)	ϕ COV (%)
100.0	25.0	707,160	66,394	9.39	22.5	0.57	2.52
100.0	10.0	532,848	52,092	9.78	23.4	0.28	1.20
100.0	5.0	431,941	35,880	8.31	25.9	0.59	2.28
100.0	1.0	232,207	12,746	5.49	29.4	0.49	1.66
100.0	0.5	175,483	7,965	4.54	29.9	0.36	1.20
100.0	0.1	102,675	6,165	6.00	29.0	0.06	0.21

Temperature (F)	Loading Frequency (Hz)	Dynamic Modulus (psi)	E* Std Dev (psi)	E* COV (%)	Phase Angle (degrees)	ϕ Std Dev (degrees)	ϕ COV (%)
130.0	25.0	309,457	32,533	10.51	26.4	0.66	2.75
130.0	10.0	226,209	21,754	9.62	27.5	0.67	2.89
130.0	5.0	166,678	12,717	7.63	30.9	1.05	4.13
130.0	1.0	74,956	5,564	7.42	30.3	2.32	8.34
130.0	0.5	55,803	6,001	10.75	29.3	2.53	8.62
130.0	0.1	32,108	5,033	15.68	27.9	2.58	9.25

AR-HMA Dynamic Modulus (E*) Test Results (Average of 3 Samples)

Temperature (F)	Loading Frequency (Hz)	Dynamic Modulus (psi)	E* Std Dev (psi)	E* COV (%)	Phase Angle (degrees)	ϕ Std Dev (degrees)	ϕ COV (%)
10.6	25	3,652,147	250,109	6.85	4.4	0.24	5.37
10.6	10	3,245,667	525,799	16.20	4.4	0.22	4.90
10.6	5	3,131,441	435,487	13.91	5.4	0.27	5.02
10.6	1	2,686,339	590,981	22.00	5.9	0.61	10.34
10.6	0.5	2,474,845	666,463	26.93	6.2	0.73	11.90
10.6	0.1	2,238,577	551,934	24.66	8.5	1.16	13.72

Temperature (F)	Loading Frequency (Hz)	Dynamic Modulus (psi)	E* Std Dev (psi)	E* COV (%)	Phase Angle (degrees)	ϕ Std Dev (degrees)	ϕ COV (%)
40.0	25	2,479,540	64,244	2.59	8.9	0.80	9.03
40.0	10	2,173,785	111,172	5.11	9.2	1.04	11.36
40.0	5	1,976,283	102,695	5.20	10.3	1.09	10.51
40.0	1	1,616,938	232,795	14.40	11.8	1.63	13.82
40.0	0.5	1,471,293	193,690	13.16	12.5	1.89	15.12
40.0	0.1	1,120,670	204,588	18.26	15.4	2.28	14.81

Temperature (F)	Loading Frequency (Hz)	Dynamic Modulus (psi)	E* Std Dev (psi)	E* COV (%)	Phase Angle (degrees)	ϕ Std Dev (degrees)	ϕ COV (%)
70.0	25	1,265,095	78,468	6.20	16.0	0.90	5.61
70.0	10	1,026,827	71,700	6.98	16.7	1.44	8.62
70.0	5	879,349	63,220	7.19	18.5	1.42	7.68
70.0	1	617,949	57,135	9.25	22.5	1.74	7.74
70.0	0.5	507,686	58,854	11.59	24.2	1.99	8.22
70.0	0.1	324,273	54,428	16.78	27.0	2.05	7.59

Temperature (F)	Loading Frequency (Hz)	Dynamic Modulus (psi)	E* Std Dev (psi)	E* COV (%)	Phase Angle (degrees)	ϕ Std Dev (degrees)	ϕ COV (%)
100.0	25	636,833	43,729	6.87	20.9	1.12	5.36
100.0	10	474,710	36,622	7.71	21.6	0.95	4.41
100.0	5	378,433	32,134	8.49	23.7	0.84	3.53
100.0	1	207,891	28,214	13.57	27.7	1.23	4.45
100.0	0.5	145,173	22,365	15.41	28.8	1.38	4.78
100.0	0.1	74,585	16,757	22.47	30.0	1.96	6.54

Temperature (F)	Loading Frequency (Hz)	Dynamic Modulus (psi)	E* Std Dev (psi)	E* COV (%)	Phase Angle (degrees)	ϕ Std Dev (degrees)	ϕ COV (%)
130.0	25	336,013	21,713	6.46	20.7	1.13	5.44
130.0	10	228,730	16,068	7.02	20.5	1.01	4.92
130.0	5	166,619	11,546	6.93	22.6	0.62	2.74
130.0	1	82,360	5,252	6.38	25.6	0.50	1.94
130.0	0.5	54,869	6,565	11.96	27.3	2.14	7.82
130.0	0.1	30,093	1,281	4.26	30.4	3.97	13.06

APPENDIX E – SIMPLE PERFORMANCE TEST

REPEATED LOAD PERMANENT DEFORMATION

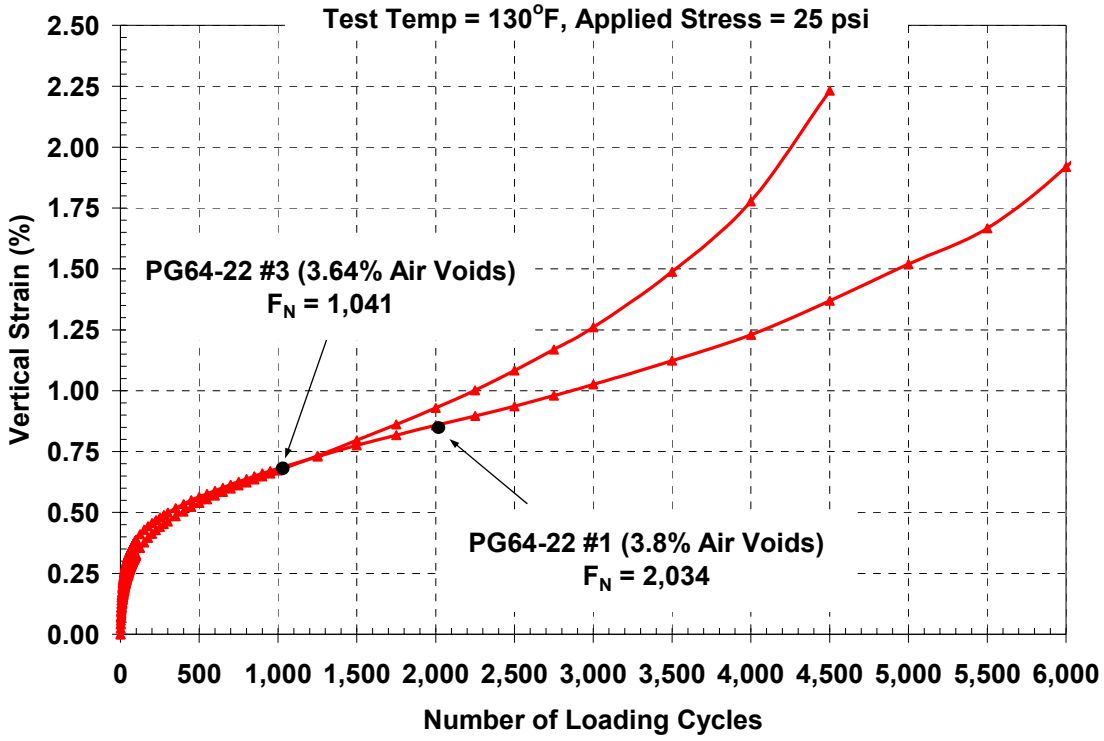

Figure E.1 – Repeated Load Permanent Deformation Results for PG64-22

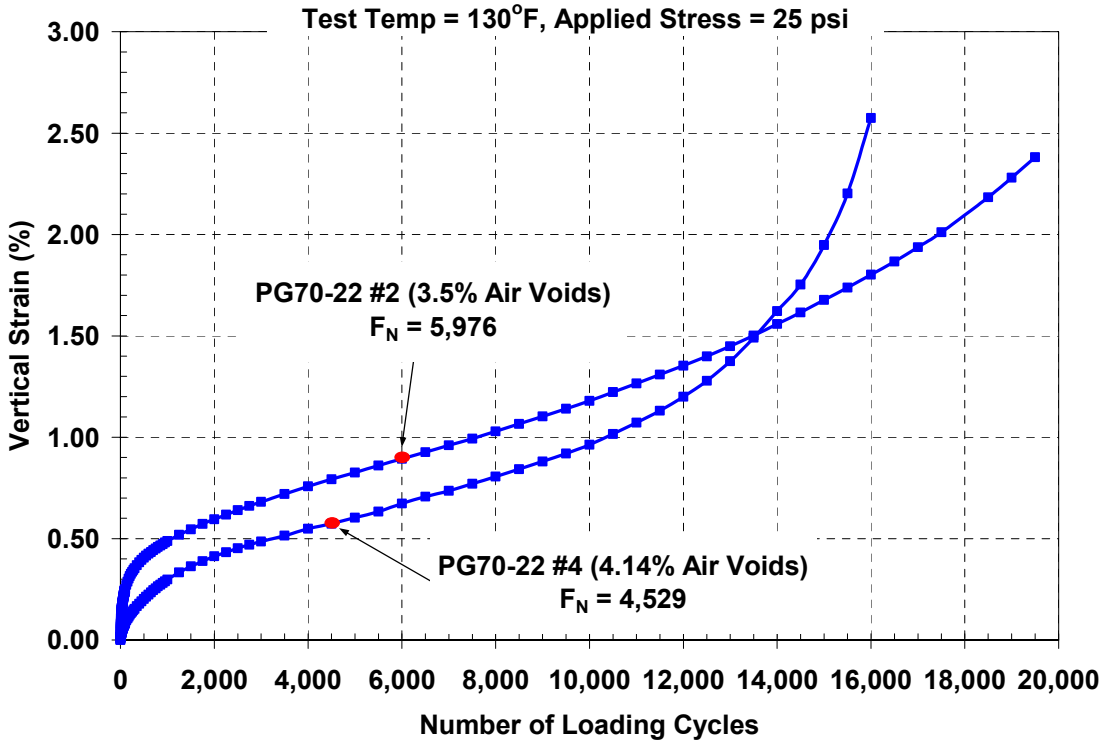

Figure E.2 – Repeated Load Permanent Deformation Results for PG70-22

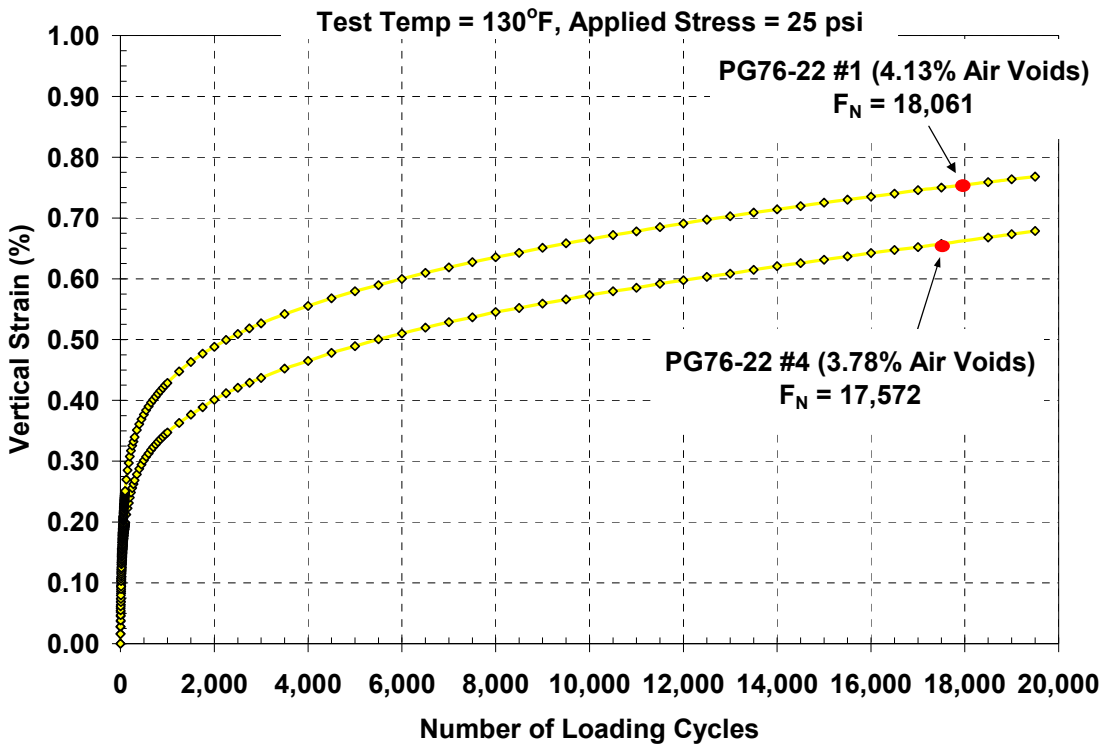

Figure E.3 – Repeated Load Permanent Deformation Results for PG76-22

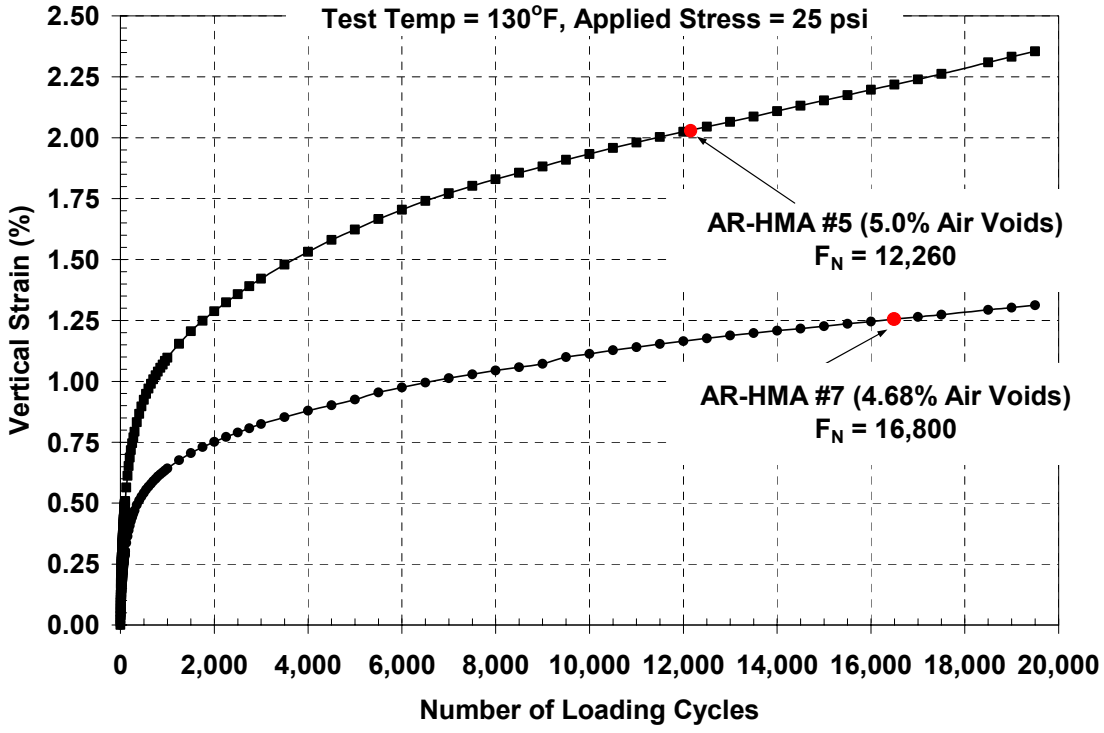

Figure E.4 – Repeated Load Permanent Deformation Results for AR-HMA